MODULATING DNA DAMAGE RESPONSES FOR IMPROVED BREAST CANCER THERAPY

APPROVED BY SUPERVISORY COMMITTEE

Sandeep Burma, Ph.D. (Mentor)
Associate Professor
Radiation Oncology

David A. Boothman, Ph.D.
Professor, Pharmacology
Radiation Oncology

James F. Amatruda, M.D., Ph.D.
Associate Professor
Pediatrics, Molecular Biology, Internal Medicine

Michael Story, Ph.D.
Division Chief/Professor
Radiation Oncology

DEDICATION

Dedicated to my inspiring parents, Ilcho and Nela Ilchevi, who worked tirelessly for the education of their children. They believe that education is the best investment one can ever make, and with perseverance, strong will and hard work they achieved that for themselves and their children. Thank you very much for all the support, encouragement and love.

MODULATING DNA DAMAGE RESPONSES FOR IMPROVED BREAST CANCER THERAPY

by

MARIYA ILCHEVA ILCHEVA

DISSERTATION

Presented to the Faculty of the Graduate School of Biomedical Sciences

The University of Texas Southwestern Medical Center

In Partial Fulfillment of the Requirements

For the Degree of

DOCTOR OF PHILOSOPHY

The University of Texas Southwestern Medical Center

Dallas, Texas

May, 2015

ACKNOWLEDGEMENTS

I would like to acknowledge my PhD mentor Dr. Sandeep Burma. I will be forever grateful for the mentorship, support, and the belief in me. I started with limited experience in science, but with his guidance, passion for science, and his effort to make his students competitive scientist, I gained confidence and the necessary tools to continue my work in the biomedical field. Thank you for the collaborative environment that you established in the laboratory, and for continuously striving to make us better scientists.

I am very grateful to Dr. David A. Boothman for the opportunity to collaborate with his lab and work on a novel anti-cancer agent. Thank you for treating me as a member of your lab, and for all the scientific guidance.

I would like to thank my husband Jerfiz Constanzo for all the support and encouragement, and of course for his constructive criticism that helped me be better at everything I do.

I am indebted to my friend and mentor Nozomi Tomimatsu for getting me up to speed with all the techniques and tools I needed to be a successful scientist. She is a great scientist and a true inspiration.

I am thankful to my friends and colleagues, Dr. Bipasha Mukherjee, Pavlina Todorova, Carlos Gil Del Alcazar, Molly Hardebeck, Cristel Camacho and Brian McEllen, for being my support group, and for their help and true friendship throughout my PhD experience; I could not have done it without them.

Special thanks go to Zachary Moore, Gaurab Chakrabarti, Lifen Cao, and Edward Motea for teaching me the techniques necessary for my project. Thank you for the welcoming environment, and the scientific discussions.

ABSTRACT

The main focus of this work is to improve the efficacy of breast cancer therapy, either by utilizing novel agents that induce specific types of DNA damage resulting in metabolic changes, or by modulating factors that are involved in the repair of toxic DNA double-strand breaks (DSBs).

The detoxifying enzyme, NQO1 (NAD(P)H:quinone oxidoreductase-1), is a promising therapeutic target due to its over-expression in many solid cancers, and very low presence in normal cells. Agents, such as β-lapachone and deoxynyboquinone (DNQ), which target NQO1 enzyme to induce programmed necrosis in solid tumors, have shown great promise. However, they have not been able to reveal the full potential of an NQO1-activated anticancer agent due to their low solubility, and more potent tumor-selective compounds are needed. Based on its structure and mode of action, isobutyl-DNQ (IB-DNQ) was recently added to the spectrum of NQO1 substrates. IB-DNQ increases NQO1 processing, enhancing both the potency and the selectivity of its anticancer properties, making it a highly efficient NQO1 substrate, and thus an outstanding anticancer agent. IB-DNQ is a promising antitumor agent whose mechanism of action has not been elucidated yet. We found that IB-DNQ killed breast cancer cells in an NQO1-dependent manner with greater potency than β-lapachone or DNQ. IB-DNQ treatment caused extensive DNA lesions, PARP1 hyperactivation, and severe NAD+ /ATP depletion leading to μ-calpain-mediated cell death (NAD^+-Keresis).

Next, we tested for synergy between IB-DNQ and the base excision repair (BER) inhibitor, methoxyamine (MeOX). Methoxyamine potentiated IB-DNQ cytotoxicity and allowed the use of very low doses of IB-DNQ, thereby potentially reducing any side-effects. Future studies in vivo will be geared toward proving the equivalent antitumor efficacy of IB-DNQ to β-lapachone and DNQ, but with much greater potency at lower doses.

In addition, this study examined factors that modulate the response of BRCA1/2-deficient breast cancers to PARP1 inhibitors. Interestingly, a significant number of BRCA1-deficient breast cancers exhibit aberrantly reduced expression of the Mre11 protein, an important player in DNA damage detection and repair. We assessed the role of Mre11 in the response of BRCA1-deficient breast cancers to PARP1 inhibitors (PARP1i) and found that Mre11 depletion resulted in a significant increase in radial chromosomal structures after IR or PARP1i treatments. These aberrations were indicative of a diminished capacity to repair DSBs by homologous recombination (HR) and subsequent repair of lesions by error-prone pathways, such as NHEJ. Loss of Mre11 abrogated HR repair pathway in BRCA1-deficient cancers, as seen with reduced Rad51 foci, and increased the sensitivity of these tumors to PARP1 inhibitors, thus Mre11 status may be an important prognostic factor in the treatment of BRCA1-deficient breast cancers with PARP inhibitors.

Another factor whose inhibition might hyper-sensitize breast cancers to PARP1 inhibitors is CDK1/2 due to the regulatory role that these kinases play in HR. Therefore, we explored the inhibition of CDK1/2 activity as a way to sensitize BRCA1-proficient cancers to PAPR1 inhibition. We found that CDK1/2 inhibition further abrogated DSB repair in BRCA1-deficient cancers, leading to heightened sensitivity to PARP1 inhibitors. These results indicate that inhibition of CDK1/2 could create a state of "BRCAness", which could expand the efficacy of PARP1 inhibitors not only for BRCA1/2-deficient cancers, but also to BRCA1-proficient ones.

TABLE OF CONTENTS

TITLE-FLY ……i

DEDICATION ……..ii

TITLE PAGE ……...……iii

ACKNOWLEDGEMENTS ……...…….iv

ABSTRACT ……..v

TABLE OF CONTENTS ……...……...viii

PUPLICATIONS ……...…….xii

LIST OF FIGURES ……...……xiii

LIST OF ABBREVIATIONS ……...……...xvii

CHAPTER I: General Introduction …….……...1

DNA damage and cancer ……2

The DNA damage response ……3

Pathway choices and resection ……7

Hereditary breast cancer …….....8

BRCA1, PARP1 and synthetic lethality …….….10

Mediation of cell death by PARP1 ……...……18

Resistance to PARP1 inhibitors …….…..20

- Increased HR capacity ……...21
- Altered NHEJ capacity ……..22
- Decreased level of activity of PARP1 …….…..23

- Loss of 53BP1 restores HR ……...23
- Decreased intracellular availability of PARP1 inhibitors …….23
- HSP90-mediated stabilization of BRCA1 mutant protein …..24
- Off-target effects of PARP1 inhibitors …….25

Need for improved therapy, and strategies to achieve it…….25

CHAPTER II: Exploiting IB-DNQ-induced DNA damage responses and metabolic changes for breast cancer therapy ……...29

Introduction ……..30

Materials and Methods ……33

Results ……..39

- NQO1: Catalase ratio is a major determinant affecting the therapeutic window of IB-DNQ ……..39
- NQO1 is required for IB-DNQ-induced lethality ……43
- Minimum time and dose for IB-DNQ-induced cell death ……45
- IB-DNQ treatment leads to dramatic DNA damage in all cell cycle phases ……...……46
- PARP1 hyperactivation and NAD+/ATP loss lead to NAD-Keresis ……...……53
- Methoxyamine synergizes with IB-DNQ ……58

Discussion ……66

CHAPTER III: Potential role of BRCA1 in modulating the sensitivity of breast cancers to IB-DNQ ……..71

Introduction ……..72

Materials and Methods ……74

Results ……..79

- Breast cancers deficient in BRCA1 are extremely sensitive to IB-DNQ ……79
- BRCA1-deficient breast cancer cells have increased number of DSBs after IB-DNQ treatment ……84
- HCC1937 BRCA1-deficient cancer cells are more sensitive to IB-DNQ due to their high NQO1 activity ……86

Discussion ……89

CHAPTER IV: Factors modulating the response of BRCA1/2-deficient breast cancers to PARP1 inhibitors ……..97

Introduction ……..98

Materials and Methods ……102

Results ……105

- Loss of Mre11 leads to increased radial chromosomes in BRCA1-deficient breast and ovarian cancer cells ……..105
- Lack of Mre11 further decreases HR in BRCA1-deficient breast and ovarian cancer cells ……...108

- Depletion of Mre11 renders BRCA1-deficient cancer hyper-sensitive to PARP1 inhibitors ……113
- Stable knockdown of BRCA1 in U2OS cancer cells recapitulates defects in HR and sensitivity to PARP1 inhibitors ……..114
- Mre11 loss leads to modest reduction of the hyper-resection in BRCA1-deficient cells ……...119
- CDK1/2 inhibition alters HR capacity ……..122
- PARP1 inhibitors require one round of replication to induce DSBs ……....122
- DSB repair kinetics show compromised resolution of damage in BRCA1-deficient cells ……..126
- Treatment with CDK1/2 inhibitors further abrogates repair in BRCA1-deficient cancer cells ……...127
- CDK1/2 inhibition renders BRCA1-deficient cancer cells hyper-sensitive to PARP1 inhibitors ……129

Discussion ……...131

CHAPTER V: Conclusions and Future Directions ……...144

Conclusions and Future Directions ……145

BIBLIOGRAPHY ……154

PUBLICATIONS

Ilcheva, M., Cao, L., Parkinson, E., Moore, Z., Chakrabarti, G., Hergenrother, P., Burma, S., Boothman, D.A. (2015) Exploiting IB-DNQ-induced DNA damage responses and metabolic changes for breast cancer therapy. (Manuscript in preparation)

Ilcheva, M., Boothman, D.A., Burma, S. (2015) Crossing the DNA damage threshold: PARP1 hyperactivation as a potent tumor-selective cancer therapy. Review. Biomolecules. (Manuscript in preparation)

Morales, J.C., Motea, E. A., Patidar, P.L., Fattah, F.J., **Ilcheva, M**., Burma, S., Story, M., Boothman, D.A. (2015) RNA transcription termination factors and persistent R-loops: potential carcinogenic determinants after high or low LET IR: implications for space travel to Mars. (Submitted to THREE)

Chakrabarti, G., Silvers, **M., Ilcheva**, M., Luo, X., Liu, Y., Li, LS., Burma, S., DeBerardinis, R., Gao, J., Gerson, S., Boothman, D.A. (2015) Inhibition of base excision repair as a strategy for sensitizing pancreatic cancer to ß-lapachone. (Submitted to Journal of Clinical Investigation)

Chakrabarti, G., Moore, Z., Luo, X., **Ilcheva, M**., Ali, M.A., Fattah, F., Padanad, M., Zhou, Y., Xie,Y., Lyssiotis, C., Scaglioni, P.P., Kimmelman, A., DeBerardinis, R., Cantley, L., Boothman, D.A. (2015) Targeting KRAS-reprogrammed glutamine metabolism sensitizes pancreatic cancer to NQO1-bioactivatable drugs. (In review, Cancer Discovery)

Tomimatsu, N., Mukherjee, B., Hardebeck, M.C., **Ilcheva, M**., Camacho, C.V., Harris, J.L., Porteus, M., Llorente, B., Khanna, K.K., Burma, S. (2014) Phosphorylation of EXO1 by CDKs 1 and 2 regulates DNA end resection and repair pathway choice. ***Nat. Commun***., 5, 3561.

Camacho, C.V., Todorova, P.K., Hardebeck, M.C., Tomimatsu, N., Gil Del Alcazar, C.R., **Ilcheva, M**., Mukherjee, B., McEllin, B., Vemireddy, V., Hatanpaa, K., Story, M.D., Habib, A.A., Murty, V.V., Bachoo, R., Burma, S.(2014) DNA double-strand breaks cooperate with loss of Ink4 and Arf tumor suppressors to generate glioblastomas with frequent Met amplification. ***Oncogene***, 29, 1-9.

LIST OF FIGURES

Figure 1.1 DNA damage responses ……4

Figure 1.2 HR vs. NHEJ during the cell cycle ……...5

Figure 1.3 Contribution of known genes to breast cancer ……9

Figure 1.4 BRCA1 structure and its interacting partners ……12

Figure 1.5 The robust cycle of PARylation ……13

Figure 1.6 Cellular roles of PARylation ……..14

Figure 1.7 Synthetic lethality ……...17

Figure 1.8 PARP1 and cellular responses to DNA damage ……19

Figure 2.1 NQO1 bioactivatable quinones ……..31

Figure 2.2 NQO1: Catalase ratio favors use of NQO1 bioactivatable drugs in breast cancer ……..40

Figure 2.3 Relative NQO1 expression ……42

Figure 2.4 NQO1 is required for IB-DNQ-induced cell death ……44

Figure 2.5 Minimum time and dose for IB-DNQ-induced cell death ……45

Figure 2.6 MCF7 cells shows high sensitivity to IB-DNQ ……46

Figure 2.7 IB-DNQ induces oxidative stress leading to DNA damage ……..48

Figure 2.8 IB-DNQ induces PARP hyperactivation, NAD+/ATP loss, μ-calpain activation and cell death ……54

Figure 2.9 Methoxyamine synergizes with IB-DNQ ……..59

Figure 2.10 Methoxyamine synergizes with IB-DNQ ……60

Figure 2.11 Methoxyamine alone is not cytotoxic ……...62

Figure 2.12 Methoxyamine synergizes with IB-DNQ in a NQO1-dependent manner ……...63

Figure 2.13 IB-DNQ induces PAR hyperactivation and NAD+/ATP depletion in a NQO1-dependent manner ……..64

Figure 2.14 Normal human cells are not sensitive to IB-DNQ and MeOX ……65

Figure 3.1 IB-DNQ treatment activates HR ……79

Figure 3.2 BRCA1-deficient breast cancers are extremely sensitive to IB-DNQ ……81

Figure 3.3 BRCA1-deficient breast cancer cells have high TUNEL+ cells after IB-DNQ treatment ……82

Figure 3.4 Generation of MCF7 cell line with stable knockdown of BRCA1…83

Figure 3.5 BRCA1-deficient breast cancer cells have increased DNA damage after IB-DNQ treatment ……84

Figure 3.6 BRCA1-deficient breast cancer cells cannot respond to IB-DNQ-induced DNA damage partly due to their HR deficiency ……....85

Figure 3.7 MCF7 shScr and shBRCA8 show equivalent sensitivity to IB-DNQ ……...86

Figure 3.8 BRCA1-deficient breast cancer cells have higher amount of ROS…87

Figure 3.9 BRCA1-deficient HCC1937 cells have high NQO1 activity, while NQO1 activity is equal between MCF7 shScr and shBRCA8 ……88

Figure 3.10 BRCA1-deficient HCC1937 cells have higher NQO1 enzyme activity……88

Figure 4.1 Structure of the MRN complex ……..98

Figure 4.2 Loss of Mre11 leads to increased radial chromosomes in BRCA1-deficient breast cancer cells ……106

Figure 4.3 Loss of Mre11 leads to increased radial chromosomes in BRCA1-deficient ovarian cancer cells ……..107

Figure 4.4 Lack of Mre11 further decreases HR in BRCA1-deficient breast cancer cells ……..109

Figure 4.5 Lack of Mre11 further decreases HR in BRCA1-deficient breast cancer cells ……..111

Figure 4.6 Mre11 loss leads to increased sensitivity to PARP1 inhibitor ABT-888 in BRCA1-null ovarian cells ……...113

Figure 4.7 Generation of U2OS cell line with stable knockdown of BRCA1…114

Figure 4.8 Loss of Mre11 leads to increased radial chromosomes in BRCA1-deficient U2OS cancer cells ……115

Figure 4.9 Lack of Mre11 further decreases HR in BRCA1-deficient breast cancer cells ……..116

Figure 4.10 Mre11 loss leads to increased sensitivity to the PARP1 inhibitor ABT-888 in U2OS BRCA1-null cancer cells …….118

Figure 4.11 Resection is increased in BRCA1-null breast cancers, and Mre11 loss leads to its modest decrease ……..……..119

Figure 4.12 BrdU/ssDNA assay confirms the increased resection in BRCA1-deficient breast cancers, and Mre11 loss lessens it ……..…120

Figure 4.13 Induction kinetics of DSBs in U2OS after ABT-888 treatment …123

Figure 4.14 PARP1 inhibitor olaparib induces DSBs in S/G2 phase …….124

Figure 4.15 PARP1 inhibitor ABT-888 induces DSBs in S/G2 phase ……125

Figure 4.16 DSB repair kinetics in U2OS cells after ABT-888 treatment …..126

Figure 4.17 Treatment with CDK inhibitor AZD-5438 further abrogates repair in BRCA1-deficient cancer cells …….127

Figure 4.18 CDK1/2 inhibitor AZD-5438 does not induce DSBs ……...128

Figure 4.19 CDK inhibition increased the sensitivity of BRCA1-deficient cancer cells to PARP1 inhibitor ABT-888 …….129

LIST OF ABBREVIATIONS

231	MDA-MB-231 breast cancer cell line
231 NQO1+	MDA-MB-231-NQO1-proficient
231 NQO1-	MDAMB-231-NQO1-deficient
53BP1	p53 Binding Protein 1
β-lap	β-Lapachone (3,4-dihydro-2, 2-dimethyl-2H-naphthol [1,2b] pyran-5, 6-dione)
AIF	Apoptosis inducing factor
AP	Apurinic/apyrimidinic site
APE1	Apurinic/apyrimidinic (AP) endonuclease 1
ATM	Ataxia telangiectasia mutated
ATP	Adenosine triphosphate
ATR	ATM and Rad3-related protein
BER	Base excision repair
BRCA1/2	Breast cancer susceptibility gene 1 or 2
BRCT	BRCA1 C Terminus (BRCT) domain
BrdU	Bromodeoxyuridine
CDK	Cyclin-dependent kinase
Chk1	Checkpoint kinase 1
CO_2	Carbon dioxide
CPT	Camptothecin

CtIP	C-terminal binding protein–interacting protein
DAPI	4', 6-diamidino-2-phenylindole
DDR	DNA damage response
DIC	Dicoumarol
DMEM	Dulbecco's Modified Eagle Medium
DMSO	Dimethyl sulfoxide
DNA	Deoxyribonucleic acid
DNA-PKcs	DNA-dependent protein kinase catalytic subunit
DNQ	Deoxynyboquinone
DSB	Double-strand break
FBS	Fetal Bovine Serum
Gy	Gray
H2AX	Histone 2A variant X
H2O2	Hydrogen peroxide
HMEC	Human mammary epithelium cells
HQ	Hydroquinone
HR	Homologous recombination
HSP90	Heat shock protein 90
IB-DNQ	Isobutyl-deoxynyboquinone
IR	Ionizing radiation
Lig IV	Ligase IV

MAR	Mono-(ADP-ribose)
MMEJ	Microhomology-Mediated End Joining
Mre11	Meiotic recombination 11
MRN	Mre11/Rad50/Nbs complex
MX	Methoxyamine
NAD	Nicotinamide adenine dinucleotide
NHEJ	Non-homologous end joining
NQO1	NAD(P)H:quinone acceptor oxidoreductase 1
OCR	Oxygen consumption rate
PAR	Poly (ADP-ribose)
PARG	Poly-(ADP-ribose) glycohydrolase
PARP1	Poly (ADP-ribose) polymerase
PBS	Phosphate buffered saline
PFA	Paraformaldehyde
P-gp	P-glycoprotein pumps
PI	Propidium iodide
Rad51	Rec A recombinase
RCC1	Regulator of chromosome condensation 1
ROS	Reactive oxygen species
RPA	Replication protein A
RPMI	Roswell Park Memorial Institute

shRNA	Short hairpin RNA
siRNA	Small interfering RNA
SOD	Superoxide dismutase
SQ	Semiquinone
SSB	Single-strand break
ssDNA	Single-stranded DNA
STS	Staurosporine
TMZ	Temozolomide
TNBC	Triple-negative breast cancer
TUNEL	Terminal deoxyribonucleotidyl transferase-mediated dUTP-nick end labeling
UV	Ultraviolet
WT	Wild-type

CHAPTER I

General Introduction

DNA damage and cancer:

Each of the ~10^{13} cells in the human body is exposed to tens of thousands of DNA lesions per day (Lindahl & Barnes, 2000). These lesions can block genome replication and transcription, and if they are not repaired or are repaired incorrectly, they lead to mutations or wider-scale genome aberrations that threaten cell or organism viability. Some DNA aberrations arise via physiological processes, such as DNA mismatches occasionally introduced during DNA replication and DNA strand breaks caused by abortive topoisomerase I and topoisomerase II activity (Iyama & Wilson, 2013). In addition, hydrolytic reactions and non-enzymatic methylations generate thousands of DNA-base lesions per cell per day (Lindahl & Barnes, 2000). DNA damage is also produced by reactive-oxygen species (ROS) arising as by-products from oxidative respiration or through redox-cycling events involving environmental toxic agents and Fenton reactions mediated by heavy metals (Valko, Rhodes, Moncol, Izakovic, & Mazur, 2006). Such by-products can attack DNA, leading to adducts that impair base pairing and/or block DNA replication and transcription, base loss, or DNA single-strand breaks (SSBs). Furthermore, when two SSBs arise in close proximity, or when the DNA-replication apparatus encounters a SSB or certain other lesions, double-strand breaks (DSBs) are formed. Although DSBs do not occur as frequently as the other lesions listed above, they are difficult to repair and extremely toxic (Khanna & Jackson, 2001).

Most carcinogens operate by generating DNA damage and causing mutations. Failure to properly repair damaged DNA contributes to the development of many diseases, including cancer.

Inherited DNA repair defects predispose to cancer, contributing to the mutator phenotype of many malignancies, and may allow tumor-cell survival and proliferation (Harper & Elledge, 2007). Notably, aberrant cell proliferation, caused by oncogene activation or inactivation of certain tumor suppressors, elicits DNA-replication stress and ongoing DNA-damage formation, which leads to genomic scarring. Such damage activates ATR/ATM-mediated signaling, causing cell death or senescence in cell-culture models and during tumorigenesis in vivo (Hoeijmakers, 2001). Indeed, the damage response is commonly activated in early neoplastic lesions and probably protects against malignancy. It has been suggested that breaches to this barrier, arising through mutational or epigenetic inactivation of cell cycle checkpoints, are subsequently selected for during tumor development, thus allowing malignant progression. This model for the DNA damage response (DDR), as an anticancer barrier helps to explain the high frequency of DDR defects in human cancers (Bassing & Alt, 2004).

The DNA damage response:

To combat threats posed by DNA damage, cells have evolved mechanisms—collectively termed the DNA-damage response (DDR)—to detect DNA lesions,

signal their presence and promote their repair **(Fig 1.1).** Cells defective in these mechanisms generally display heightened sensitivity towards DNA-damaging agents and, as described above, many such defects cause human diseases. Although responses differ for different classes of DNA lesions, they usually occur by a common general pathway: DNA damage sensors->recruitment of mediators->transducers and effectors->cellular responses (**Fig 1.1**).

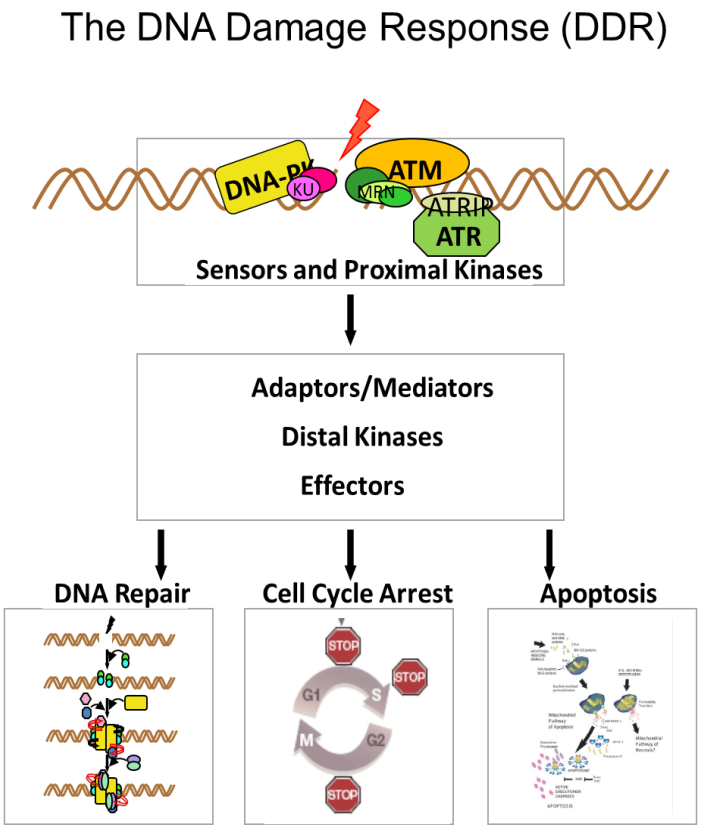

Figure 1.1. DNA damage response. When a DSB occurs it is sensed by sensor proteins (PARP1, MRN, Ku, ATRIP) and proximal kinases (ATM, DNA-PKcs, ATR). The signal is passed to adaptors, mediators, distal kinases and effectors which elicit three scenarios: DNA repair and cell cycle arrest, or apoptosis (depending on the extent of damage).

Among all genomic lesions, DNA DSBs are the most lethal if remained unrepaired. To cope with them, the cell utilizes two principal repair pathways: non-homologous end-joining (NHEJ) and homologous recombination (HR) (**Fig 1.2**).

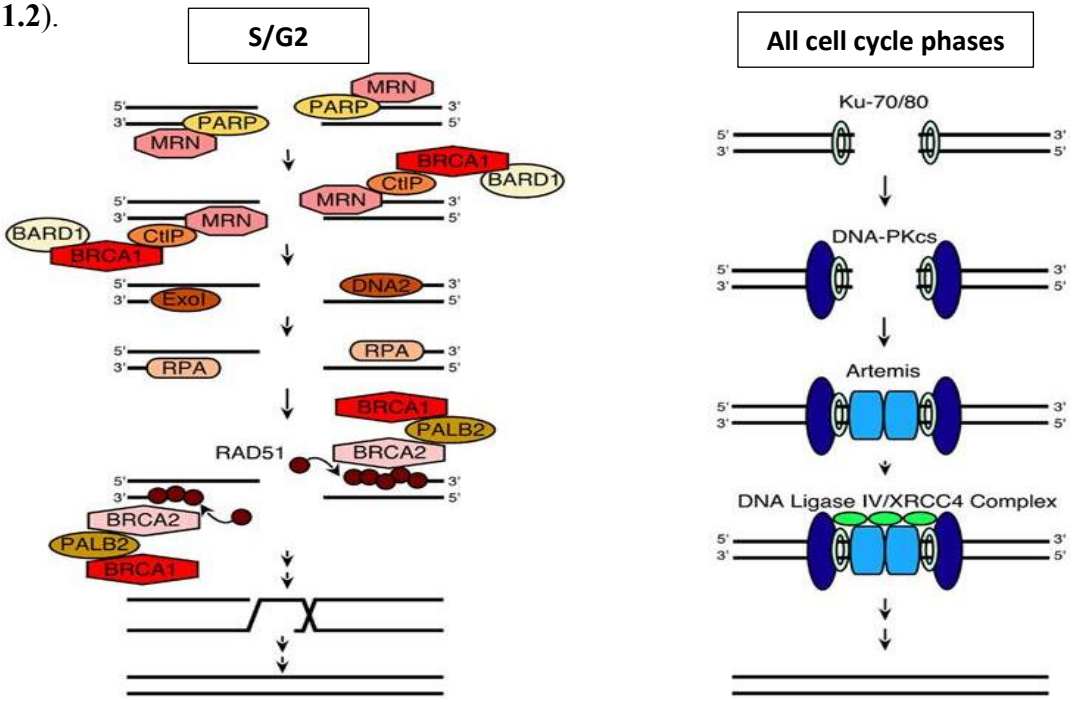

Figure 1.2. HR vs. NHEJ during the cell cycle. DSBs can be repaired via HR (left), or NHEJ pathway (right). NHEJ process involves the following steps: (1) the Ku70/80 heterodimer detects and binds to the DSB; (2) Ku70/80 bound to the DSB recruits DNA-PKcs; (3) DNA-PKcs undergoes autophosphorylation, favoring the processing of DNA ends by Artemis; and (4) the XRCC4/DNA ligase IV complex ligates the processed DNA ends. However, when a DSB occurs during the S and G2 phases of the cell cycle, repair occurs preferentially via the HR pathway (left), which involves the following steps: (1) PARP1 binds to the DSB and competes with Ku binding to DNA ends; (2) the MRN complex is recruited to the DSB (together with CtIP and BRCA1/BARD1) and mediates the initial stages of DSB resection; (3) extensive end resection is catalyzed by EXO1 and/or DNA2/BLM resulting in long stretches of ssDNA; (4) this ssDNA is coated by RPA; (5) the BRCA2/PALB2/BRCA1 complex facilitates replacement of RPA with Rad51; (6) RAD51 filaments induce strand invasion into homologous DNA sequences; (*Figure adapted from Silvana De Lorenzo, 2013*).

During NHEJ repair, DSBs are recognized by the Ku protein that then binds and activates the protein kinase DNA-PKcs, leading to recruitment and activation of end-processing enzymes, polymerases and DNA ligase IV (Waters, Strande, Wyatt, Pryor, & Ramsden, 2014). A Ku-independent NHEJ pathway, called microhomology-mediated end-joining (MMEJ) or alternative end-joining, also exist, which always results in sequence deletions (McVey & Lee, 2008). Although both NHEJ and MMEJ are error-prone, they can operate in any phase of the cell cycle. By contrast, HR is generally restricted to S and G2 phases because it uses sister-chromatid sequences as the template to mediate faithful repair. Although there are several HR sub-pathways (San Filippo, Sung, & Klein, 2008), HR is always initiated by ssDNA generation, which is promoted by various proteins including the MRE11–RAD50–NBS1 (MRN) complex and CtIP. In events catalyzed by Rad51 and the breast-cancer susceptibility proteins BRCA1 and BRCA2, the ssDNA then invades the undamaged template and, following the actions of polymerases, nucleases, helicases and other components, DNA ligation and substrate resolution occur. HR is also used to restart stalled replication forks and to repair interstrand DNA crosslinks, the repair of which also involves the Fanconi anaemia protein complex (Kennedy & D'Andrea, 2005).

Pathway choice and resection:

When a DSB occurs how does the cell decide which pathway to choose for its repair? Several factors determine whether a DSB is repaired by HR or NHEJ (Aparicio, Baer, & Gautier, 2014). One of the key decision makers between the two pathways is DNA end resection. Resection occurs in several distinct steps that prepare a broken DNA substrate for strand invasion into a homologous template and eventual resolution of strand invasion intermediates. The first step is the resection of 5' strands from the DSB ends to develop 3′ tails of single-stranded DNA (ssDNA) that are bound initially by replication protein A (RPA), which is subsequently exchanged for the Rad51 recombinase. Resection is a prerequisite for HR, and it is regulated during the cell cycle to occur preferentially in the S and G2 phases. Once resection has initiated, the DNA ends become poor substrates for binding by NHEJ proteins, and cells are committed to HR repair.

The lack of BRCA2, Rad51, and a suitable sister chromatid as a template prevent HR during the G0 and G1 phases of the cell cycle. During S and G2 phases, on the other hand, there is a competition between HR and NHEJ. For example, Ku70 and Ku80 binding impairs DSB end resection, whereas resection prevents binding of the Ku70/Ku80 complex (Rouse & Jackson, 2002). Additional studies have shown that MRN plays a primary role in removing or displacing Ku from DNA ends to allow resection to take place (Langerak, Mejia-Ramirez, Limbo, & Russell, 2011). When damage occurs during G1 phase of the

cell cycle, the 53BP1/Rif1 complex restricts CtIP recruitment and stimulation of Mre11-mediated resection as described above, thereby facilitating NHEJ (Kumar & Cheok, 2014). During S and G2 phases of the cell cycle, on the other hand, Rif1 is inhibited by a BRCA1-CtIP complex, allowing HR to occur. Furthermore, the cyclin-dependent kinase CDK2, which is active primarily at the G1/S transition and in S phase, catalyzes a priming phosphorylation of CtIP that is required before DNA damage can induce CtIP binding to MRN and subsequent Mre11-initiated end resection (Buis, Stoneham, Spehalski, & Ferguson, 2012).

The above listed competing interactions illustrate the complexity of processes that regulate DNA repair and provide an explanation for the observation that mechanisms involved in DNA DSB repair shift from NHEJ to HR during cell cycle progression.

Hereditary breast cancer:

Among all types of cancer, breast cancer is the leading cause of death for women in the United States (American Cancer Society, 2015). In 2014, an estimated 235,030 cases were diagnosed, and 40,430 deaths from breast cancer will occur. However, breast cancer has made a significant therapeutic progress for the past decade, with early detection and improved chemotherapy (National Cancer Institute, 2014).

Multiple genes are associated with breast cancer. Two decades ago, the gene for the tumor suppressor BRCA1 was cloned and mapped to Ch17q21 (Miki et al., 1994). Since then hundreds of mutations have been found in affected families and 80% of individuals carrying BRCA1 defects succumb to these diseases. Disruption of one of the alleles of BRCA1 occurs in 40–50% of germline and 10% of sporadic breast cancers and in virtually all families with histories of breast and ovarian cancer (Russell et al., 2000). Secondary cancers such as pancreatic, prostate and melanoma also commonly arise at later stages in male and female breast cancer patients (Hemminki et al., 2005). Other identified genes at risk include: p53, PTEN, CDH1, STK11, CHEK2, ATM and PALB2 (**Fig 1.3**).

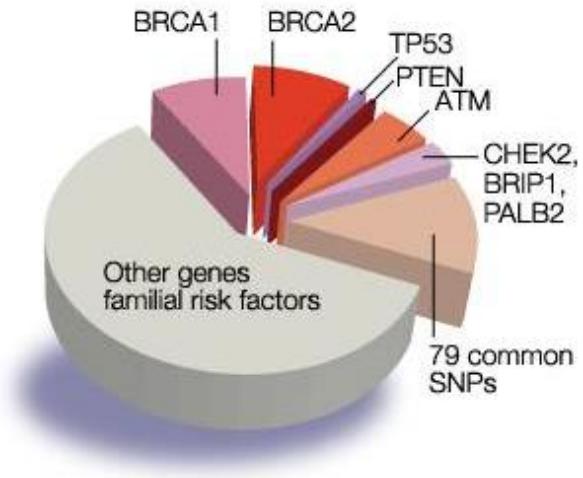

Figure 1.3. Contribution of known genes to breast cancer. Known predisposition genes account for 45% of all familial breast cancers. The other 55% are unexplained. The pie chart shows the proportion of cases accounted for by genes known to contain mutations that predispose to breast cancer and by common genetic risk factors (common SNPs). *Figure adapted from Discovery's Edge, Mayo Clinic's Online Research Magazine.*

BRCA1 is haploinsufficient for the suppression of replication stress in primary human mammary epithelial cells (HMECs) and fibroblasts (Pathania et al., 2014). BRCA1+/- cells can preferentially direct their limited stores of intact BRCA1 protein to checkpoint activation, HR, centrosome, SLUG (zinc-finger transcription factor) control and spindle pole function, and less effectively to stalled fork repair. When the replication stalling rises above a threshold level in cells, which are already deprived of a full complement of intact BRCA1, the available BRCA1 pool is dedicated first to preventing and repairing collapsed forks. This leaves even less BRCA1 available to form complexes that are required for the execution of HR at DSB that are not associated with fork collapse (Pathania et al., 2014). Therefore, patients with BRCA1/2 mutations have increased chances of developing breast or ovarian cancers (85% and 40%, respectively). Thus, tumor cells bearing BRCA1/2 mutations are hypersensitive to DSB-inducing agents, such as ionizing radiation (IR).

BRCA1, PARP1 and synthetic lethality:

One of the main players in DSB repair is the BRCA1 tumor suppressor. Multiple functions of BRCA1 may contribute to its tumor suppressor activity, including roles in cell cycle checkpoint, transcription, protein ubiquitination, apoptosis, chromatin remodeling (Yi, Kang, & Bae, 2014). BRCA1 has been found in large nuclear protein complexes (**Fig 1.4**) that are believed to be

important sensors to monitor the genome for damage and to signal to downstream proteins. For example, the BRCA1C complex is composed of CtIP and the MRN complex (M. L. Li & Greenberg, 2012). To facilitate proper HR during S and G2 phases of the cell cycle, a DSB must be processed to generate a single-stranded DNA region. CtIP, from the BRCA1C complex, promotes DNA end resection by interacting and stimulating the nuclease activity of the MRN complex. Interestingly, CtIP interacts with BRCA1 during the S-G2 phase of the cell cycle which makes BRCA1 essential for efficient ssDNA generation (Huen, Sy, & Chen, 2010). Because BRCA1 is not known to have any nuclease or helicase domains, it is speculated that BRCA1 might act as a scaffold to stabilize the MRN-CtIP complex which is important for DNA end resection. Also, BRCA1 might act as a switch to activate CtIP-dependent DNA resection specifically during S-G2 phase (Yun & Hiom, 2009a). Accumulating data shows that BRCA1 is critical for DNA end resection.

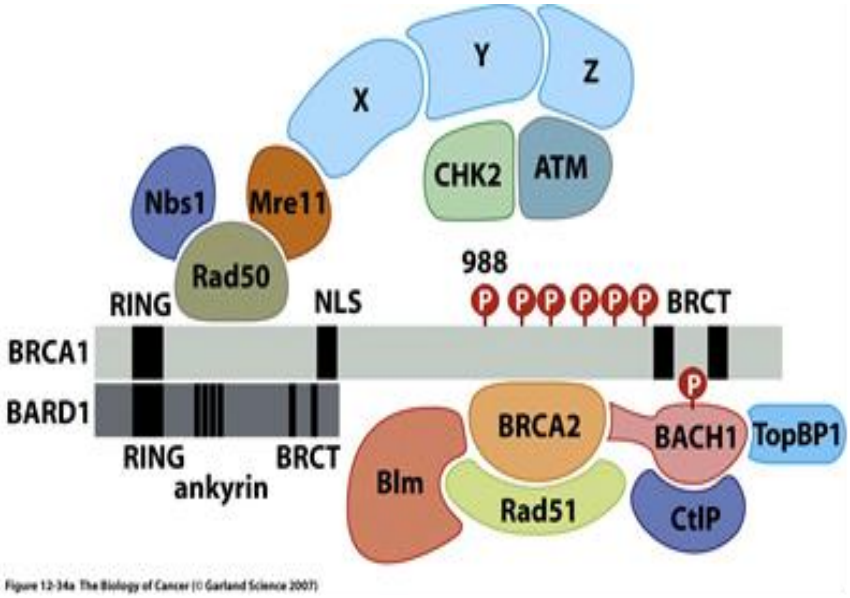

Figure 1.4. BRCA1 structure and its interacting partners. BRCA1 and BRCA2 proteins act, at least in part, as scaffolds to assemble a cohort of other DNA repair proteins into large physical complexes. Once assembled, these multiprotein complexes aid in the repair of DSBs, usually via HR. *Image taken from The Biology of Cancer by Robert Weinberg.*

Another mammalian conserved protein that plays a role in DNA repair is Poly (ADP-ribose) polymerase 1 (PARP1). PARP1 is an abundant nuclear enzyme that synthesizes poly(ADP-ribose) polymer when activated by DNA nicks or breaks (**Fig 1.5**).

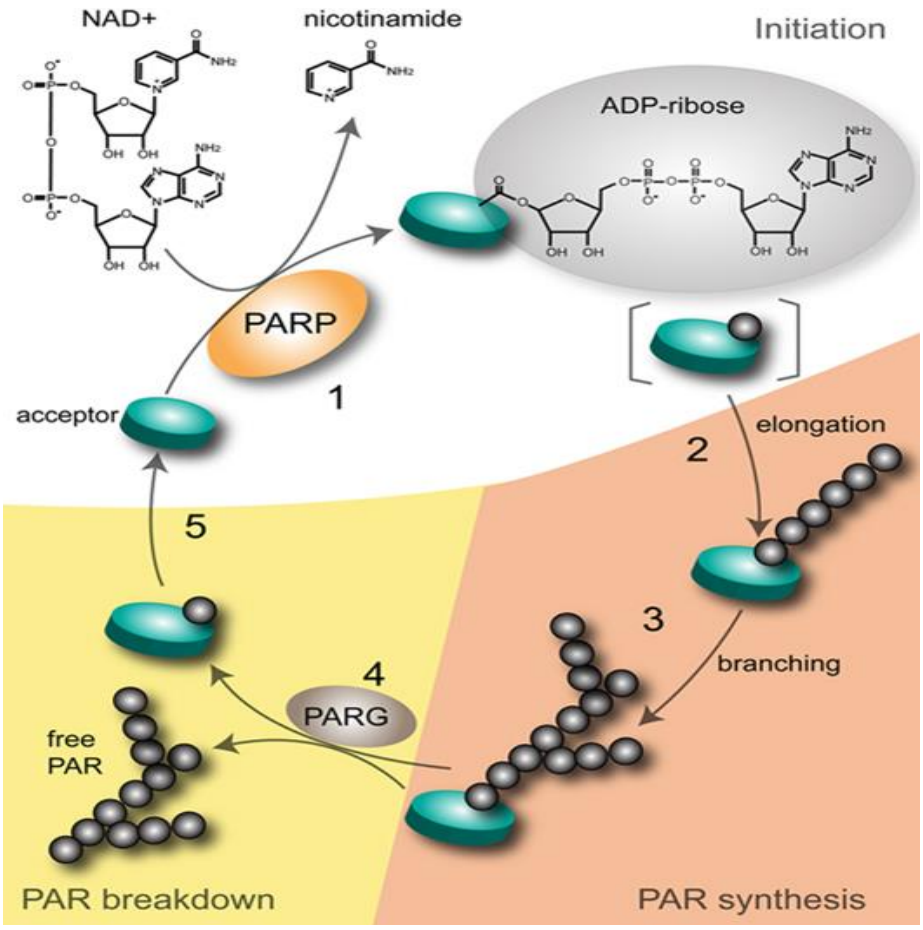

Figure 1.5. The robust cycle of PARylation. 1. PARP1 uses cellular NAD+ to add ADP-ribose moieties to acceptor proteins. 2-3. PARP1 passes elongation step where linear or branched structures are formed. 4-5. PARylation is a transient post-translational modification as PARG enzyme cleaves off PAR. *Image adapted from Karen Kate David et al, 2009.*

Activation of PARP1 has important effects on a variety of cellular processes, including base excision repair (BER), transcription, and cellular bioenergetics among others (Thomas & Tulin, 2013) (**Fig 1.6**).

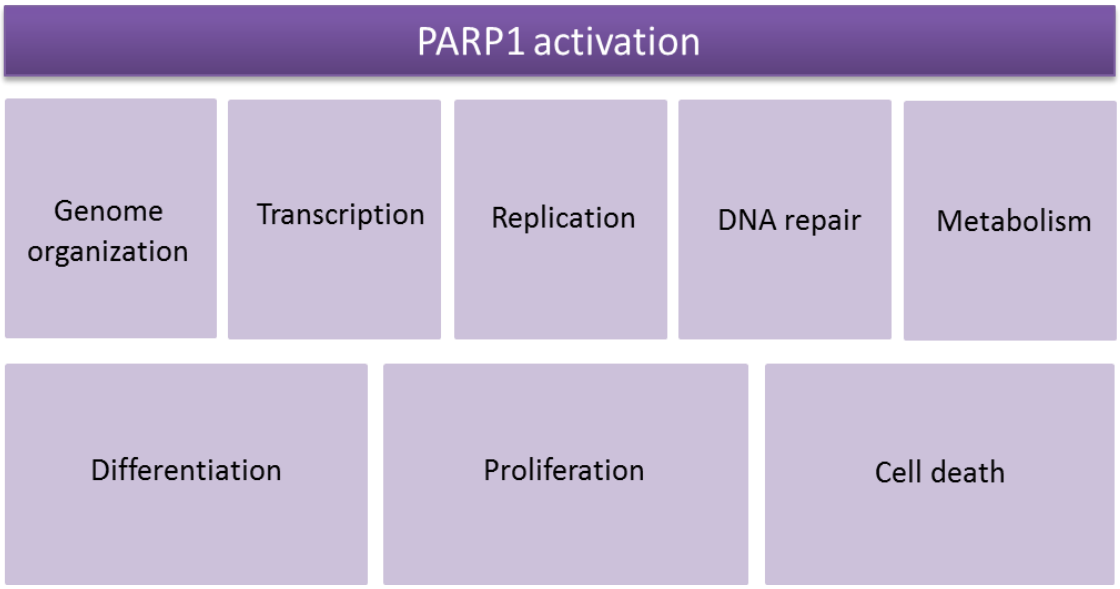

Figure 1.6. Cellular roles of PARylation. PARP1 regulates molecular events by four mechanisms: (a) PARylation of target proteins; (b) non-covalent binding of free or protein-bound PAR polymer to target proteins; (c) protein–protein interactions between PARP1 and partner proteins; and (d) modulation of cellular levels of NAD and ATP. These molecular events form the basis for the cellular roles of PARP1 in the regulation of chromatin organization, transcription, replication, DNA repair and metabolism. Combinations of these cellular effects are responsible for the regulatory roles of PARP1 in cell differentiation, proliferation and cell death. *Image was adapted from Hegedus et al., 2014*

Due to the important role PARP1 plays in many processes, there are several PARP1 inhibitors that have entered the clinic. At the moment there are nine PARP1 inhibitors in clinical development (**Table 1**). In December 2014, Olaparib was FDA approved for the treatment of BRCA-associated ovarian cancers (Walsh, 2015).

Table 1
Poly(ADP-ribose) polymerase (PARP) inhibitors in clinical development

Agent/company. Date first into clinic	Route	Disease	Single agent/combination	Clinical status
AG014699/PF0367338/CO338 **Rucaparib** Pfizer/Clovis 2003	Intravenous and oral	Solid tumours Melanoma BRCA-related tumours Ovarian cancer	Various combinations Single agent	Phase I complete Phase II ongoing
KU59436/AZD2281 **Olaparib** AstraZeneca 2005	Oral	BRCA-related cancers Solid tumours	Single agent Various combinations	Phase I complete Several Phase II ongoing
ABT888 **Veliparib** Abbott 2006	Oral	Solid Haematological	Single agent Various combinations	Phase 0/I complete Several Phase II ongoing
Iniparib BiPar/Sanofi 2006		breast cancer (TNBC)	temozolomide combinations	Phase III complete
INO-1001 Inotek/Genentek 2003/6	Intravenous	Melanoma glioblastoma multiforme (GBM)	Temozolomide combinations	Phase II (? Status)
MK4827 **Niraparib** Merck/Tesaro 2008	Oral	Solid BRCA ovarian	Single	Phase I complete
CEP-9722 Cephalon 2009	Oral	Solid tumours	Temozolomide combinations and single agent	Phase I complete
GPI 21016/E7016 (E7449 2011) MGI Pharma/Eisai 2010	Oral	Solid tumours	Temozolomide combinations Single agent and combination	Phase I ongoing
LT673/BMN 673 Biomarin 2011	Oral	Solid tumours and haematological malignancies BCRA-related cancers	Single agent	Phase I complete, Phase III ongoing

Table1 was taken from Plummer R, Poly(ADP-ribose)polymerase (PARP) inhibitors: From Bench to Bedside, Clinical Oncology (2014), http://dx.doi.org/10.1016/j.clon.2014.02.007

Only mild side effects have been reported from PARP1 inhibitor treatment (Fong et al., 2009). Normal cells, with intact HR, are not significantly affected, in line with evidence that PARP1$^{-/-}$ mice are alive and healthy in general (de Murcia et al., 1997).

The observation that PARP1 inhibition is particularly lethal to cells deficient in HR proteins (such as BRCA1) has generated additional excitement in the cancer chemotherapy community. The current explanation for this hypersensitivity focuses on a mechanism in which loss of PARP1 activity is thought to result in accumulation of DNA SSBs, which are subsequently converted to DSB by the cellular replication machinery (Dedes et al., 2011). These DSBs, which are repaired by HR in BRCA-positive cells, are presumed to accumulate in BRCA1-deficient cells, leading to subsequent cell death. The genetic interaction between BRCA1 and PARP1 can be described as synthetic lethal. Synthetic lethality between two genes occurs when individual loss of either gene is compatible with life, but simultaneous loss of both genes results in cell death. It has for a long time been suggested that a synthetic lethal approach could be used in the treatment of cancer (Hartwell, Szankasi, Roberts, Murray, & Friend, 1997) and the BRCA1-PARP1 interaction provides the first example of a successful synthetic lethal approach (**Fig 1.7**)

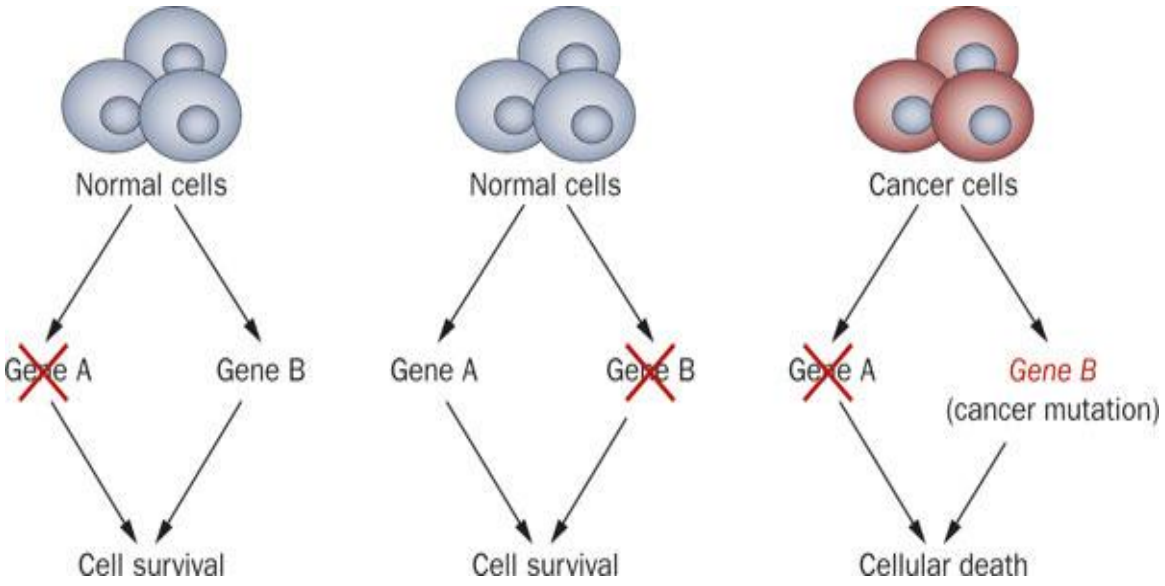

Figure 1.7. Synthetic lethality. Loss of either gene A or gene B in normal cells is compensated by the action of the remaining gene. In tumor cells, however, a mutation in one of these genes leaves the cell vulnerable to loss of the other gene by drug inhibition. This approach is the basis of drugs that target synthetic lethal relationships (e.g. BRCA1 and PARP1 inhibitors). By contrast, normal tissues are spared any toxic effects. *(Rehman, Lord, & Ashworth, 2010*)

Mediation of cell death by PARP1

PARP1 plays a role not only in DNA repair, but it also orchestrates cellular stress responses, where it processes diverse signals and, in response, directs cells to specific fates (e.g. survival vs. cell death). The specific role of PARP1 in deciding cell fate depends on the type, duration, and strength of the stress stimuli, as well as the metabolic and proliferative status of the cell (Luo & Kraus, 2012). It has become clear that while in the presence of a low level of DNA damage PARP1 activation may promote cell survival. In the presence of widespread DNA damage, excessive activation of these enzymes (PARP hyperactivation) causes programmed necrosis (Moroni, 2008) (**Fig 1.8**). Since PARP1 responds to DNA damage in a dose-dependent manner, it can be hyperactivated leading to cellular depletion of NAD+ through (ADP)-ribosylation of nuclear substrates. Thus, PARP1 hyperactivation is an energetically expensive process. Rapidly declining NAD+ levels can reduce ATP levels, since NAD+ synthesis is ATP-dependent (Ying, 2013). PARP1 hyperactivation in response to cellular trauma such as ischemia-reperfusion (Eliasson et al., 1997), myocardial infarction (Pieper et al., 2000), and reactive oxygen species-induced injury (Khanna & Jackson, 2001) has been well documented. Under these conditions pharmacological inhibition of PARP1 can protect cells from death.

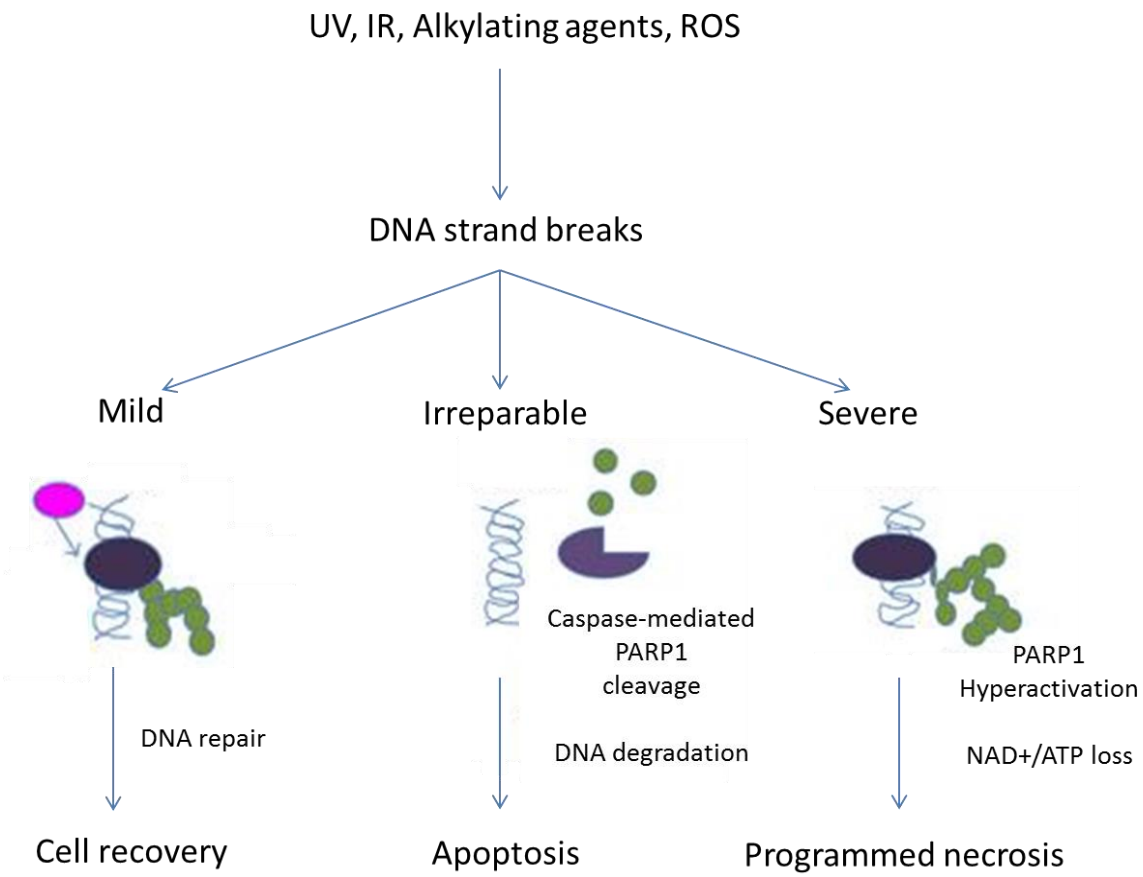

Figure 1.8. PARP1 and cellular responses to DNA damage. The intensity of DNA damage determines cellular pathways: survival, apoptosis, or necrosis. In the case of mild DNA damage, poly(ADP-ribosylation) enhances DNA repair and cell survival. When the damage is beyond repair, PARP1 facilitates apoptosis, preventing ATP depletion and DNA repair through PARP1 caspase-mediated cleavage. Severe DNA damage leads to PARP1 hyperactivation, cellular energy depletion, and programmed necrotic cell death (NAD-KERESIS) (Moore et al., 2015). *Adapted from Virág and Szabó, 2002.*

Scientists have named poly(ADP-ribose)-mediated cell death "parthanatos" based on the observation that excessive amount of PAR is toxic to the cell: mitochondria exposed to PAR are no longer functional, do not synthesize ATP and release apoptosis initiating factor (AIF). AIF translocates into the nucleus causing chromatin disruption and a caspase-independent type of cell death (Andrabi et al., 2006). This may be true in some cases, however, in this study we describe another type of programmed necrosis: "NAD-KERESIS" named after the death spirits in Greek mythology called Keres, who pull the life out of those who die violently in war. In our case IB-DNQ induces severe NAD+/ATP depletion leading to cell death that is independent of PAR moieties (Moore et al., 2015).

Resistance to PARP1 inhibitors

Despite initial responses, the development of resistance to PARP1 inhibitors limits their clinical efficacy. Early indicators from trials involving PARP1 inhibitors for triple-negative breast cancer (TNBC) show partial, but not complete response (Lovato, Panasci, & Witcher, 2012). There are several categories of known and potential mechanisms of resistance to PARP1 inhibitors in breast cancer cells, such as:

1) Increased HR capacity

- Reverse mutations of BRCA1/2

The resistance of BRCA tumors to PARP1 inhibitors was identified to be due to reverse mutations in BRCA1/2 and restoration of HR (Ashworth, 2008). For BRCA2, reverse mutation was in part due to intragenic deletion of the c.6174delT mutation and restoration of the open reading frame (Ashworth, 2008). The genomic instability associated with BRCA1/2 loss could be a cause for reverse mutations of BRCA1/2 (Aly & Ganesan, 2011). Also, certain BRCA1-deficient tumors carry hypomorphic BRCA1 mutations within its population (Drost et al., 2011). Thus, a population of cells with restored BRCA1/2 function could confer resistance to PARP inhibitors.

- Overexpression of *BRCA* via downregulation of miR-182 or PARP1

BRCA1 expression is negatively regulated by the microRNA miR-182, therefore miR-182 overexpression sensitizes BRCA1-proficient breast cancer cells to PARP1 inhibitors, whereas its downregulation made them resistant to PARP1 inhibitors (Moskwa et al., 2011). PARP1 and its activity is a negative modulator of BRCA2, because PARP1 binds to the silencer-binding region of the BRCA2 promoter (J. Wang et al., 2008). PARP1 inhibitors that mediated suppression of PARP1 activity could lead to overexpression of BRCA2 and resistance to PARP inhibitors.

- ATM mediates HR during loss of 53BP1 in BRCA-deficient tumors

BRCA1 and 53BP1 determine the balance between NHEJ and HR, because the loss of BRCA1 results in a profound defect in HR and increased NHEJ repair, whereas loss of 53BP1 suppresses NHEJ and promotes HR (Bunting et al., 2010). Additional loss of 53BP1 allowed a partial ATM-dependent HR repair (Aly & Ganesan, 2011), making these cells resistant to PARP1 inhibitors (Cao et al., 2009). Thus, increased ATM alone could induce resistance to PARP1 inhibitors.

- Increased activity of Rad51

Rad51 is a key HR protein and any factor that increases Rad51 levels or activity can potentially lead to resistance to PARP1 inhibitors. The levels of Rad51 are suppressed by miR-96 (Y. Wang, Huang, Calses, Kemp, & Taniguchi, 2012) and Aurora-1 (Sourisseau et al., 2010) and increased by PTEN (Dedes et al., 2010). It is likely that decreased miR-96 and Aurora-1 or increased PTEN can increase Rad51 and HR activity leading to the resistance to PARP1 inhibitors.

2) Altered NHEJ capacity

One of the causes for synthetic lethality of PARP1 inhibitors in HR-deficient cells is an upregulation of the error-prone NHEJ pathway. Any decrease in NHEJ capacity in these cells could increase their resistance to PARP1 inhibitors, as shown in BRCA2-deficient cells by inhibition or downregulation of 53BP1, Ku80, Artemis, or DNA-PK (Patel, Sarkaria, & Kaufmann, 2011). Thus, decreased NHEJ capacity of cells could lead to resistance to PARP1 inhibitors.

3) Decreased level or activity of PARP1

Reduced levels of PARP1 could result in resistance to PARP1 inhibitors as seen with the colorectal carcinoma HCT116 cells that are resistant to PARP1 inhibitors and temozolomide (X. Liu et al., 2009). The effectiveness of PARP1 inhibitors is also linked to the catalytic activity of PARP1. Cancer cells with normal levels of PARP1 but decreased enzymatic activity as noted by reduced levels of endogenous PARylation are more resistant to PARP inhibitors (Oplustilova et al., 2012). In contrast, HR-deficient tumor cells with higher endogenous PARylation activity are more sensitive to PARP inhibitors (Gottipati et al., 2010).

4) Loss of 53BP1 restores HR

A low level or loss of 53BP1 in human BRCA1-mutant breast cancer cells increased their resistance to PARP1 inhibitors (Bunting et al., 2010). 53BP1 is displaced from DSB ends by BRCA1, which allows resection to take place and HR to be executed. Given the preferential loss of 53BP1 in BRCA-defective and triple-negative breast carcinomas, our findings justify assessment of 53BP1 among candidate predictive biomarkers of response to PARP1 inhibitors (Oplustilova et al., 2012).

5) Decreased intracellular availability of PARP1 inhibitors

Cancer cells can efficiently elliminate PARP1 inhibitors and can become relatively resistant to this therapy. The p-glycoproteins (P-gp) also called multi-

drug resistance proteins are involved in the efflux of PARP1 inhibitors. In mouse mammary tumor models, PARP1 inhibitors were more effective when P-gp knockout condition was added to BRCA1-deficient cells (Jaspers et al., 2013). The P-gp belongs to ABC transporter family which is inhibited by ADP-ribose, a product of catalytic activity of PARP1 (Dumitriu et al., 2004). It is possible that PARP1 inhibitors that would prevent formation of ADP-ribose can permit full activity of P-gp to eliminate PARP1 inhibitors from the cells.

6) HSP90-mediated stabilization of BRCA1 mutant protein

BRCA1 gene mutations may produce truncated proteins that lose the ability to interact with associated proteins. Additionally, mutations in the BRCA C-terminal (BRCT) domain of BRCA1 create protein folding defects that result in protease-mediated degradation (Williams & Glover, 2003). Parental cells treated with the proteosome inhibitors MG132 or bortezomib had detectable levels of mutant BRAC1 protein, suggesting protein was being generated but rapidly degraded due to folding defects (Johnson, 2013). Neil Johnson and colleagues have shown that HSP90-mediated stabilization of a BRCT domain of BRCA1 can render some cancer cells resistant to PARP1 inhibitors. Treatment of resistant cells with HSP90 inhibitor reduced mutant BRCA1 protein levels and restored their sensitivity to PARP1 inhibition. Under PARP1 inhibitor selection pressure, HSP90 interacted with and stabilized mutant BRCA1 protein. The stabilized C-terminal truncated protein is semi-functional, as it is unable to interact with CtIP,

but retains the protein domains necessary to mediate interactions with PALB2-BRCA2-Rad51, capable of promoting Rad51 loading onto DNA following DNA damage. Stabilization of the mutant BRCA1 protein is critical for the restoration of Rad51 focus formation (Johnson et al., 2013).

7) Off-target effects of PARP1 inhibitors

Other reports show that very high concentrations of commonly used PARP1 inhibitors are needed to suppress the growth of TNBC cell lines in vitro (Chuang, Kapuriya, Kulp, Chen, & Shapiro, 2012). The micromolar concentrations of inhibitors needed to suppress proliferation is likely well beyond those required to block PARP1 activity (Bryant et al., 2005) and may reflect secondary effects of these inhibitors. Early studies have shown that PARP1 inhibitors have only 30-40% response rate in BRCA1/2-deficient breast and ovarian cancers (De Lorenzo, Patel, Hurley, & Kaufmann, 2013).

Need for improved therapy and strategies to achieve it

Many factors can influence the efficiency of PARP1 inhibitors, such as HR and NHEJ status, PARP1 levels or its activity and other factors that influence intracellular concentrations of PARP1 inhibitors. Therefore, it would be necessary to assess the status of these controlling factors before beginning the treatment with PARP1 inhibitors (Ashworth, 2008). Patients should be stratified before treatment on the basis of not only germline BRCA gene mutation status but also their tumor DNA sequence. For example, germline and somatic mutation, as well

as gene methylation status for BRCA1, BRCA2 and other genes that control HR, should be established before treatment, as should the presence and frequency of any HR alleles carrying secondary mutations that are predicted to restore function. In general, this would mean using clinical trial designs that generate a series of biopsies encompassing blood and tumor samples from the treatment-naive, pre–PARP1 inhibitor treatment, during-treatment and post–PARP1 inhibitor treatment (resistant) stages of the cancer, which could be a difficult task.

We must identify conditions that can resensitize tumor cells to PARP1 inhibitors, leading to improved therapy. We have to find new treatments or identify new cancer targets that in combination with PARP1 inhibitors will lead to cell death, with no chance of resistance. Most of the treatment strategies for BRCA1/2-deficient cancers include PARP1 inhibitors. However, in this study I am exploiting the opposite scenario: hyperactivating PARP1 to induce programmed cell death.

In addition, this study examined factors that modulate the response of BRCA1/2-deficient breast cancers to PARP1 inhibitors. Interestingly, a significant number of BRCA1-deficient cancers exhibit aberrantly reduced protein expression of Mre11, an important player in DNA damage detection and repair. An important goal of this study was to assess the role of Mre11 in the response of BRCA1-deficient breast cancers to PARP1 inhibitors. We speculated that reduced levels of Mre11 would further abrogate the HR repair pathway, and increase

sensitivity of these tumors to PARP1 inhibitors, and also exclude the risk for resistance.

Furthermore, I explored the inhibition of CDK1 activity as a way to sensitize BRCA1-proficient cancers to PAPR1 inhibition. CDK1 phosphorylates BRCA1, and this is essential for efficient formation of BRCA1 foci (Johnson et al., 2011). Therefore, inhibition of CDK1 created a state of "BRCAness", which could expand the efficacy of PARP1 inhibitors not only for BRCA1/2-deficient cancers, but also to BRCA1-proficient ones.

CHAPTER II

Exploiting IB-DNQ-induced DNA damage responses and metabolic changes for breast cancer therapy

INTRODUCTION

The primary goal of personalized medicine is to utilize inducible or over-expressed cancer targets. During oncogenic or cellular stress new genes are (over)- expressed that could turn into potential exploitable targets. Discriminating between normal and cancer cells is a crucial, but often challenging task, as it requires identifying a cellular component that is altered in cancer cells, but not in normal cells. The enzyme NQO1 (NAD(P)H:quinone oxidoreductase-1) is an excellent candidate for a therapeutic target due to its overexpression in many solid cancers and very low presence in normal cells.

NQO1 is a flavoenzyme that catalyzes the two-electron reduction of quinones to their hydroquinone forms. This enzyme uses reduced pyridine nucleotide cofactors NADH or NADPH to catalyze the direct two-electron reduction of a broad range of quinones (Bentle, Bey, Dong, Reinicke, & Boothman, 2006). The direct two-electron reduction of quinones to hydroquinones by NQO1 is considered a detoxification mechanism because this reaction by-passes the formation of the highly reactive semiquinone (Bentle, Bey, et al., 2006). Dicoumarol (DIC) is a potent and selective NQO1 inhibitor which competes with NAD(P)H for the NQO1 active site (Bentle, Reinicke, Bey, Spitz, & Boothman, 2006).

Normally, NQO1 detoxifies quinones resulting in the formation of a stable hydroquinone that is subsequently conjugated to glutathione, sulfate, or glucose

and excreted from the cell. However, reduction by NQO1 can turn certain rare quinones into potent cell death-inducing compounds (Parkinson, Bair, Cismesia, & Hergenrother, 2013). A couple of quinones of this type have been reported including β-lapachone (β-lap) and deoxynyboquinone (DNQ) (Huang et al., 2012). Such quinones, β-lap for instance, generate a futile redox cycle in which one mole of β-lap generates ~120 moles of superoxide within two minutes, consuming > 60 moles of NAD(P)H (Bey et al., 2013). This occurs when the bioreduction of a quinone results in the formation of an unstable hydroquinone, capable of undergoing futile redox cycling, generating reactive oxygen species (ROS).

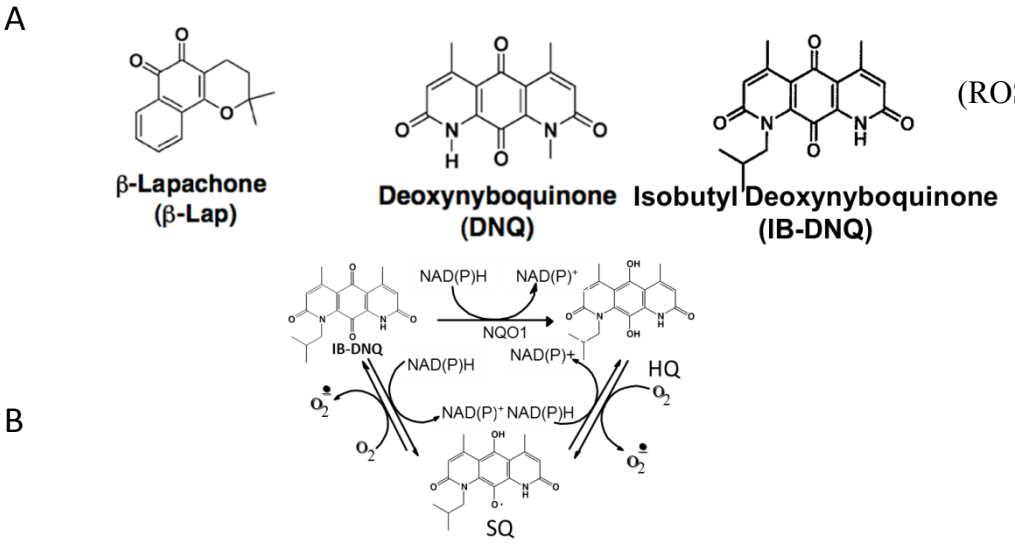

Figure 2.1. NQO1 bioactivatable quinones. A. Quinone structure of NQO1 substrates. B. Futile redox cycling of IB-DNQ. NQO1 performs a two-electron reduction of the parent IB-DNQ molecule to its hydroquinone form (HQ), which avoids enzymes that perform one-electron reductions to form the semiquinone (SQ). Unfortunately, the IB-DNQ HQ is unstable and spontaneously reverts back to its parental, oxidized form through two, one-electron reactions utilizing cellular oxygen and generating superoxide radicals.

Even though these quinones have demonstrated great promise, they have not been able to show the full potential of an NQO1-bioactivated anticancer agent either due to low solubility or intolerable side effects.

Based on its structure and mode of action, IB-DNQ (isobutyl-DNQ) was recently added to the spectrum of NQO1 substrates allowing us to fully elucidate the relationship between NQO1, quinones, and cancer cell death. IB-DNQ increased NQO1 processing, enhancing both the potency and the selectivity of its anticancer properties, however, the mechanism of action of this novel agent is not known.

This study revealed the mechanism of action of a new anticancer agent, IB-DNQ, and explored the synergy between IB-DNQ and the base excision repair (BER) inhibitor methoxyamine (MeOX). We showed that IB-DNQ induced cell death by NQO1-dependent ROS formation and oxidative stress. The generation of elevated levels of long –lived hydrogen peroxide (H_2O_2) caused extensive DNA base lesions, single-strand breaks (SSB), double-strand breaks (DSB), and AP sites. These DNA lesions caused PARP1 hyperactivation, inhibiting its essential repair functions. Additionally, PARP1 hyperactivation caused dramatic NAD^+/ATP loss resulting in dramatic energy depletion, μ-calpain activation and subsequent programmed necrosis (NAD-Keresis). IB-DNQ treatment caused extensive base lesions (8-oxo-G), which are normally repaired by BER. Addition of the potent BER inhibitor, MeOX, potentiated IB-DNQ cytotoxicity and

allowed the use of very low doses of IB-DNQ, significantly reducing potential side effects.

MATERIALS AND METHODS

Chemicals, reagents, and antibodies. Isobutyl-deoxynyboquinone was synthesized as described (Parkinson, 2013). Deoxynyboquinone and β-lapachone were synthesized as described (Pink et al., 2000). Staurosporine, Hoechst 33258, Hydrogen peroxide (H_2O_2), Propidium iodide, and Dicoumarol were purchased from Sigma-Aldrich. All quinones were dissolved in dimethyl sulfoxide (DMSO). Caspase inhibitor VI, zVAD-FMK (Z-VAD) was purchased from Calbiochem. Staurosporine (STS) was obtained and used as described (Dong et al., 2010). Human NQO1 antibody was provided by Dr. David Ross (University of Colorado Health Science Center, Denver, CO) and used at a 1:1000 dilution overnight, 4◦C. α-PAR (BD Pharmingen), which detects poly(ADP-ribosylated) (PAR) proteins, typically ADP-ribosylated PARP1, and α-PARP1 (sc-8007, Santa Cruz Biotechnology) antibodies were used at 1:1000 dilution. α-Actin (Sigma) was monitored for loading. PARP1 inhibitor, veliparib (ABT-888), was purchased from Selleckchem. Antibodies for Chk1, phospho-Chk1 (S317), Chk2 (Bethyl), phospho-Chk2 (T68) (Cell Signaling), Rad51 (H-92), 53BP1 (H-300; Santa Cruz), Cyclin A (6E6), γH2AX, H2AX, were used as described (Tomimatsu et al., 2014)

Microarray datasets. Breast cancer gene expression data series were extracted from the Gene Expression Omnibus (GEO) subject to the following criteria: 1) Public on or before September 30, 2011, 2) More than 50 samples in the full study, 3) Platform used Affymetrix HG- U133 Plus 2, 4) Triple Negative status indicated and 5) acceptable data quality. Three series meeting these criteria were chosen for inclusion in the cohort: GSE10780, GSE10890, and GSE26639. The resulting data cohort includes 266 tumor samples, 143 normal breast samples and 58 breast cancer cell line specimens, for a total of 469 specimens. Within this assembled cohort are 52 triple negative breast cancer specimens.

Cell Lines and Culture. Cell lines were obtained from either American Type Culture Collection or the Boothman lab (University of Texas Southwestern Medical Center). NQO1-*2 polymorphic human MDA-MB-231 triple-negative breast, and genetically matched NQO1+, cancer cells were generated by the Boothman lab. All cancer cells were grown in RPMI 1640 medium, or Dulbecco's minimal essential medium (DMEM) with 5% fetal bovine serum (FBS) depending on the instructions of ATCC. Cells were cultured at 37 °C in a 5 % CO_2-95 % air humidified atmosphere.

Survival Assay. Relative survival assays were assessed as described (Dong et al., 2010) and correlated well with colony forming assays (Wuerzberger et al., 1998). Briefly, cells were seeded at 10,000 cells/well in 48-well plates and allowed to attach overnight. Cells were then treated with various concentrations

of β-lapachone, DNQ, or IB-DNQ in the presence or absence of 50 μM DIC for 2 h with at least six technical replicates. Drug-free medium was then added and cells were allowed to grow for 7 days until control cells reached ~100 % confluence. Viability of adherent cells was then assessed using Hoechst dye. Plates were then read for luminescence on Perkin Elmer Devices. Percent death was calculated by subtracting background from all wells and setting 100 % survival to DMSO-treated controls. Results were reported as means ± standard error (SE) from at least 3 independent experiments done in sextuplicate.

Western Blot Analysis. Cells were grown to 70-80 % confluence at which point they were treated and harvested as indicated. The cells were lysed with RIPA lysis buffer containing 1% protease inhibitor cocktail set III (Calbiochem). Protein concentration was determined by the Pierce BCA Assay (Thermo Scientific, Rockford, IL) and whole cell lysate was resolved by SDS-PAGE gel electrophoresis. The membranes were blotted for molecules of interest with the corresponding antibodies listed above in chemicals, reagents, and antibodies. The following secondary antibodies were used: horseradish peroxidase-conjugated secondary antibodies (Bio-Rad) and Alexa488/568/647-conjugated secondary antibodies (Invitrogen). The membranes were stripped in acidic methanol and re-probed as necessary.

Alkaline comet assay. DNA single- and double-strand breaks and base damage were assessed using alkaline comet assays (TREVIGEN). Digital

photomicrographs of comet tail lengths were quantified using Komet Version 6.0 software from experiments done 3 times.

Nucleotide analyses. Changes in intracellular NAD^+ and ATP pools were measured using Luminescence NAD/NADH Glo Assay (Promega). Briefly, NAD cycling enzyme converts NAD+ to NADH. In the presence of NADH, reductase enzymatically reduces a proluciferin reductase substrate to luciferin. Luciferin is detected using Ultra-Glo rLuciferase, and the amount of light produced is proportional to the amount of NAD+ and NADH in a sample. NAD^+ and ATP levels were graphed as means, ±SE from at least 3 independent experiments carried out in quadruplets each.

Flow cytometry. MCF7 cells were analyzed by BD CYTOMICS FC500 Flow Cytometer (Becton, Dickinson and Company) as described in (Tomimatsu, Mukherjee, & Burma, 2009). For quantification of H2AX phosphorylation and cell cycle stage, cells were stained for both DNA content (propydium iodine, red) and phosphorylated H2AX using anti-γH2AX antibody (green).

TUNEL Assay. MCF7 cells were seeded at $1x10^6$ cells per 10 cm^2 dish. Log-phase cells were then treated for 4 h with 0.4 μM IB-DNQ, as described above. Medium was collected from experimental as well as control conditions after 24 h. Attached along with floating cells were monitored for cell death using TUNEL 3'-biotinylated DNA end labeling via the APO-DIRECT kit (BD Pharmigen). TUNEL positive cells were analyzed and quantified using a BD

LSRFortessa (BD Biosciences) flow cytometer equipped with BD FACSDiva™ acquisition software for processing.

Immunofluorescence. Cells were seeded onto chamber slides (BD Falcon) and next day were treated with reagents as indicated. Cells were fixed in 4 % PFA for 20 min on ice, permeabilized with 0.5 % Triton X-100, blocked in 5 % BSA/PBS, and primary antibodies were added overnight at 4^{o}C. For γH2AX and 53BP1 foci, cells were co-immunostained with Cyclin A antibody, as described (Tomimatsu et al., 2009). The average number of 53BP1 foci for Cyclin A-positive (S/G2 phase) and Cyclin A-negative (G1) nuclei was determined after scoring at least 50 nuclei. Images were captured using Leica DH5500B fluorescence microscope (40 X objective lens) coupled to a Leica DFC340 FX camera using Leica Application Suite v3 acquisition software.

Irradiation and UV. Cells in culture media were irradiated with gamma rays from a cesium source ^{137}Cs (JL Shepherd and Associates) at the indicated doses. As a positive control for Chk1, cells were exposed to 2 mJ/cm^2 of UV (Clone Zone, USA Scientific, Ocala, FL) and harvested 1 h later.

Data Processing and Analysis. The 469 specimen data files included in the cohort were downloaded as raw CEL files for post-processing together, following the standard gene expression data preparation workflow (Irizarry et al., 2003). Data was processed using the linear model from RMA, then fit robustly using probe level models as described in (Robinson & Speed, 2007). We used the R package aroma.affymetrix, which uses persistent memory to allow very large datasets to be analyzed. Probe level models are fit to RMA-background corrected and quantile normalized data to get gene-level summaries. Gene-level summarization used the standard CDF provided by Affymetrix. All data analysis was performed in R. DNA repair data were analyzed by unpaired, 2-tailed *t* tests with Welch correction using the Graphpad Prism software package. Mouse survival data were plotted using the Kaplan–Meier method and compared using the log-rank test. Tumor growth profiles between different groups were compared by the mixed model method. An AR(1) covariance structure for repeated tumor volume measures was used in the model. SAS 9.3 for Windows was used for analysis.

RESULTS

NQO1: Catalase ratio is a major determinant affecting the therapeutic window of IB-DNQ. Cells have intrinsic mechanisms to eliminate toxic H_2O_2, in particular, catalase enzyme functions to decompose H_2O_2 to water and oxygen (Bey et al., 2013). Erik Bey et al. recently reported that catalase spared β-lapachone-treated cells from H_2O_2 formation, PARP1 hyperactivation, AIF activation, atypical PARP1 and p53 proteolysis, blocked TUNEL+ staining, and enhanced clonogenic survival. The ratio of NQO1: catalase expression in tumor versus normal tissue may be a major determinant of the efficacy of any antitumor regimen involving NQO1-bioactivatable drugs. We, therefore, conducted a screen for NQO1: catalase expression ratio in 266 breast tumor samples, and 143 normal breast samples, for a total of 409 specimens. Within this assembled cohort were 52 triple negative breast cancer specimens. As seen in **(Fig 2.2)** NQO1: catalase ratio favored the use of NQO1 bioactivatable drugs in breast cancer. Specifically, matched-pair analysis showed significant differences in NQO1 expression between tumors and associated normal breast tissue for most patients. NQO1 expression is significantly elevated in breast tumors compared to normal breast tissue, while catalase expression is suppressed in breast tumors compared to normal tissue. Endogenous NQO1 and catalase expression levels in a panel of thirteen breast cancer cell lines showed different ratios, thus making assessment of the two enzymes obligatory **(Fig 2.2C).** These data predict that normal tissue,

which typically has higher catalase levels than cancer cells, could be selectively spared from IB-DNQ-induced toxicity. We also examined NQO1 levels in tumor microarray data from 66 breast cancer patients and determined that 55 % of the tumor samples expressed high level of NQO1 **(Fig 2.3).**

A

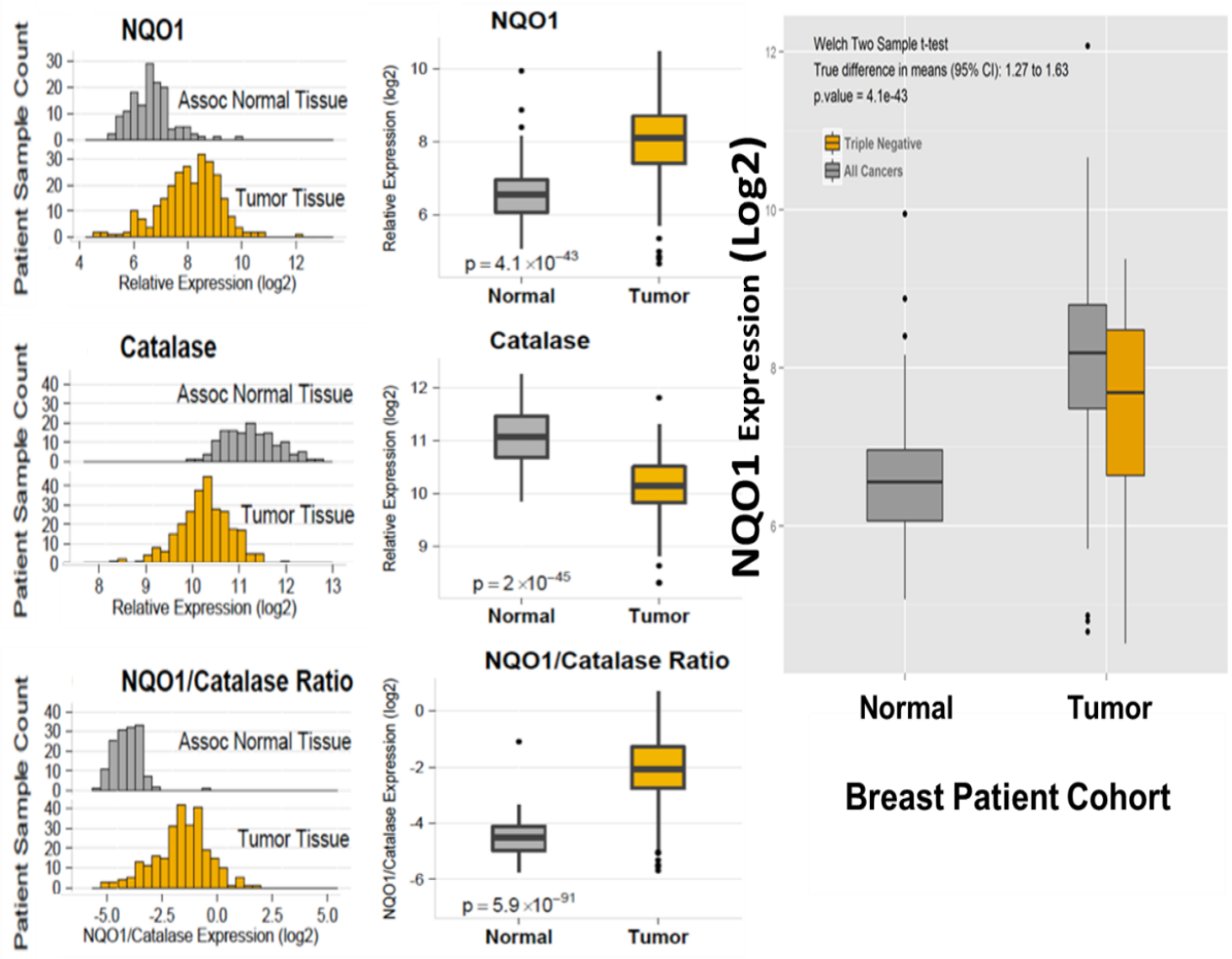

B

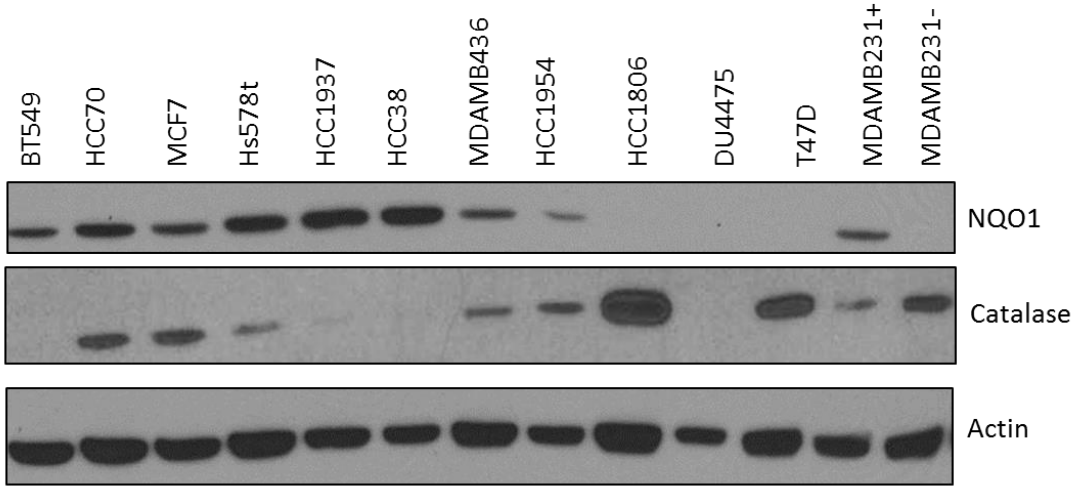

NQO1 : Catalase Ratio	0	1.47	0.93	4.96	0	0	1.60	0.35	0	0	0	1.71	0
NQO1 activity (nmol/min/mg protein)	2400 (200)	2100 (100)	1900 (100)	1900 (100)	1600 (50)	1500 (60)	1050 (50)	570 (90)	180 (30)	100 (2)	8 (4)	1500 (60)	<1
IB-DNQ IC_{50} (μM)	0.112 (0.006)	0.083 (0.007)	0.25 (0.05)	0.39 (0.04)	0.068 (0.001)	0.106 (0.004)	1.69 (0.04)	1.12 (0.03)	2.5 (0.1)	1.1 (0.3)	61 (6)	1.8 (0.9)	31 (3)
Protect (25 μM DIC)	8	14	5	8	12	22	4	3	2	1	1	8	

Figure 2.2. NQO1:Catalase ratio favors use of NQO1 bioactivatable drugs in breast cancer. A. Matched-pair analysis shows significant differences in NQO1 expression between tumors and associated normal breast tissue. NQO1 expression is significantly elevated in breast tumors compared to normal breast tissue (difference in means (95 % CI): 1.27 to 1.63, $p = 4 \times 10^{-43}$). Catalase expression is significantly suppressed in breast tumors compared to normal breast tissue (difference in means (95 % CI): -1.11 to -.88, $p= 2 \times 10^{-45}$). Orange represents the triple negative breast cancer subset. B. Endogenous NQO1 and catalase expression levels in various breast cancer cell lines. NQO1 activity (top), sensitivity to IB-DNQ (middle), and protection from IB-DNQ by the NQO1 inhibitor Dicoumarol (25 μM, bottom) are stated in the table. Standard errors of values are shown in parenthesis.

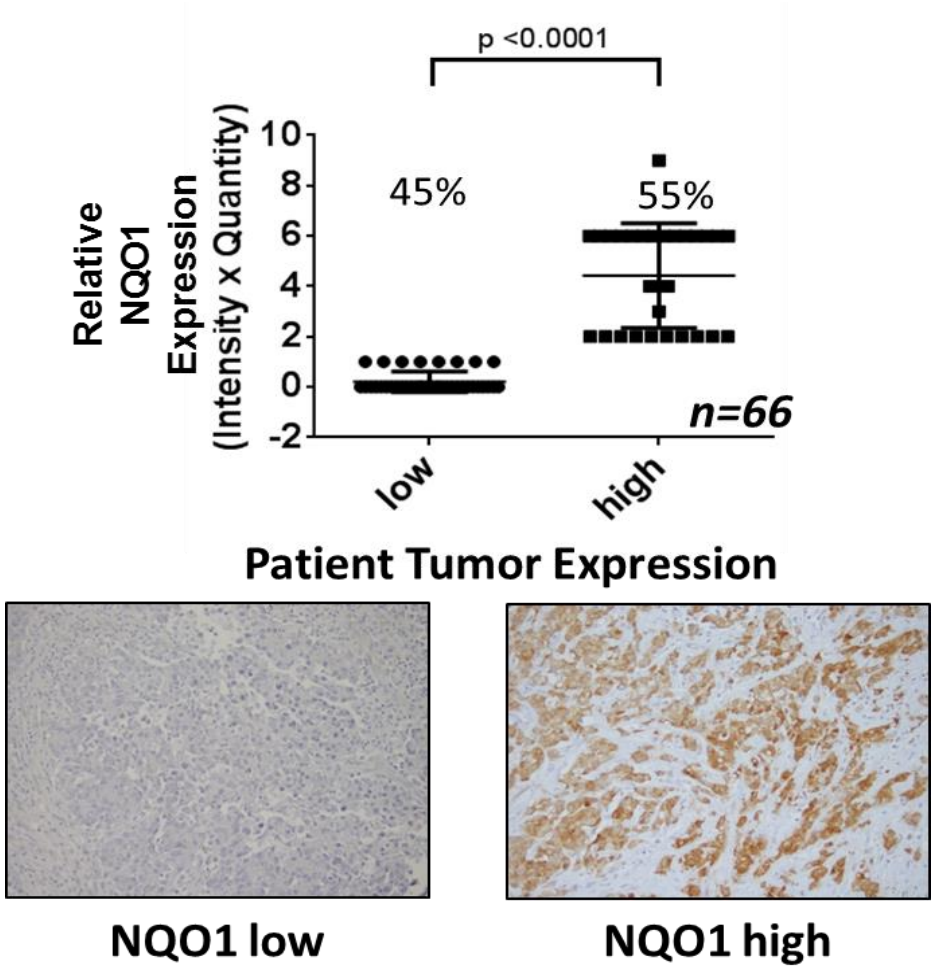

Figure 2.3. Relative NQO1 expression. Relative NQO1 level was assessed in tissue microarray data from 66 breast cancer patients (tissue microarray purchased from US Biomax, Inc.) 55 % of the tumor samples expressed high level of NQO1 (intensity x quantity). Intensity of NQO1 was scored as 0 = absent, 1 = weak, 2 = moderate, 3 = strong. Quantity of NQO1 was scored as 0 = absent, 0 %, 1 = rare, < 10 %, 2 = focal, 10-50 %, 3 = diffuse, > 50 %.

These results indicated that a significant proportion of breast cancer patients could potentially benefit from NQO1-bioactivable anticancer agents, such as IB-DNQ.

NQO1 is required for IB-DNQ-induced lethality. We examined the requirement of NQO1 for β-lapachone, DNQ and IB-DNQ-induced lethality using two breast cancer cell lines, MDA-MB-231 and MCF7. MDA-MB-231cell line has no NQO1 enzyme due to *2 polymorphism (Ross et al., 2000). The polymorphism (NQO1*2 allele) is a C to T change at position 609 of the cDNA which codes for a proline to serine change in the structure of the human protein. The lack of NQO1 protein as a result of the NQO1*2/*2 genotype appears to be due to accelerated degradation of the mutant NQO1 protein mediated by the ubiquitin/proteasomal system. We re-expressed NQO1 in order to compare the effect of NQO1 in a genetically matched pair. On the other hand, MCF7 cells have high NQO1 level and to study the role of NQO1 we used Dicoumarol (DIC), a potent and selective inhibitor of NQO1. IB-DNQ-induced lethality was compared to β-lapachone and DNQ **(Fig. 2.4 A, B, and C).** Dicoumarol spared the cells from all three quinones, with minimal protection from β-lap with > 5 μM dose **(Fig. 2.4 D, E, F)**. Both cell lines showed that only when NQO1 is present and active, the antitumor agents could elicit their cytotoxic effects.

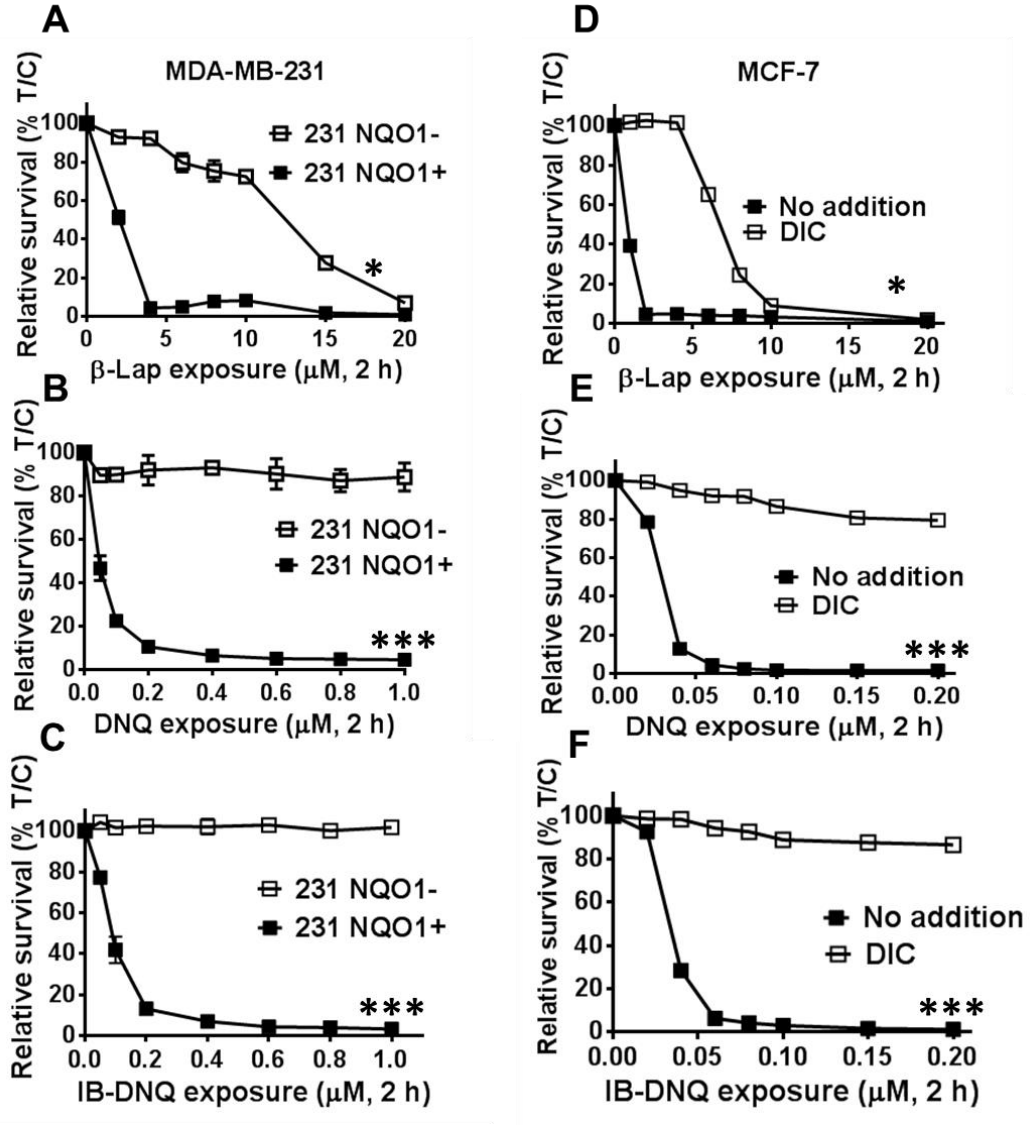

Figure 2.4. NQO1 is required for IB-DNQ-induced cell death. A-C. Long-term relative survival assays of MDA-MB-231(231 NQO1+ vs. 231 NQO1-) cells treated for 2 h with β-lap, DNQ, or IB-DNQ respectively at the indicated doses. Shown are means ± SE for three independent experiments performed in triplicate. D-F. MCF7 cells were exposed for 2 h to increasing doses of β-lap, DNQ, or IB-DNQ respectively, with or without 50 μM DIC, and long-term relative survival assays were performed. Results (means ± SE) in A-F are representative of experiments performed at least three times.

Minimum time and dose for IB-DNQ-induced cell death. MCF7 cells were exposed to increasing doses of IB-DNQ, with or without DIC (50 µM), at various times to assess the long-term survival potential therapeutic window. In MCF7 cells, IB-DNQ exhibited a much broader therapeutic window than DNQ (Huang et al., 2012). IBDNQ-treated MCF7 cells were rescued by DIC **(Fig 2.5. A–F)**. From these observations we could conclude that 2 h exposure to 0.2 µM IB-DNQ was sufficient to induce cell death, and that DIC reversed the NQO1-mediated lethality.

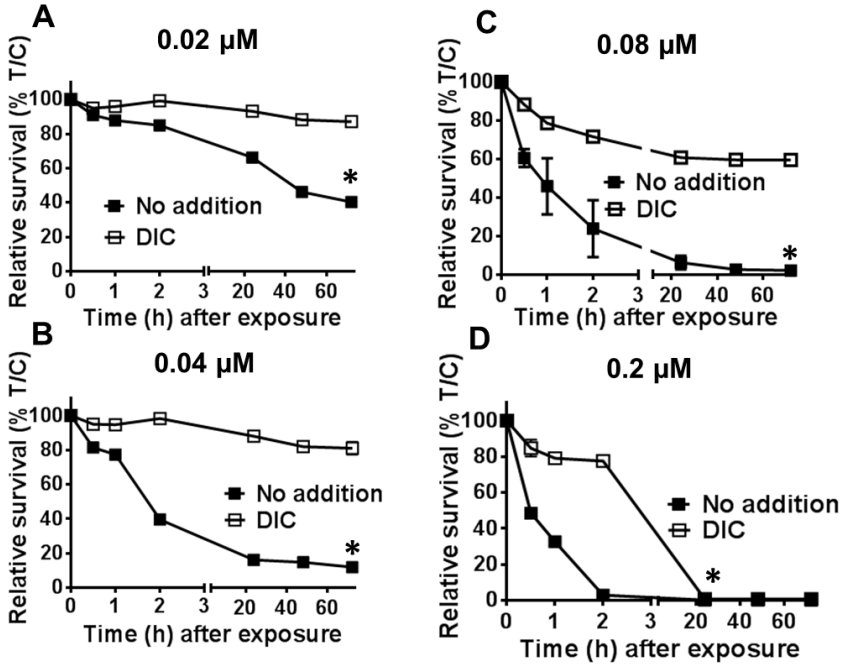

Figure 2.5. **Minimum time and dose for IB-DNQ-induced cell death.** A-D. MCF7 cells were treated with increasing doses of IB-DNQ, with or without 50 µM DIC, and long-term relative survival assays were performed. Drugs were removed at various times up to 72 h to determine minimum exposure time required for lethality. Results (means ± SE) in A-D are representative of experiments performed at least three times.

IB-DNQ treatment leads to dramatic DNA damage in all cell cycle phases. The standard of care for breast cancer is chemotherapy and radiation. We compared the sensitivity of MCF7 cells to IR, β-lap, H_2O_2, and IB-DNQ. Based on the survival curves IB-DNQ was the most toxic agent among all with ten-fold greater toxicity than β-lap. **(Fig. 2.6).**

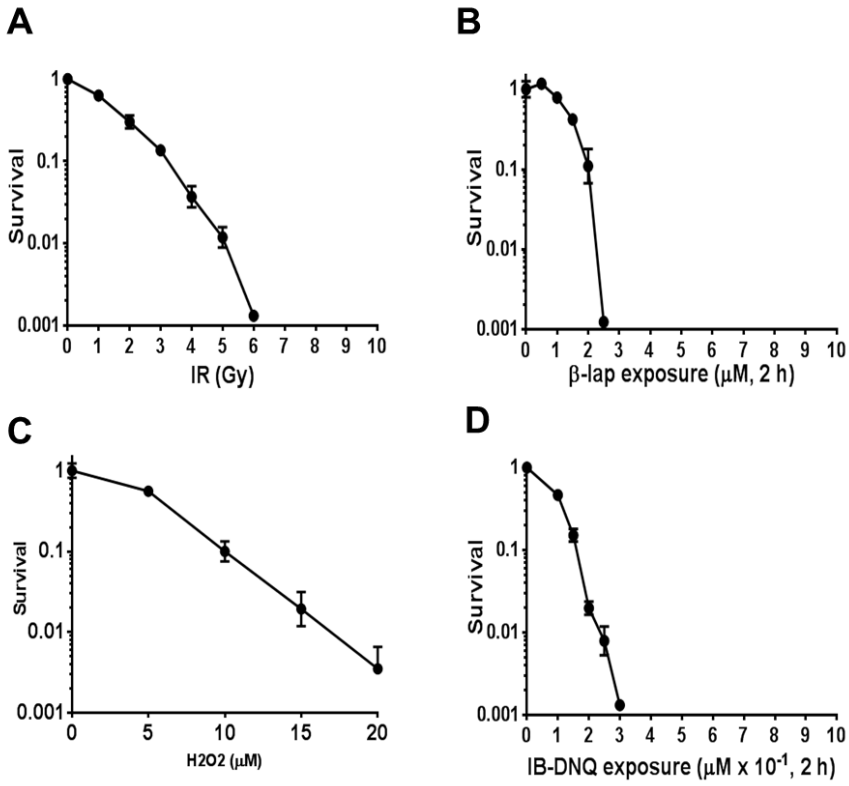

Figure 2.6. MCF7 cells show high sensitivity to IB-DNQ. Sensitivity to IR, β-lap, H_2O_2, and IB-DNQ was measured with clonogenic assay. Cells were seeded at 500 cells/dish on 60 mm tissue culture dishes and allowed 16 h to attach to the dishes. Drugs were added for 2 h at various concentrations. Colonies from control and treated conditions were allowed to grow in drug-free media for 14 days, the time required for a control colony to reach ~50 cells. Individual plates were stained with crystal violet, counted and plotted on a log scale.

It is clear that IB-DNQ is a very potent anticancer agent at low doses, but how exactly it achieves its cytotoxicity is yet unknown, thus we set to investigate the mechanism of action of IB-DNQ.

First, we focused on the futile redox cycling of IB-DNQ mediated by NQO1, specifically its back reaction in which the hydroquinone is converted to a semi-quinone and then back to IB-DNQ **(Fig 2.1B)**, extensive amount of ROS is generated, which induce severe DNA lesions. Utilizing the alkaline comet assay to study DNA damage after treatment with increasing doses of IB-DNQ, we found dramatic increase in comet tail length indicating high DNA damage. As a positive control, 2 mM of H_2O_2 for 15 min treatment was used **(Fig 2.7A)**.

Single-strand breaks induced by IB-DNQ can be converted to lethal DSBs during replication, therefore we measured γH2AX level, a marker for DSBs (Sharma, Singh, & Almasan, 2012), after 2 h IB-DNQ treatment in MCF7 cells. Phosphorylation of H2AX in different stages of the cell cycle was assayed by dual-parameter flow cytometry **(Fig 2.7C).** MCF7 cells were irradiated with 4 Gy as a positive control for DNA damage. As the dose of IB-DNQ increased, so did the amount of γH2AX, indicating increased DNA DSBs. Addition of DIC reversed the effect of IB-DNQ. It is interesting to note that DNA damage was induced in all cells regardless of the cell cycle phase, similar to the irradiation treatment.

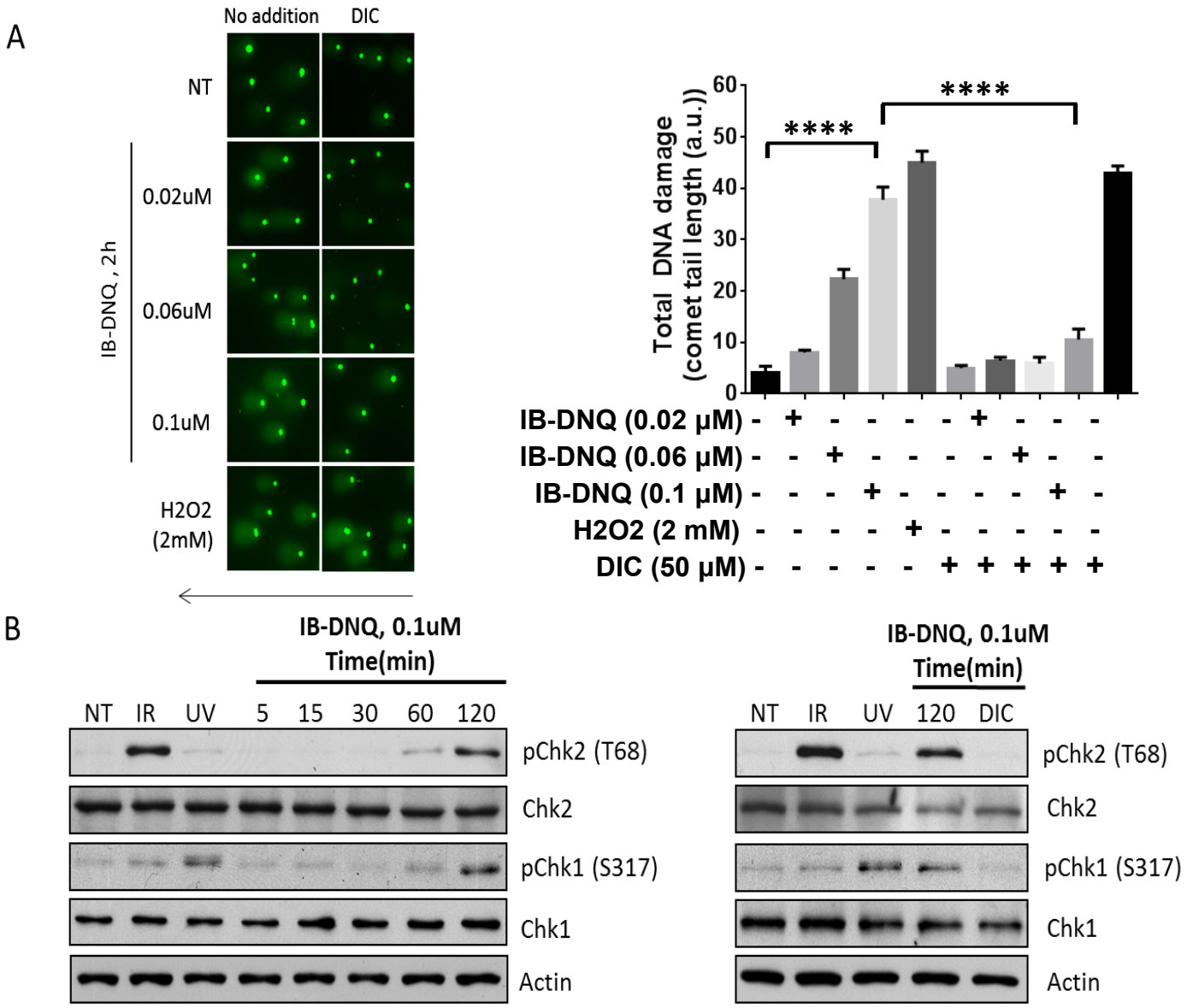
A
No addition
DIC
NT
0.02uM
0.06uM
0.1uM
H2O2
(2mM)
IB-DNQ , 2h
Total DNA damage
(comet tail length (a.u.))
****
****
IB-DNQ (0.02 μM)
IB-DNQ (0.06 μM)
IB-DNQ (0.1 μM)
H2O2 (2 mM)
DIC (50 μM)
B
IB-DNQ, 0.1uM
Time(min)
NT IR UV 5 15 30 60 120
pChk2 (T68)
Chk2
pChk1 (S317)
Chk1
Actin
IB-DNQ, 0.1uM
Time(min)
NT IR UV 120 DIC
pChk2 (T68)
Chk2
pChk1 (S317)
Chk1
Actin

C

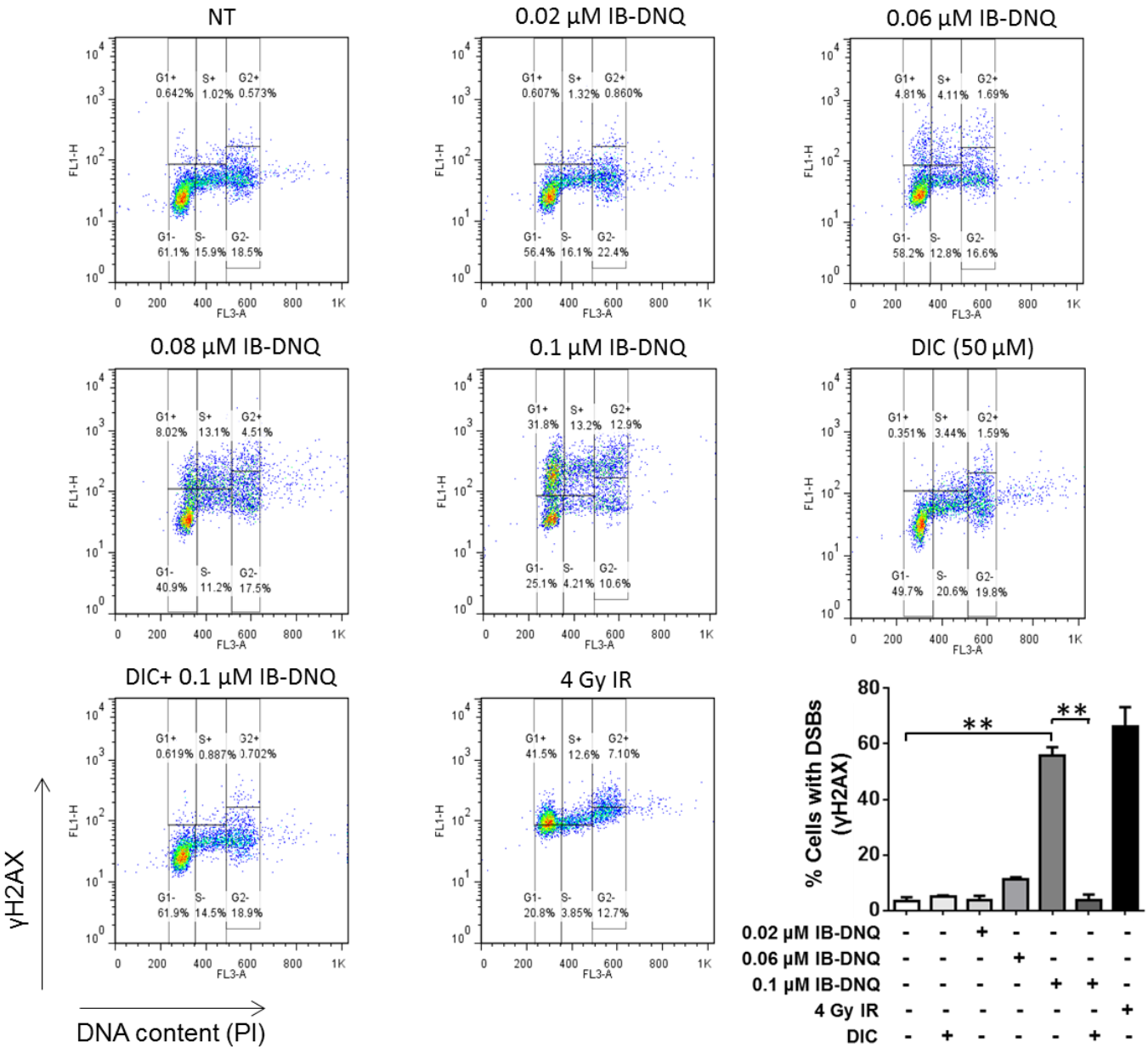
NT
G1+ 0.642% S+ 1.02% G2+ 0.573%
G1- 61.1% S- 15.9% G2- 18.5%
0.02 µM IB-DNQ
G1+ 0.607% S+ 1.32% G2+ 0.860%
G1- 56.4% S- 16.1% G2- 22.4%
0.06 µM IB-DNQ
G1+ 4.81% S+ 4.11% G2+ 1.69%
G1- 58.2% S- 12.8% G2- 16.6%
0.08 µM IB-DNQ
G1+ 8.02% S+ 13.1% G2+ 4.51%
G1- 40.9% S- 11.2% G2- 17.5%
0.1 µM IB-DNQ
G1+ 31.8% S+ 13.2% G2+ 12.9%
G1- 25.1% S- 4.21% G2- 10.6%
DIC (50 µM)
G1+ 0.351% S+ 3.44% G2+ 1.59%
G1- 49.7% S- 20.6% G2- 19.8%
DIC+ 0.1 µM IB-DNQ
G1+ 0.619% S+ 0.887% G2+ 0.702%
G1- 61.9% S- 14.5% G2- 18.9%
4 Gy IR
G1+ 41.5% S+ 12.6% G2+ 7.10%
G1- 20.8% S- 3.85% G2- 12.7%
FL1-H
FL3-A
γH2AX
DNA content (PI)
% Cells with DSBs (γH2AX)
**
**
0.02 µM IB-DNQ
0.06 µM IB-DNQ
0.1 µM IB-DNQ
4 Gy IR
DIC

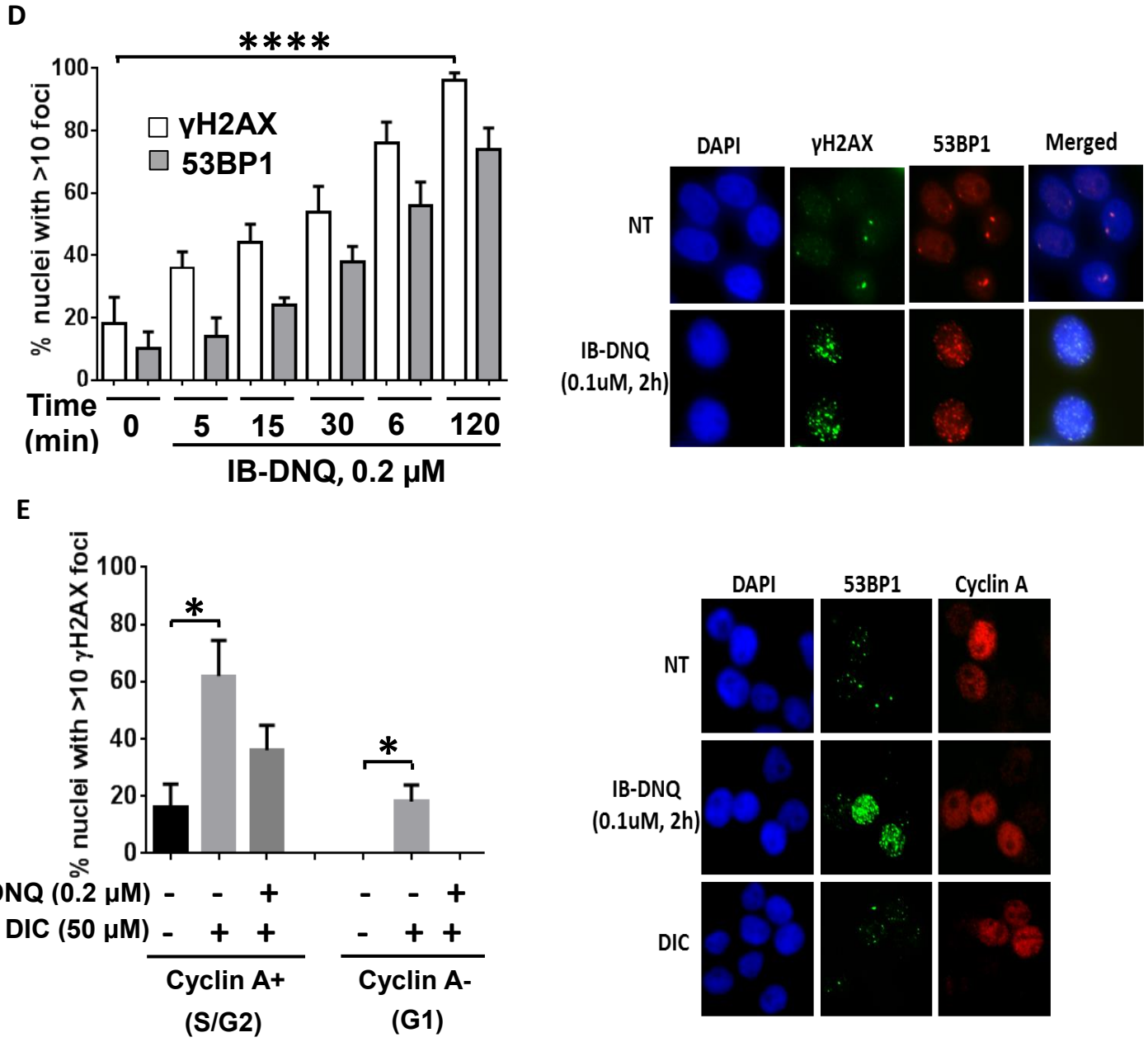

Figure 2.7. **IB-DNQ induces oxidative stress leading to DNA damage**. A. MCF7 cells were exposed to IB-DNQ with or without 50 μM DIC and assessed for DNA damage by the alkaline comet assay. Cells were exposed to 2 mM H_2O_2

for 15 min (in PBS) as positive control. Comet tail lengths were measured by Komet Version 6.0 software (a.u., arbitrary unit). Shown are representative images of experiments performed at least three times. Graphed are means ± SE from three experiments. B. Western blot analysis of phosphorylated Chk2 and Chk1 in MCF7 cells. Cells were γ-irradiated (5 Gy) as a positive control for DNA DSBs, and UV (2 mJ/cm^2) radiated as positive control for replication-associated damage. Cells were treated with 0.1 μM IB-DNQ and harvested at the indicated times. Addition of 50 μM DIC prevented phosphorylation of Chk2 and Chk1. C. Phosphorylation of H2AX in different stages of the cell cycle, in the presence of increasing doses of IB-DNQ or IB-DNQ + DIC (50 μM), was assayed by dual-parameter flow cytometry in MCF7 cells. Staining for DNA content (*x* axis) and H2AX phosphorylation (*y* axis) is shown. Percent cells with γH2AX signals are indicated for each cell cycle stage. Cells were γ-irradiated (4 Gy) as a positive control. D. IB-DNQ induced DSBs in all phases of the cell cycle. MCF7 cells were treated with 0.1 μM IB-DNQ for the indicated times, fixed and immunofluorescence stained with γH2AX and 53BP1 antibodies. Representative images and graphical representation of data are shown. The results shown are the average of three independent experiments and error bars indicate SEM. *$P \leq 0.05$ and ***$P \leq 0.001$. E. MCF7 cells were exposed to 0.1 μM IB-DNQ or IB-DNQ+DIC (50 μM) for 2 h, fixed and co-stained with γH2AX and Cyclin A antibodies to delineate cells in G1 (Cyclin A-negative) and cells in S/G2 phase (Cyclin A+positive). Graphical representation of Cyclin A+ vs. Cyclin A- populations is shown. $P < 0.001$

After treatment with β-lapachone, DNQ, and IB-DNQ, there is a whole spectrum of DNA lesions produced: SSB, base damage, AP sites, and DSBs (Bentle, Reinicke, Dong, Bey, & Boothman, 2007). We followed DSBs induction kinetics after IB-DNQ exposure. MCF7 cells were treated with IB-DNQ for a short time-course and co-stained for γH2AX and 53BP1, as surrogate markers for DSBs. Continuous induction of DSBs was observed over 120 min of IB-DNQ exposure, and at the end of the time-course almost all cells had DSBs. In addition, we analyzed whether cells in G1 versus cells in S/G2 phase of the cell cycle would respond with the same extent to the IB-DNQ-induced damage. We stained MCF7 cells with Cyclin A in order to delineate cells in G1 (Cyclin A-negative) versus cells in S/G2 phase (Cyclin A-positive). Both populations had the same response to IB-DNQ, there was a 3-fold higher induction of DSBs above background level, however, cells in S/G2 had the propensity for more breaks possibly due to replication stress and increased conversion of SSBs to DSBs **(Fig 2.7 E).**

Furthermore, we followed the formation of DSB after IB-DNQ treatment in MCF7 cells by examining the activation of Chk1 and Chk2, substrates for ATR and ATM, respectively (Tomimatsu et al., 2009). After 2 h exposure to IB-DNQ, we observed phosphorylation of Chk2 and Chk1, delineating DSBs occurring in G1(pChk2), as well as in S/G2 phase (pChk1) indicating that DNA DSBs were occurring in all phases of the cell cycle **(Fig 2.7 B)**. IR (5 Gy) and UV (2 mJ/cm^2)

were used as positive controls for pChk2 and pChk1, respectively. Addition of dicoumarol completely averted NQO1-mediated, IB-DNQ-induced DNA DSBs.

PARP1 hyperactivation and NAD+/ATP loss lead to NAD-Keresis. IB-DNQ participates in a NQO1-mediated futile cycle where oxygen is being consumed and ROS generated. We monitored the oxygen consumption rate (OCR) of MCF7 after treatment with 0.1 μM and 0.4 μM IB-DNQ using Seahorse analyses. The assay measured the OCR at base level and the OCR after drug addition, for a time period of three hours. Oligomycin, FCCP (uncoupling agent), and Rotenone were added as positive controls to ensure normal mitochondrial activity (Mito capacity test). As soon as IB-DNQ was added, cells responded with dramatic OCR increase that was dose dependent and reached a maximum peak in 15 min, after which OCR quickly descended. Dicoumarol blocked OCR suggesting that O_2 consumption was NQO1 mediated **(Fig. 2.8A)**.

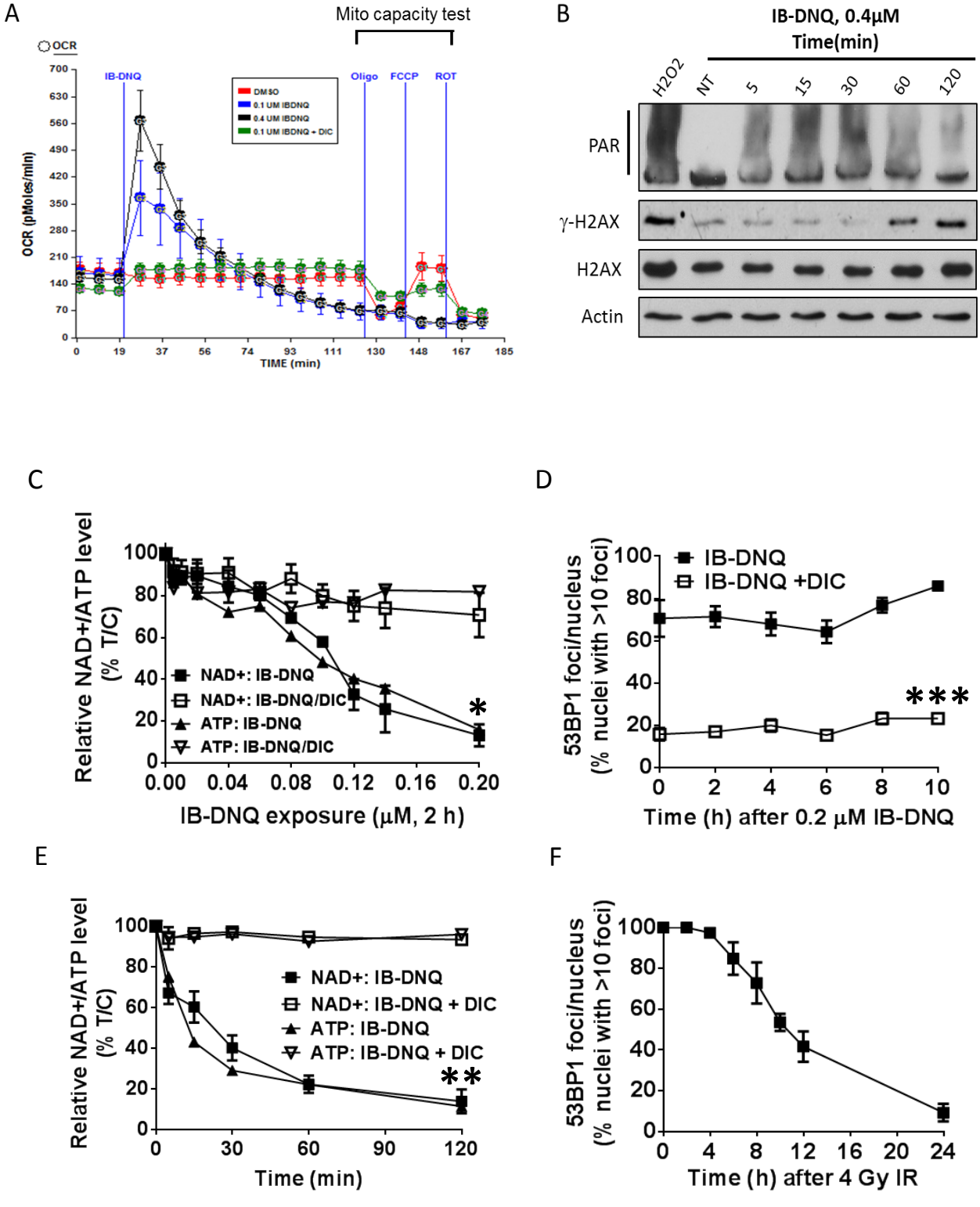
A
Mito capacity test
OCR
IB-DNQ
Oligo
FCCP
ROT
DMSO
0.1 UM IBDNQ
0.4 UM IBDNQ
0.1 UM IBDNQ + DIC
OCR (pMoles/min)
TIME (min)
B
IB-DNQ, 0.4µM
Time(min)
H2O2
NT
5
15
30
60
120
PAR
γ-H2AX
H2AX
Actin
C
Relative NAD+/ATP level (% T/C)
NAD+: IB-DNQ
NAD+: IB-DNQ/DIC
ATP: IB-DNQ
ATP: IB-DNQ/DIC
IB-DNQ exposure (µM, 2 h)
D
53BP1 foci/nucleus (% nuclei with >10 foci)
IB-DNQ
IB-DNQ +DIC
Time (h) after 0.2 µM IB-DNQ
E
Relative NAD+/ATP level (% T/C)
NAD+: IB-DNQ
NAD+: IB-DNQ + DIC
ATP: IB-DNQ
ATP: IB-DNQ + DIC
Time (min)
F
53BP1 foci/nucleus (% nuclei with >10 foci)
Time (h) after 4 Gy IR

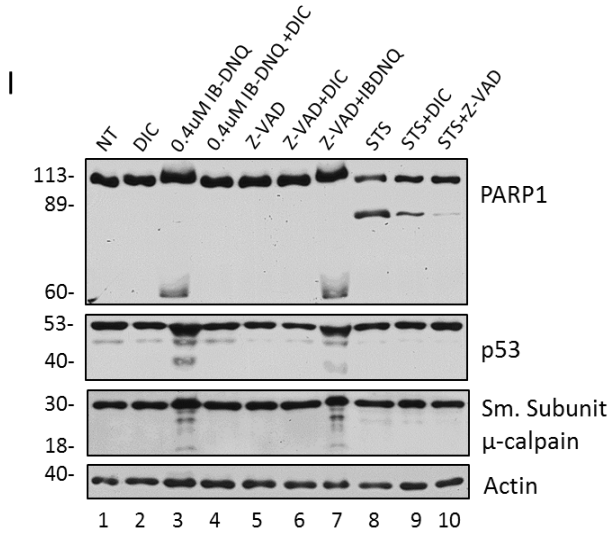

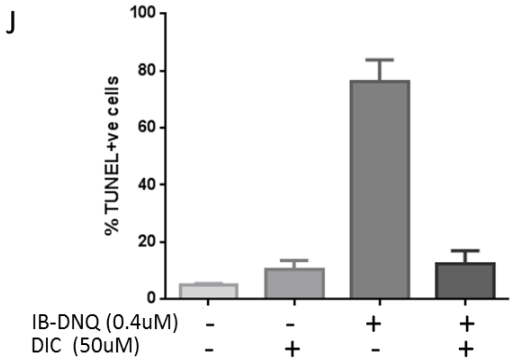

%	subG1	G1	S	G2/M
NT	0.11	0.17	0.15	0.11
DIC	0	0.47	0.31	0.52
IB-DNQ	10	15.8	21.9	18.8
IB-DNQ + DIC	2.35	0.11	0	0.28

Figure 2.8. **IB-DNQ induces PARP hyperactivation, NAD+/ATP loss, μ-calpain activation and cell death.** A. Seahorse analysis of MCF7 cells assessing oxygen consumption rate after addition of IB-DNQ (0.1 μM and 0.4 μM), or IB-DNA+DIC. B. Western blot confirmed PAR formation (PAR-PARP1, ~120 kDa) in MCF7 cells treated with or without 0.4 μM IB-DNQ at indicated times. Cells were treated with 2 mM H_2O_2 (15 min, in PBS) as a positive control for PAR formation. Also, induction of DSBs was assessed by γH2AX. Loading was controlled by H2AX, and actin levels. Dose and time-dependent NAD+ and ATP (C and E) loss in MCF7 cells after treatment with IB-DNQ. D and F. DNA repair is inhibited after IB-DNQ treatment, but not after IR. MCF7 cells were treated with 0.1 μM IB-DNQ and 4 Gy IR and percent cells with > 10 foci (53BP1) were quantified. I. Atypical PARP1 and p53 proteolysis was measured in MCF7 cells exposed to DIC (50 μM, 24 h), IB-DNQ (0.4 μM, for 4 h), IB-DNQ+DIC (0.4 μM, for 4 h), Z-VAD (75 μM, 24 h), IB-DNQ+ Z-VAD (24 h), Z-VAD+DIC (24 h), STS (1 μM, 16 h), STS+DIC (16 h), STS+ Z-VAD (16 h), under identical conditions. Shown are representative western blots of whole cell extract from experiment performed three times. J. IB-DNQ induced an increase in TUNEL+ cells. MCF7 cells were treated with 0.4 μM IB-DNQ for 4 h with or without DIC, and 24 h later cells were analyzed by TUNEL reaction and flow cytometry. IB-DNQ caused a significant increase in TUNEl+ cells, and DIC reverted that lethality. Cell death was observed in all phases of the cell cycle (table).

PARP1 catalyzes the covalent transfer of poly(ADP-ribose) (PAR) onto a variety of nuclear acceptor proteins, including PARP1 itself as part of its autoregulation. After transient exposure of MCF7 cells to low dose IB-DNQ we found extensive PARP1 hyperactivation as measured by (PAR) formation within 5 min of treatment with the drug **(Fig 2.8B).** PAR levels decreased significantly after 30 min, and were almost absent after 120 min **(Fig 2.8B).** This observation is most likely attributed to NAD+ loss, because PARP1 uses cellular NAD+ as a substrate for ADP-ribosylation of nuclear proteins (Luo & Kraus, 2012). Also, poly(ADP-ribose) glycohydrolase (PARG) liberates PAR both from acceptor proteins and PARP1, decreasing the overall PAR-PARP1 level over time. Simultaneously, DSBs formation was followed by probing for γH2AX, and their appearance was evident after 30 min with continuous induction seen even after 120 min, suggesting that PARP1 hyperactivation precedes DSBs formation.

NAD+ is an obligate substrate for PARP1, and it is synthetized by ATP, thus we speculated that the levels of these essential nucleotides would be depleted following the same time-course as PAR formation. We measured NAD+ and ATP levels after treatment with increasing doses of IB-DNQ for 2 h and found that at 0.2 μM IB-DNQ there was significant depletion of NAD+ and ATP **(Fig 2.8.C).** The kinetics of NAD+ and ATP depletion was assessed using 0.2 μM IB-DNQ, and we found that after 30 min more than 50 % of the cellular NAD+ and ATP pools were lost, and after 120 min there was essentially no NAD+ and ATP left in

the cell **(Fig 2.8.D).** As expected, NAD+/ATP depletion coincided exactly with PAR formation, suggesting that PARP1 hyperactivation led to NAD+/ATP loss.

Another consequence of PARP1 hyperactivation was inhibition of DNA repair evidenced by persistent DSBs **(Fig 2.8.G-H).** This was in contrast with 4 Gy IR-induced DSBs, which were completely repaired after 24 h. IB-DNQ treatment resulted in PARP1 hyperactivation depleting NAD+ and ATP levels and inactivating energy-dependent DNA repair processes.

Similar to β-lap and DNQ, IB-DNQ shifted the cell death decision from apoptosis to programmed necrosis as seen with atypical PARP1 and p53 proteolysis (60 kDa and 40 kDa, respectively) and μ-calpain small subunit cleavage (18 kDa) **(Fig 2.8.I)** due to μ-calpain activation (Tagliarino et al., 2003). In contrast, treatment of the same cells with staurosporine (STS) yielded classic apoptosis-related, 89 kDa PARP1 proteolysis **(Fig 2.8.I, lane 8)**. We noted that the pan-caspase inhibitor, z-VAD, had no effect on IB-DNQ–induced cell death or downstream PARP1/p53 atypical proteolysis **(Fig 2.8.I, lane 6),** but inhibited STS-related 89 kDa PARP1 cleavage **(Fig 2.8.I, lane 10)**. Furthermore, IB-DNQ-induced cell death was confirmed with dramatic increase in TUNEL+ cells (~ 80 %), and DIC reverted that lethality. TUNEL+ cells were observed in all phases of the cell cycle, confirming again that IB-DNQ acts in a cell-cycle independent manner **(Fig 2.8.J)**

Methoxyamine synergizes with IB-DNQ. The alkaline comet assay **(Fig 2.4B)** showed increased DNA damage after IB-DNQ treatment, and it has been reported that oxygen radical species lead to 8-oxoguanine DNA adducts (Lindahl & Wood, 1999). To determine the extent of 8-oxoguanine produced after IB-DNQ treatment we immunofluorescently stained MCF7 cells for 8-oxoguanine **(Fig 2.9A)**. We found an increase in 8-oxoguanine levels after 30 min exposure to 0.1 μM IB-DNQ. The main pathway that repairs these types of DNA damage is base excision repair (BER) (Scott, Rangaswamy, Wicker, & Izumi, 2014). We hypothesized that if we inhibited BER that would potentiate the cytotoxic effects of IB-DNQ. A specific inhibitor of BER is methoxyamine (MeOX), a chemical able to react with the aldehydic C1 atom of AP sites (L. Liu, Taverna, Whitacre, Chatterjee, & Gerson, 1999). MeOX-adducted AP sites are resistant to cleavage by AP endonuclease 1 (APE1). Methoxyamine on its own did not increase 8-oxoguanine levels above background **(Fig 2.9A)**. However, adding MeOX to IB-DNQ further sensitized cancer cells to the anti-cancer agent IB-DNQ **(Fig 2.9A-B)**.

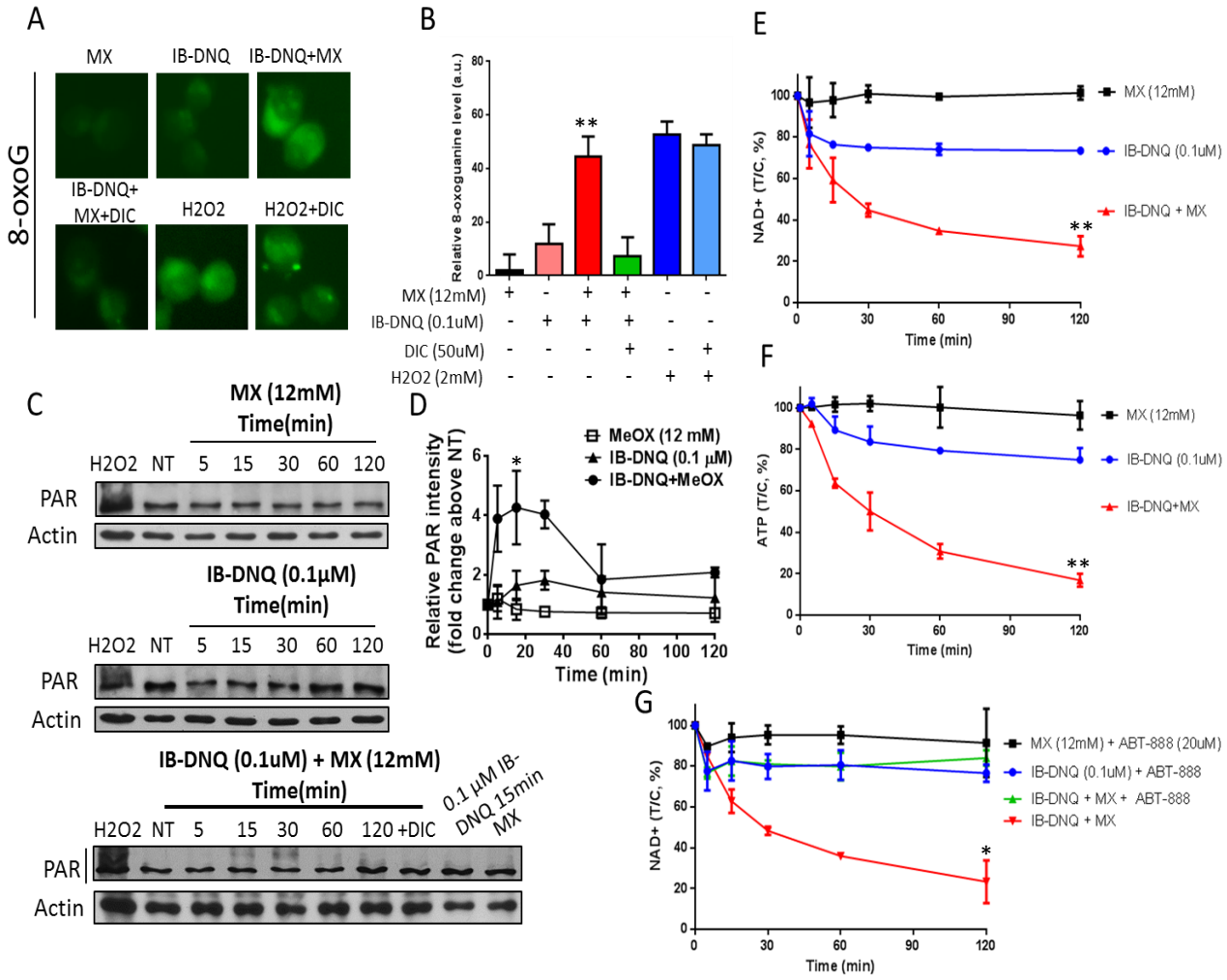

Figure 2.9. **Methoxyamine synergizes with IB-DNQ**. A. 8-oxoG levels in MCF7 were measured by immunofluorescence with antibody against 8-oxoG. B. Intensity of 8-oxoG signal was quantified with ImageJ and graphed. C. PAR formation western blot after short time-course exposure to 12 mM MeOX, 0.1 μM IB-DNQ, or 0.1 μM IB-DNQ + 12 mM MeOX. 2 mM H2O2 in PBS for 15 min served as positive control. D. Relative PAR level was measured using ImageJ and graphed. E-F. NAD+ and ATP depletion over short time-course after exposure to12 mM MeOX, 0.1 μM IB-DNQ, or 0.1 μM IB-DNQ + 12 mM MeOX. G. NAD+ levels in MCF7 were measured overtime after addition of PARP1 inhibitor ABT-888 (20 μM).

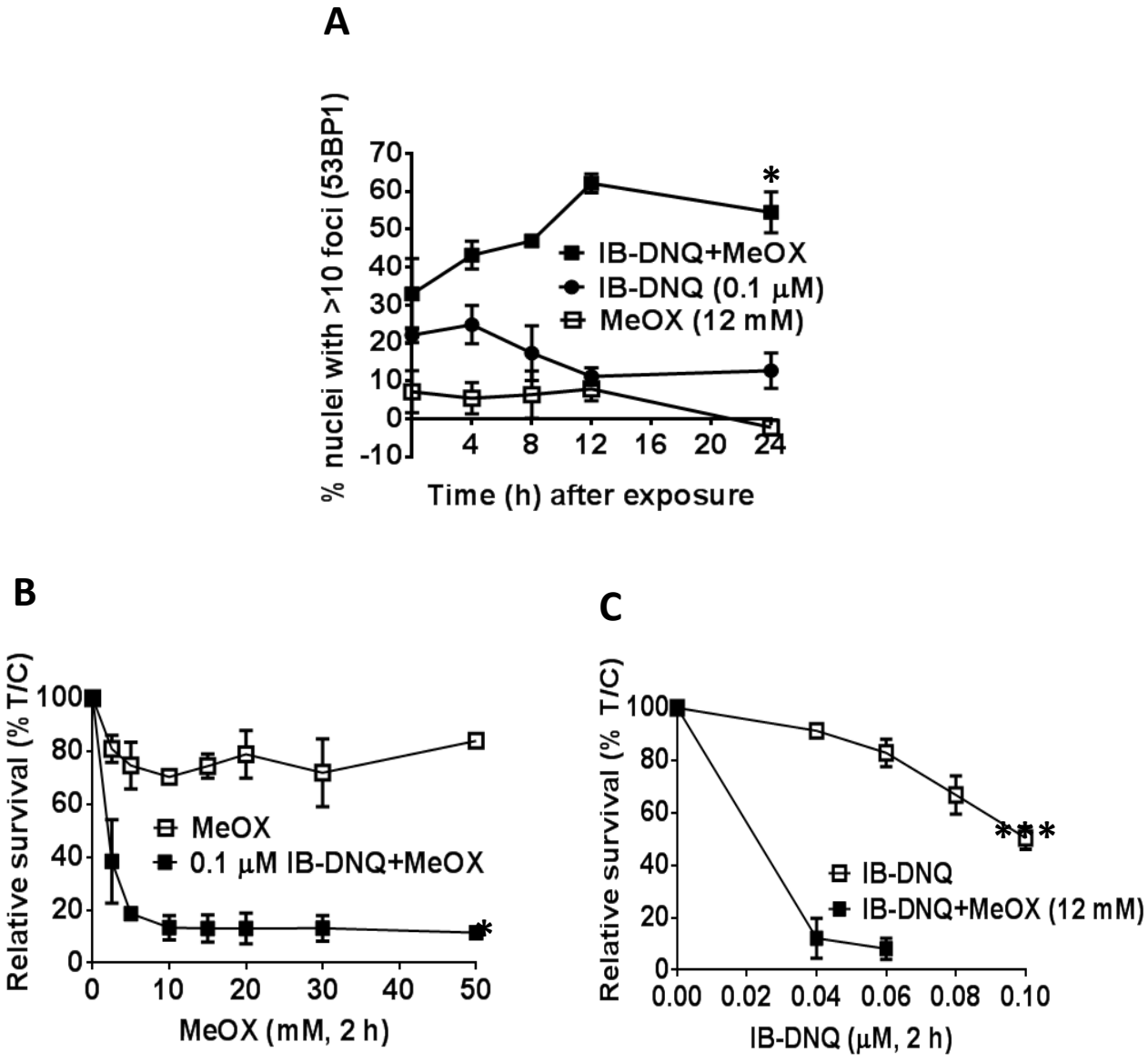

Figure 2.10. Methoxyamine synergizes with IB-DNQ. A. Percent of cells with ≥ 10 53BP1 foci per nucleus was quantified in MCF7 after exposure to 12 mM MeOX, or 0.1 uM IB-DNQ, or 0.1 uM IB-DNQ + 12 mM MeOX (background level was subtracted). B. Long-term relative survival of MCF7 cells after treatment with increasing doses of MeOX and constant dose of 0.1 μM IB-DNQ. C. Sensitivity of MCF7 cells to increasing doses of IB-DNQ, and IB-DNQ + 12 mM MeOX was measured with long-term relative survival assay. The results shown are the average of three independent experiments and error bars indicate SEM. *$p < 0.05$; **$p < 0.01$; ***$p < 0.001$.

APE1 cannot bind and process AP sites when MeOX is present (Wilson & Simeonov, 2010); on the other hand PARP1 can freely bind AP sites and becomes activated (Prasad et al., 2014). PARP1 hyperactivation was seen after 15 min of MeOX and IB-DNQ treatment **(Fig 2.9B).** Due to the rapid PARP1 hyperactivation and its demand for NAD+, as its substrate, the essential nucleotides NAD+ and ATP were depleted after MeOX and IB-DNQ treatment **(Fig 2.9C-D).** To further validate the crucial role of PARP1 hyperactivation, we followed NAD+ level in MCF7 over two-hour time period after addition of PARP1 inhibitor Veliparib (ABT-888) **(Fig. 2.9D).** The dramatic decrease of NAD+ and ATP levels observed after co-treatment with MeOX and IB-DNQ was prevented by addition of the PARP1 inhibitor ABT-888. NAD+ levels did not change significantly and the cells were spared from the energy catastrophe. This result proved once again that the cytotoxic effect that we observed with IB-DNQ is PARP1- dependent. Methoxyamine alone was not toxic to the cells as seen with colony formation assay **(Fig 2.11).**

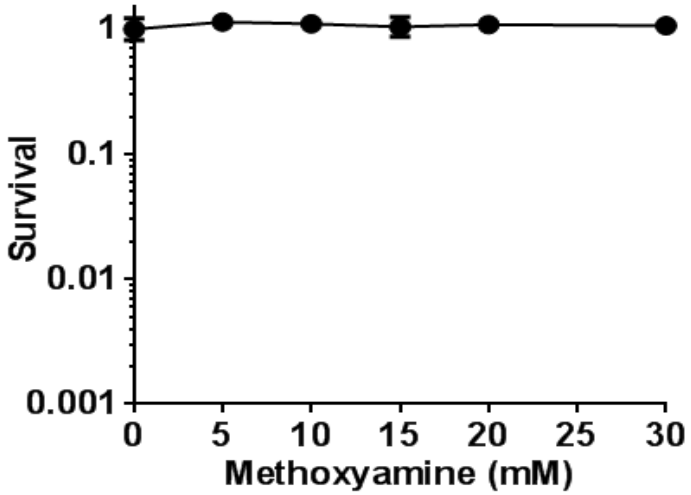

Figure 2.11. Methoxyamine alone is not cytotoxic. MCF7 cells were treated with increasing doses of MeOX for 2 h and then released in fresh media. Cells were allowed to grow until > 50 cells/colony. Colonies were fixed stained with methanol/crystal violet, and counted.

In addition to the dramatic energy loss, there were more DNA DSBs formed after the combination treatment, as quantified by 53BP1 foci, and these persistent lesions most likely contributed to the inevitable cell death **(Fig 2.10A).** Methoxymine potentiated IB-DNQ cytotoxicity and made breast cancer cells extremely sensitive to low dose IB-DNQ **(Fig 2.10B-C).** The high sensitivity to IB-DNQ was recapitulated in MDA-MB-231 triple negative breast cancer cell line **(Fig 2.12).**

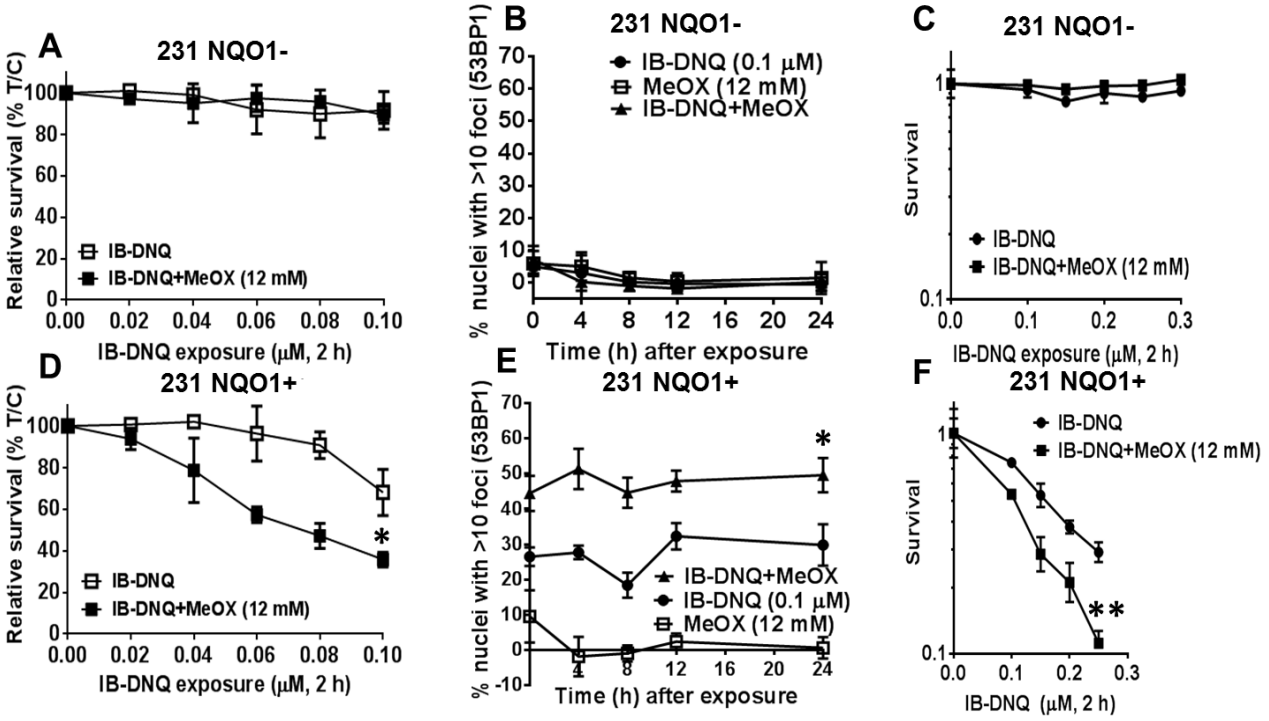

Figure 2.12. Methoxyamine synergizes with IB-DNQ in a NQO1-dependent manner. A-C. Treatment of MDA-MB 231 NQO1- with MeOX, IB-DNQ or combination of the two drugs showed no effect, both via DNA assay, immunofluorescence and colony survival. D-F. MDA-MB-231 NQO1+ had high sensitivity to the combination treatment as seen with DNA assay, immunofluorescence and colony survival.

Similar to MCF7, IB-DNQ caused PARP1 hyperactivation and energy failure in MDA-MB-231 cells **(Fig. 2.13).**

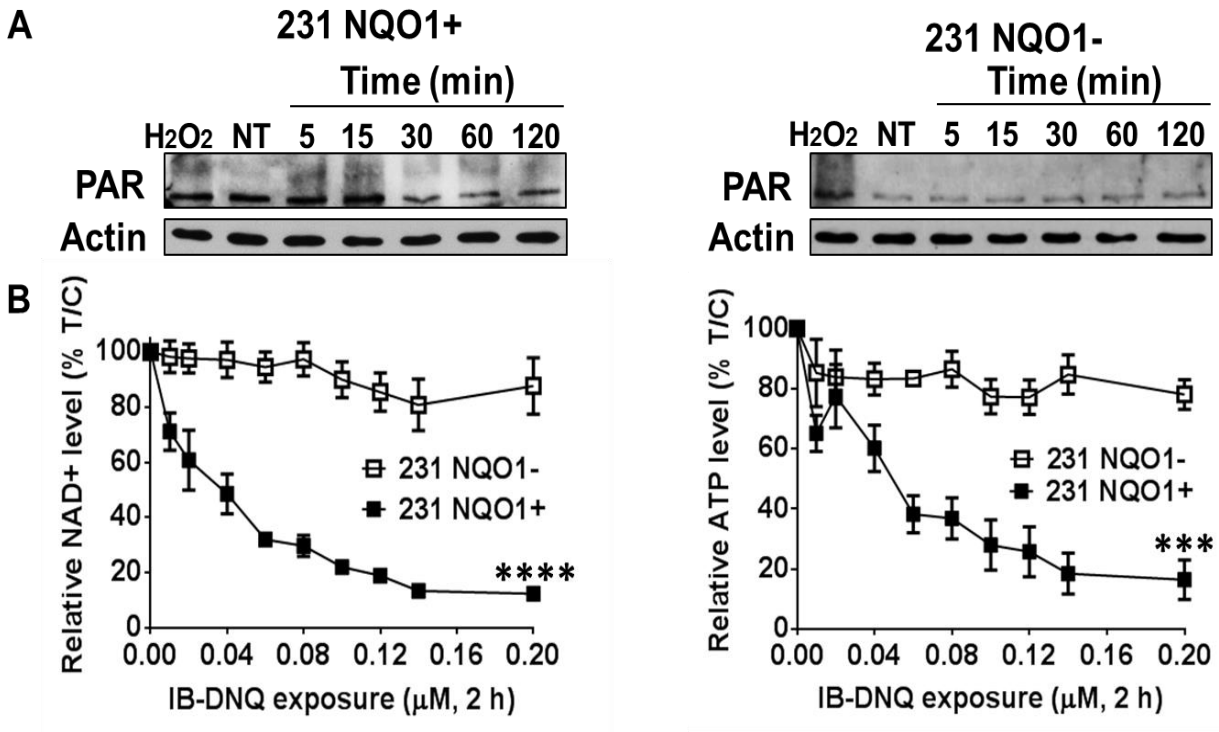

Figure 2.13. IB-DNQ induces PAR hyperactivation and NAD+/ATP depletion in a NQO1-dependent manner. A. Western blot analyses confirmed PAR formation (PAR-PARP1, ~120 kDa) after 15 min of 0.4 μM IB-DNQ treatment of MDA-MB-231 + NQO1 cells only; no PAR was detected in MDA-MB-231- NQO1. Cells were treated with 2 mM H2O2 (15 min, in PBS) as a positive control for PAR formation. Loading was controlled by actin levels. B. Dose-dependent NAD+ and ATP loss in MDA-MB-231 (+/- NQO1) cells after treatment with IB-DNQ for 2 h. The results shown are the average of three independent experiments and error bars indicate SEM. *$p < 0.05$; **$p < 0.01$; ***$p < 0.001$.

The same treatment conditions as with MCF7 and MDA-MB-231 were applied to IMR-90 cells (normal human embryonic fibroblasts) and no significant response to the agents was noted, proving again the tumor specificity of IB-DNQ **(Fig. 2.14).**

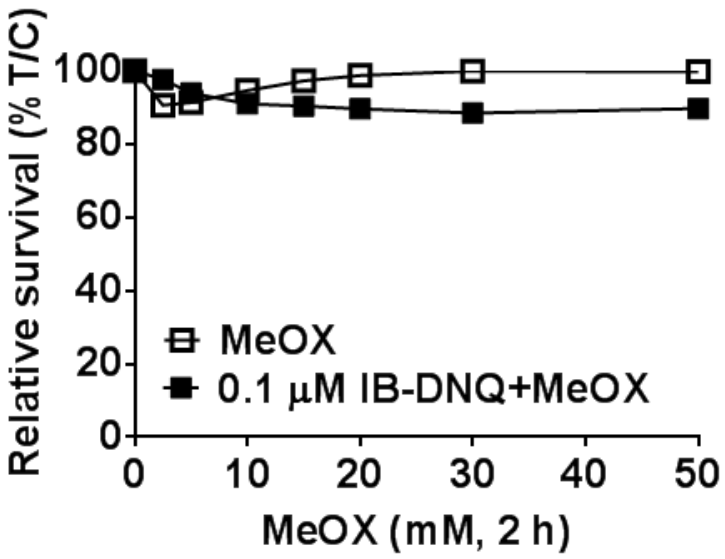

Figure 2.14. Normal human cells are not sensitive to IB-DNQ and MeOX. IMR-90 (lung fibroblasts) were treated with increasing doses of MeOX for 2 h, with or without 0.1 μM IB-DNQ, and long-term relative survival assay was performed.

DISCUSSION

Current cancer therapeutic strategies focus on proliferative differences between tumor and associated normal tissue. These approaches frequently result in minimal efficacy, and undesirable normal tissue toxicity. There is a growing need to exploit inducible or over-expressed genes that arise during oncogenic or cellular stress. The product of such genes could become an exploitable target allowing us to discriminate between the two populations, low level in normal cells vs. high level in tumor cells, and eliminate only the tumor cells. The NQO1 enzyme is a promising cancer target due to its up-regulation after carcinogenic cell stress, it is an early marker for carcinogenesis, and it is over-expressed in many solid cancers including 60 % of breast cancers (Bey et al., 2013). In the past decade, several tumor selective agents that require the NQO1 enzyme have been developed. We have focused our efforts on understanding and exploiting the most recently developed NQO1 bioactivatable drug, IB-DNQ. Treatment with IB-DNQ showed tumor-selective DNA damage and changes in metabolism that could be exploited to improve the efficacy of breast cancer therapy.

First, it was important to consider factors that could affect the therapeutic window for IB-DNQ. Cellular catalase could cause marked cytoprotection against NQO1 bioactivatable drugs making it an important resistance factor to consider. Normal tissues, which typically have higher catalase levels than cancer cells (Alexander, 1957), could be selectively protected from toxicity-causing NQO1

bioactivatable drugs. Alternatively, cancer cells overexpressing catalase would require higher doses of IB-DNQ to avoid sublethal drug treatments. Thus, the ratio of NQO1:catalase expression in tumor versus normal tissue is a major determinant of tumor selectivity for IB-DNQ. NQO1 expression was significantly elevated in breast cancers and triple negative breast cancers compared to normal breast tissue **(Fig. 2.1B).** A recent paper by Li et al., demonstrated that β-lapachone –mediated cell death required ~ 90 enzymatic units of NQO1 activity, and patients with elevated NQO1 level could potentially benefit from the antitumor activity of such agents (L. S. Li et al., 2011).

Even though β-lapachone has proven to be a promising antitumor agent, it has a modest potency in vitro (IC_{50}= 2-10 μM), with limited aqueous solubility that complicates formulation and delivery (Blanco et al., 2010). Although nanoparticles strategies for β-lap delivery solved formulation issues, resulting in dramatic antitumor efficacy, there is a clear need for higher potency drugs with reduced side-effects. Recently, Parkinson et al. had identified a significant number of DNQ derivatives that are both outstanding NQO1 substrates and selective anticancer agents, with IB-DNQ showing the most optimal parameters.

A lethal dose of 0.4 μM IB-DNQ and a minimum exposure time of two hours ensured lethality in vitro. Any dose below that was sub-lethal probably due to endogenous mechanisms, such as catalase, which prevented the induction of damage. The addition of DIC spared the cells proving that indeed NQO1 is

required for IB-DNQ-induced lethality. At low doses, IB-DNQ elicited elevated DNA damage in the form of SSB, base damage, AP sites, and DSB in a dose dependent manner. Dicoumarol reversed this effect and did not cause significant DNA damage above background level. Normally, SSBs would be converted to DSBs, especially during replication (Speit, Hochsattel, & Vogel, 1984). Indeed, the induction of DNA DSBs was observed after transient exposure to IB-DNQ as assayed by Chk1 and Chk2 phosphorylation, substrates for ATM and ATR respectively. After addition of DIC, no DSBs were detected. IB-DNQ induced massive DNA damage, comparable to 4 Gy of radiation, regardless of the cell cycle phase **(Fig 2.5C).**

One of the first proteins to respond to a DNA lesion is PARP1. PARP1 uses NAD+ as a substrate to carry out PAR posttranslational modification of proteins, including itself, where PAR-PARP1 is inactive (Berger, 1985). Due to the massive DNA damage induced by IB-DNQ PARP1 becomes hyperactivated within 5 min of exposure **(Fig 2.6B).** After 30 min PARP1 activity significantly decreased possibly due to PARG activity, and the loss of essential NAD+ and ATP. It is now clear that in the presence of low levels of DNA damage PARP1 activation may promote cell survival; in the existence of irreparable DNA damage the cell commits to programmed apoptosis, while during severe DNA damage, excessive activation of PARP1 causes caspase-independent cell death (Han, Zhong, & Zhang, 2011). Examples of such severe DNA damage that leads to

PARP1 hyperactivation are during ischemia-reperfusion, myocardial infarction and ROS-induced injury (Eliasson et al., 1997). Since PARP1 responds to DNA damage in a dose-dependent manner, it can be hyperactivated, leading to cellular depletion of NAD+ and ATP, exactly what we observed after treatment of MCF7 breast cancer cells with increasing doses of IB-DNQ **(Fig 2.8C).** The end result for the cell is a rapid and dramatic energy loss leading to cell death, as confirmed here by the long-term survival and TUNEL assays **(Fig 2.8J).** It is known that caspase pathways are commonly abrogated or altered in breast cancer, and strategies for treating cycling, as well as dormant cancer cells that exploit caspase-independent cell death pathways (programmed necrosis) are needed. No drugs mechanistically act to induce PARP1-mediated programmed necrosis in a tumor specific manner and at clinically relevant doses. Current breast cancer therapeutic strategies attack proliferative differences between tumor and associated normal breast tissue. Unfortunately, these approaches show minimal efficacy, normal tissue toxicity, drug resistance, and increased metastatic potential. IB-DNQ-induced PARP1 hyperactivation led to caspase-independent cell death. The typical 89-kDa PARP1 cleavage fragment seen in caspase-mediated apoptosis was not observed; instead a 60-kDa atypical PARP1 cleavage mediated by μ-calpain was present after treatment with IB-DNQ. Furthermore, unlike caspase-mediated apoptosis, cell death caused by IB-DNQ was not prevented by the pancaspase inhibitor, z-VAD. IB-DNQ-stimulated, μ-calpain-

mediated atypical PARP1 cleavage was blocked by co-treatment with DIC. Therefore, agents that can hyperactivate PARP1 have multitude of benefits including the ability to: (1) kill independently of p53 and caspases; (2) augment anticancer agents that damage DNA, including agents that were not efficacious due to the formation of SSBs instead of the more lethal DSBs; and (3) kill cancer cells that have up-regulated levels of pro-survival factors that protect against caspase-mediated processes. To the best of our knowledge IB-DNQ is the only agent that addresses all these points with the added benefit of low dose and short exposure time.

A major concern with bioactivatable drugs such as β-lapachone and DNQ is the side effect of methemoglobinemia (Cortazzo & Lichtman, 2014). Usually, methemoglobinemia occurs when hemoglobin undergoes oxidation and an electron is removed from one of the iron atoms of the heme groups. This change in oxidation state converts the ferrous or Fe^{2+} iron to the ferric or Fe^{3+} state (Cortazzo & Lichtman, 2014). Under such conditions the hemoglobin can carry oxygen, but it is unable to release it efficiently to the tissues. An effective way to minimize, or even eliminate this side effect is to reduce the dose of the exogenous agent that causes it. After identifying IB-DNQ's mechanism of action, its NQO1 and PARP1 dependence, and the base DNA lesions it induces due to high H_2O_2 levels, we predicted that IB-DNQ would synergize with BER inhibitors, such as methoxyamine. By adding MeOX to IB-DNQ we could significantly reduce its

dose, and still preserve its anti-tumor properties. A key benefit that allowed all this to take place is that MeOX-adducted AP sites do not allow APE1 to bind and cleave the DNA, but they do not halt PARP1 binding. Unrepaired base damage activates PARP1, and in this scenario we speculate that it is the number of PARP1 proteins being simultaneously engaged at numerous AP sites that causes its hyperactivation. PARP1 functions as a cellular "rheostat" that produces different responses for different types, durations and strength of stimuli (Luo & Kraus, 2012). IB-DNQ and MeOX treatment caused severe and sustained stress that led to hyperactivation of PARP1, and irreversible cell death. This therapeutic strategy could be applied not only to breast cancers, but to any solid tumor that overexpresses NQO1 and has functional PARP1.

We found that the severe NAD+/ATP depletion caused by PARP1 hyperactivation led to metabolic catastrophe and cell death that is independent of PAR moiety accumulation. We refer to this mode of cell death as NAD-Keresis, named after the death spirits in Greek mythology called Keres who pull the life out of those who die violently in war. This subtype of programmed necrosis was also observed after β-lapachone treatment (Moore et al., 2015), and it is PAR independent unlike the mitochondria-linked cell death called parthanatos (David, Andrabi, Dawson, & Dawson, 2009). Our findings offer preclinical proof-of-concept for IB-DNQ as a potent chemotherapeutic agent for the treatment of breast cancers, especially in combination with MeOX.

Chapter III

Potential role of BRCA1 in modulating the sensitivity of breast cancers to IB-DNQ

INTRODUCTION

About 1 in 8 (12 %) women in the United States will develop invasive breast cancer during their lifetime (Jemal, Siegel, Xu, & Ward, 2010). Among all breast cancers, those with familial BRCA1/BRCA2 mutations have benefited the most from the development of PARP1 inhibitors (Farmer et al., 2005). PARP1 is an abundant nuclear enzyme that synthesizes poly(ADP-ribose) polymer when activated by DNA nicks, base damage, SSBs, DSBs or AP sites. Activation of PARP1 has important effects on a variety of cellular processes, including base excision repair (BER), transcription, and cellular bioenergetics (Luo & Kraus, 2012). The observation that PARP inhibition is particularly lethal to cells deficient in HR, such as BRCA1/2-null cancers, has generated additional excitement in the cancer chemotherapy community (Farmer et al., 2005). Despite the initial responses, the development of resistance to PARP1 inhibitors limits their clinical efficacy (Fojo & Bates, 2013). Currently, BRCA1-deficient breast cancer treatment is focusing on inhibiting PARP1, with no studies exploring the exact opposite, PARP1 hyperactivation, which could potentially synergize with BRCA1/2 deficiency.

After describing the mechanism of action of the new anticancer agent, IB-DNQ (Chapter II), we explored the synergy between IB-DNQ and BRCA1-deficient breast cancer cells. The elevated long-lived ROS, produced after treatment with IB-DNQ, caused massive DNA base lesions and SSBs. These

SSBs caused PARP1 hyperactivation, inhibiting its essential base and SSB repair functions. Additionally, PARP1 hyperactivation caused dramatic NAD^+/ATP loss due to ADP ribosylation, resulting in extensive energy depletion, μ-calpain activation and subsequent programmed necrosis, NAD-Keresis.

We have already seen induction of toxic DSBs after 120 min of IB-DNQ exposure **(Fig 2.7E).** Furthermore, after staining MCF7 cells with cyclin A, to delineate cells in G1 vs S/G2 phases, we observed that both populations had the same response to IB-DNQ (3-fold increase compared to background). However, cells in S/G2 had the propensity for more breaks possibly due to replication stress and the increased conversion of SSBs to DSBs. Cells in S/G2 phase repair DSBs primarily through HR, and we investigated if HR is activated after IB-DNQ treatment. Indeed, MCF7 cells exposed to IB-DNQ for 2 h had increased number of Rad51 foci, a marker for HR, which was similar to baseline level after DIC addition **(Fig 2.7E).** Due to HR activation after IB-DNQ treatment, we speculated that BRCA1-deficient breast cancer cells would be more sensitive to IB-DNQ treatment possibly due to the overwhelming, unrepaired breaks. In fact, we wanted to investigate whether IB-DNQ was superior to PARP1 inhibitors in targeting BRCA1-deficient cancers. IB-DNQ could be synthetic lethal to BRCA1-deficient cancers, and our findings could offer preclinical 'proof-of-concept' for IB-DNQ as a potent chemotherapeutic agent for the treatment of breast cancers,

especially those deficient in BRCA1. Thus, patients with BRCA1/2 loss and increased NQO1 activity could benefit greatly from treatment with IB-DNQ. In this study we assess the role of BRCA1 in modulating the sensitivity of breast cancers to IB-DNQ.

MATERIALS AND METHODS

Chemicals, reagents, and antibodies. Isobutyl-deoxynyboquinone was synthesized as described (Parkinson et al., 2013). Hoechst 33258, Hydrogen peroxide (H_2O_2), Propidium iodide, and Dicoumarol were purchased from Sigma-Aldrich. All quinones were dissolved in dimethyl sulfoxide (DMSO). Human NQO1 antibody was provided by Dr. David Ross (University of Colorado Health Science Center, Denver, CO) and used at a 1:1000 dilution overnight, 4◦C. α-Actin was monitored for loading. PARP1 inhibitor, ABT-888 was purchased from Selleckchem. Antibodies for Chk1, phospho-Chk1 (S317), Chk2 (Bethyl), phospho-Chk2 (T68) (Cell Signaling), Actin (Sigma), Rad51 (H-92), 53BP1 (H-300; Santa Cruz), Cyclin A (6E6), BRCA1, γH2AX, were used as described (Tomimatsu et al., 2014).

Cell Lines and Culture. Cell lines were obtained from either American Type Culture Collection or the Boothman lab (University of Texas Southwestern Medical Center). The HCC1937 breast cancer cell line was a generous gift from Dr. Gail Tomlinson (University of Texas Southwestern Medical Center), and

HCC1937 pcBRCA1 cells were developed in Dr. Weixin Wang' laboratory (Wiltshire et al., 2007) with a protocol identical to that used to reconstitute wild-type BRCA1 in the ovarian cancer cell line UWB1.289 . The vector pcDNA3-BRCA1 plasmid was generously provided by Dr. David Livingston (Dana-Farber Cancer Institute, Boston, MA) to Dr. Weixin Wang and was transfected into HCC1937 using 5 μg Fugene 6 (Roche, Indianapolis, IN) per 100-mm plate of cells, according to the manufacturer's recommendations. Stable cell lines were established by selection of positive clones that grew in media containing G418. All cancer cells were grown in RPMI 1640 medium, or Dulbecco's minimal essential medium (DMEM) with 10 % fetal bovine serum (FBS). Cells were cultured at 37 °C in a 5 % CO_2-95 % air humidified atmosphere. MCF7 cell line with stable shRNA-mediated knockdown of BRCA1 was generated by transfection with a pGIPZ vector (5'-TATGTGGTCACACTTTGTG-3'; No.: V2LHS_254648, Thermo Scientific) using Lipofectamine2000 (Invitrogen) followed by selection and continued maintenance in puromycin (1 μg/ml^{-1}, Invitrogen). Control cells were generated by transfection with a pGIPZ vector expressing scrambled shRNA (No.: RHS4346, Thermo Scientific).

Survival Assays. Relative survival assays were assessed as described (Dong Y, 2010) and correlated well with colony forming assays (Wuerzberger Sm, 1998). Briefly, cells were seeded at 10 000 cells/well in 48-well plates and allowed to attach overnight. Cells were then treated with various concentrations

of IB-DNQ in the presence or absence of 50 μM DIC for 2 h with at least six technical replicates. Drug-free medium was then added and cells were allowed to grow for 7 days until control cells reached ~100 % confluence. Viability of adherent cells was then assessed using Hoechst dye. Plates were then read for luminescence on Perkin Elmer Devices. Percent death was calculated by subtracting background from all wells and setting 100 % survival to DMSO-treated controls. Results were reported as means ± standard error (SE) from at least 3 independent experiments done in sextuplicate.

Western Blot Analyses. Cells were grown to 70-80 % confluence and were trypsinized and harvested. After centrifugation and washing, the cells were lysed with RIPA lysis buffer containing 1 % protease inhibitor cocktail set III (Calbiochem). Protein concentration was determined by the Pierce BCA Assay (Thermo Scientific, Rockford, IL) and whole cell lysate (20-40 μg) was resolved by 8-10 % SDS-PAGE gel electrophoresis at 120 V for 90 min after which proteins were transferred onto PVDF membranes (25 V for 1 h) and blocked in 5 % milk for 1 h. The membranes were blotted for molecules of interest with the corresponding antibodies listed above in Chemicals, reagents, and antibodies. The following secondary antibodies were used: horseradish peroxidase-conjugated secondary antibodies (Bio-Rad). The membranes were stripped in acidic methanol and re-probed as necessary.

Flowcytometry. HCC1937 cells were analyzed by BD CYTOMICS FC500 Flow Cytometer (Becton, Dickinson and Company) as described in (Tomimatsu et al., 2009). For quantification of H2AX phosphorylation and cell cycle stage, cells were stained for both DNA content (propydium iodine, PI, red) and phosphorylated H2AX using anti-γH2AX antibody (green).

TUNEL Assays. HCC1937 cells were seeded at $1x10^6$ cells per 10 cm^2 dish. Log-phase cells were then treated for 4 h with 0.4 μM IB-DNQ, as described above. Medium was collected from experimental as well as control conditions after 24 h. Attached along with floating cells were monitored for apoptosis using TUNEL 3'-biotinylated DNA end labeling via the APO-DIRECT kit (BD Pharmigen). Apoptotic cells were analyzed and quantified using a BD LSRFortessa (BD Biosciences) flow cytometer equipped with BD FACSDiva™ acquisition software for processing.

Immunofluorescence. Cells (70,000/well) were seeded onto chamber slides (BD Falcon) and next day were treated with IB-DNQ or IB-DNQ + DIC as indicated. Cells were fixed in 4 % PFA for 20 min on ice, permeabilized with 0.5 % Triton X-100, blocked in 5 % BSA/PBS, and primary antibodies were added overnight at 4 C. For γH2AX and Rad51 foci, cells were co-immunostained with Cyclin A antibody, as described (Tomimatsu et al., 2009). The average number of Rad51 foci for Cyclin A-positive (S/G2) nuclei was determined after scoring 50

nuclei. Images were captured using a Leica DH5500B fluorescence microscope (40 X objective lens) coupled to a Leica DFC340 FX camera using Leica Application Suite v3 acquisition software.

ROS (H_2O_2) assays. HCC1937 cells were treated with increasing doses of IB-DNQ for 2 h and H_2O_2 level was measured. Briefly, H_2O_2 substrate is employed that reacts directly with H_2O_2 to generate a luciferin precursor. Upon addition of ROS-Glo detection reagent containg Ultra-Glo recombinant luciferase and d-cysteine, the precursor is converted to luciferin by the d-cysteine, and the produced luciferin reacts with Ultra-Glo recombinant luciferase to generate a luminescent signal that is proportional to H_2O_2 concentration.

NQO1 enzyme assays. NQO1 enzyme levels were determined from triplicate whole cell extract using NADH (200 μM) as an immediate electron donor and menadione (10 μM) as an intermediate electron acceptor as described (Pink et al., 2000). Enzyme units (U) of NQO1 were calculated as nmol of cytochrome c reduced/min/μg of protein, based on initial rate of change in absorbance at 550 nm.

RESULTS

Breast cancers deficient in BRCA1 are extremely sensitive to IB-DNQ. Due to HR activation after IB-DNQ treatment **(Fig 3.1)**, we wanted to investigate whether breast cancers compromised in HR repair, such as BRCA1-deficient breast cancers, would respond better to the anticancer agent IB-DNQ.

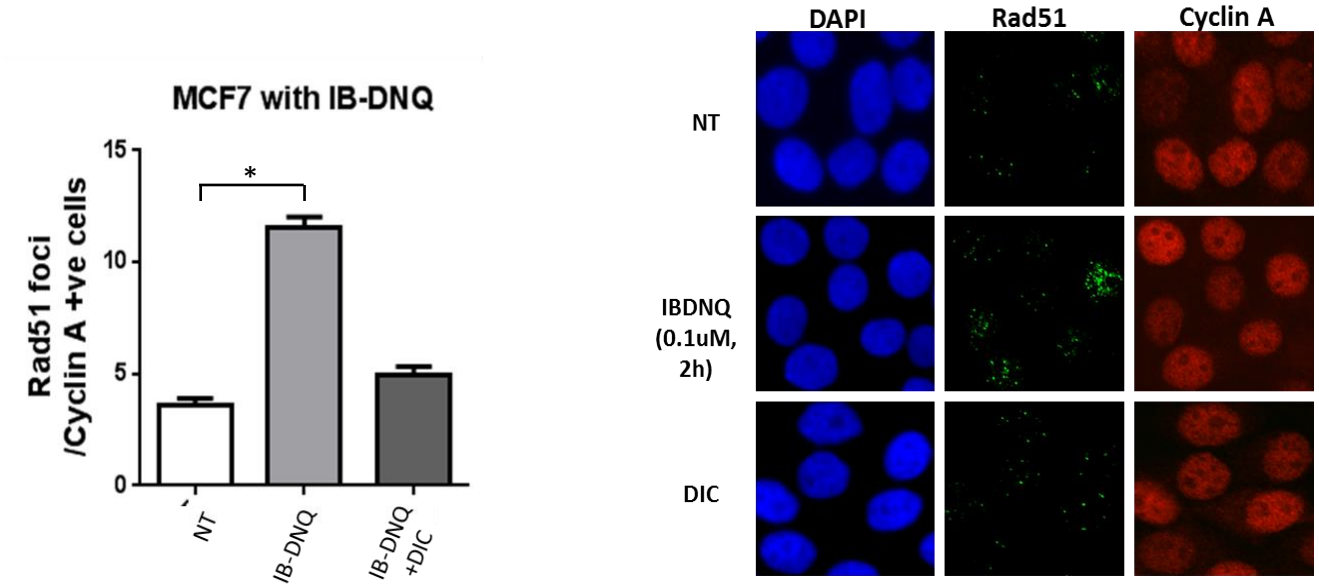

Figure 3.1. IB-DNQ treatment activates HR. MCF7 cells were treated with 0.1 µM IB-DNQ or IB-DNQ+DIC and fixed after 2 h. Immunofluorescence co-staining was carried out using Rad51 and Cyclin A antibodies. The average number of Rad51 foci for Cyclin A positive (S/G2) nuclei was determined after scoring at least 50 nuclei.

To address this question, we used HCC1937 breast cancer cells that are deficient in BRCA1 due to mutation (5381 C->T) in BRCT domain. HCC1937 cells were complemented with a wild type BRCA1, and both cells (BRCA1+ and BRCA1-) had equal level of NQO1 as determined by western blotting **(Fig 3.2A).** Long-term survival studies with HCC1937 cells after exposure to IB-DNQ showed that BRCA1-deficient cells were extremely sensitive to the compound. Treating the cells with even lower doses of IB-DNQ showed the same trend. Cells lacking BRCA1 were very sensitive to IB-DNQ compared to BRCA1-proficient cells. Dicoumarol protected the cells from the cytotoxic IB-DNQ to a reasonable extent, and the incomplete protection is probably due to the one-electron oxydoreductases B5R and P450R metabolizing IB-DNQ **(Fig 3.2A-B).**

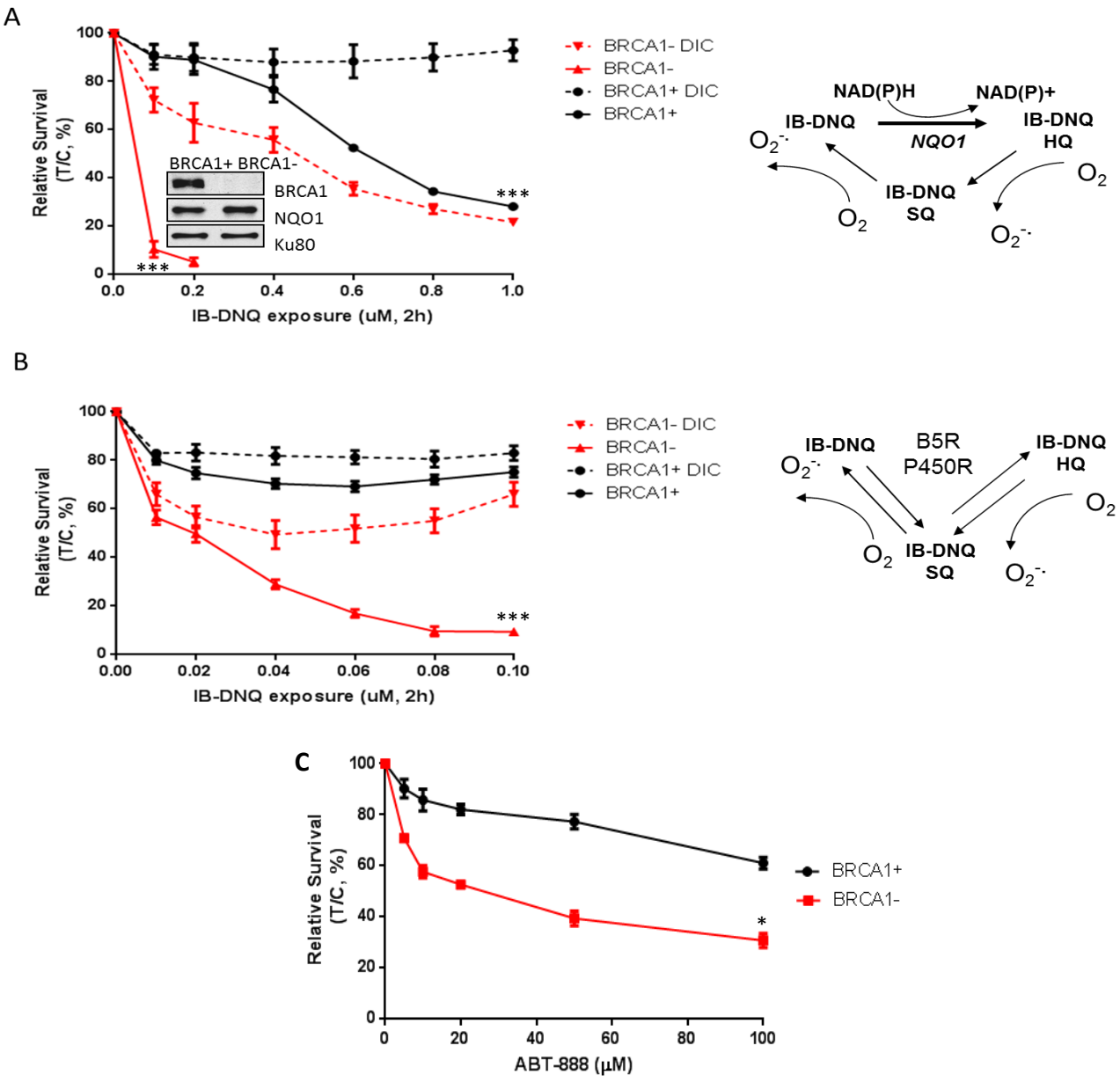

Figure 3.2. BRCA1-deficient breast cancers are extremely sensitive to IB-DNQ. A. Western blot showing BRCA1 and NQO1 status in HCC1937 breast cancer cells. A-B. Long-term survival of HCC1937 (BRCA1+ vs. BRCA1-) cells treated with increasing doses of IB-DNQ for 2 h, with or without 50 μM DIC, in B the doses of IB-DNQ are 10-fold lower than those in A. C. Long-term survival of HCC1937 (BRCA1+ vs. BRCA1-) treated with increasing doses of PARP1 inhibitor ABT-888 for the whole duration of the assay (7 days).

The high sensitivity of BRCA1-deficient cells to IB-DNQ was also observed with increased TUNEL+ cells in a dose-dependent manner **(Fig 3.3).**

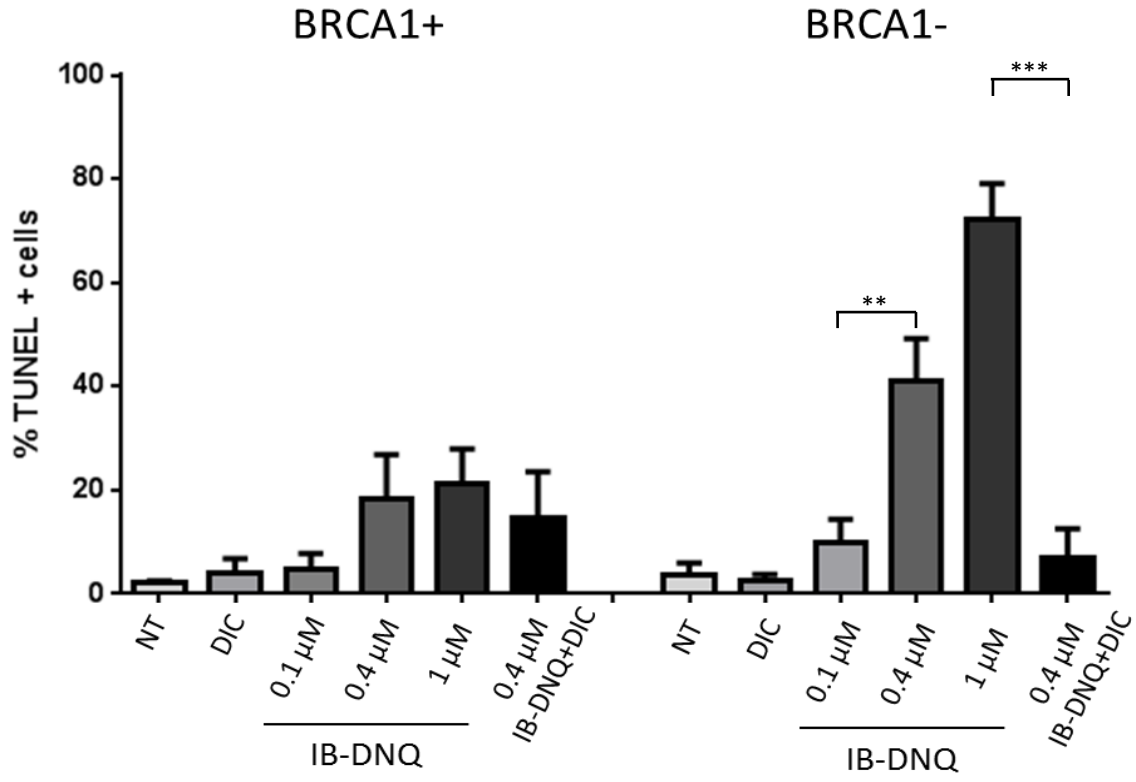

Figure 3.3. BRCA1-deficient breast cancer cells have high TUNEL+ cells after IB-DNQ treatment. IB-DNQ caused a greater increase in TUNEL+ cells in BRCA1-deficient cells compared to BRCA1-proficient cells (> 3-fold). HCC1937 cells (BRCA1+/-) cells were treated with increasing doses of IB-DNQ for 4 h and 24 h later cells were analyzed by TUNEL reaction and flow cytometry. Addition of 50 μM DIC reversed that lethality. Cell death was observed in all phases of the cell cycle.

To further confirm these findings, we generated MCF7 breast cancer cell line with stable knockdown of BRCA1 **(Fig 3.4).**

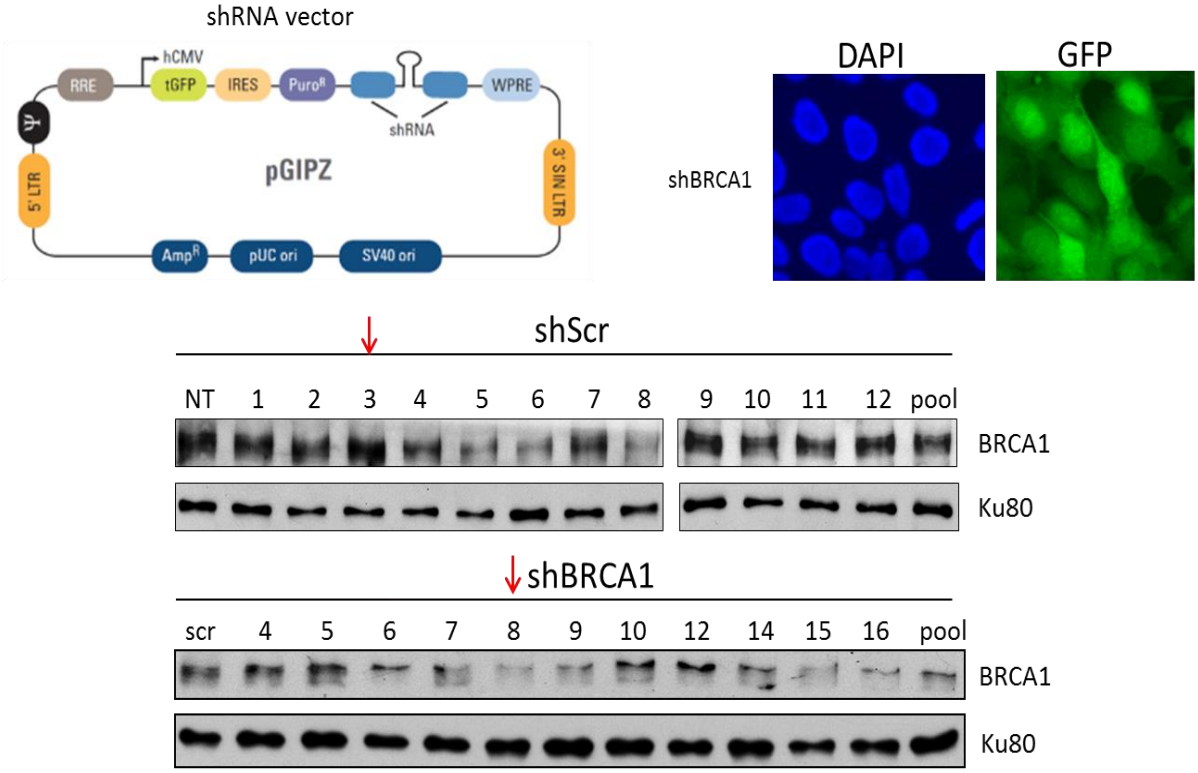

Figure 3.4. Generation of MCF7 cell line with stable knockdown of BRCA1. MCF7 cell line with stable shRNA-mediated knockdown of BRCA1 was generated by transfection with pGIPZ vector (5′-TATGTGGTCACACTTTGTG-3′; No.: V2LHS_254648, Thermo Scientific) using Lipofectamine2000 (Invitrogen) followed by selection and continued maintenance in puromycin (1 μg/ml, Invitrogen). Control cells were generated by transfection with a pGIPZ vector expressing scrambled shRNA (No.: RHS4346, Thermo Scientific). For the following experiments we used shScr3 and shBRCA8.

BRCA1-deficient breast cancer cells have increased number of DSBs after IB-DNQ treatment. The heightened sensitivity to IB-DNQ might be due to more DNA DSBs induced in BRCA1-deficient cells compared to BRCA-proficient cells, and to confirm that we co-stained HCC1937 cells (BRCA1+ and BRCA1-) for γH2AX and Cyclin A. Transient exposure to low dose IB-DNQ induced DNA damage in BRCA1-deficient cancer cells and low/no damage in BRCA1-proficient cancer cells **(Fig 3.5).**

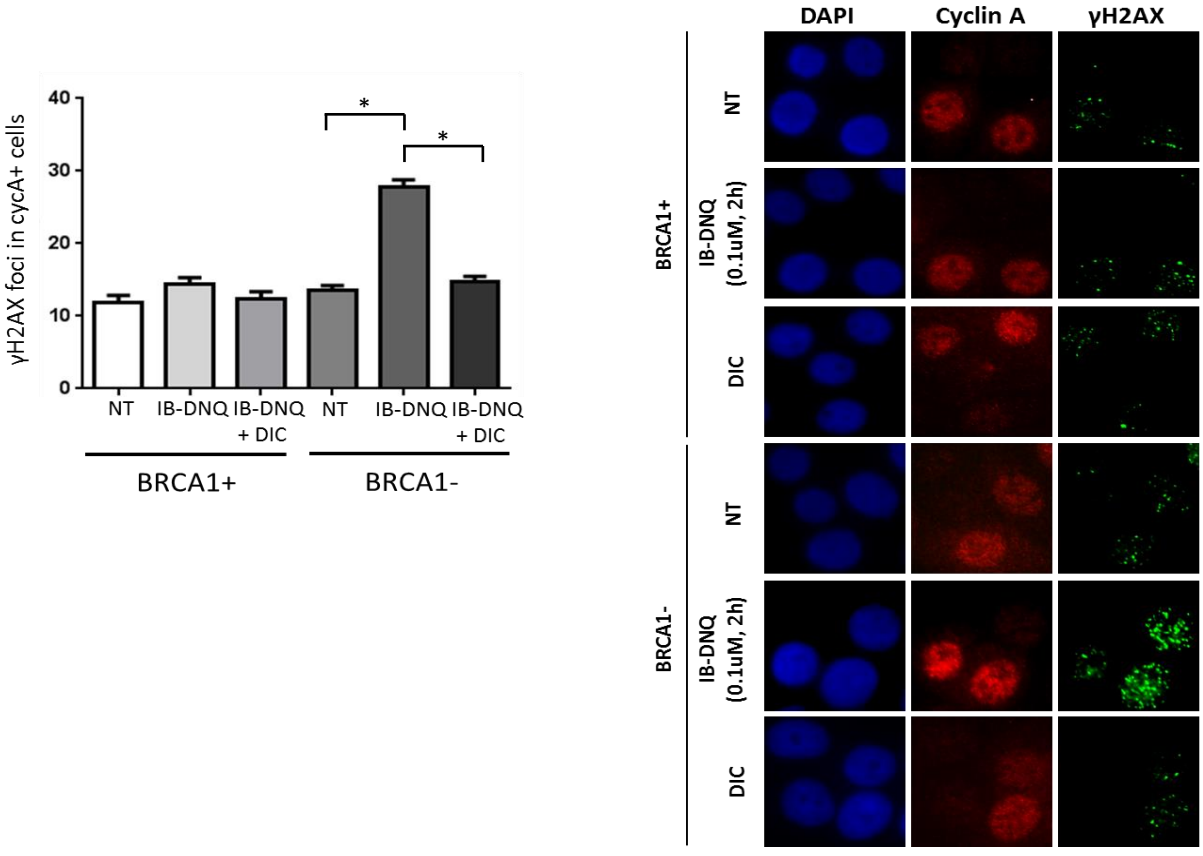

Figure 3.5. **BRCA1-deficient breast cancer cells have increased DNA damage after IB-DNQ treatment**. HCC1937 (BRCA1+/-) cells were treated with 0.1 μM IB-DNQ for 2 h and stained for γH2AX and Cyclin A to delineate damage in S/G2 phase cells.

The increased sensitivity to IB-DNQ observed in HCC1937 cells may be partly due to the compromised HR pathway in these cells. To test that we evaluated HR pathway in HCC1937 cells by Rad51 foci in Cyclin A positive cells (S/G2 cells), and as expected we found that HR is indeed impaired in BRCA1-deficient cells. BRCA1-deficient breast cancer cells could not respond to the overwhelming IB-DNQ-induced damage possibly due to their HR deficiency **(Fig 3.6).**

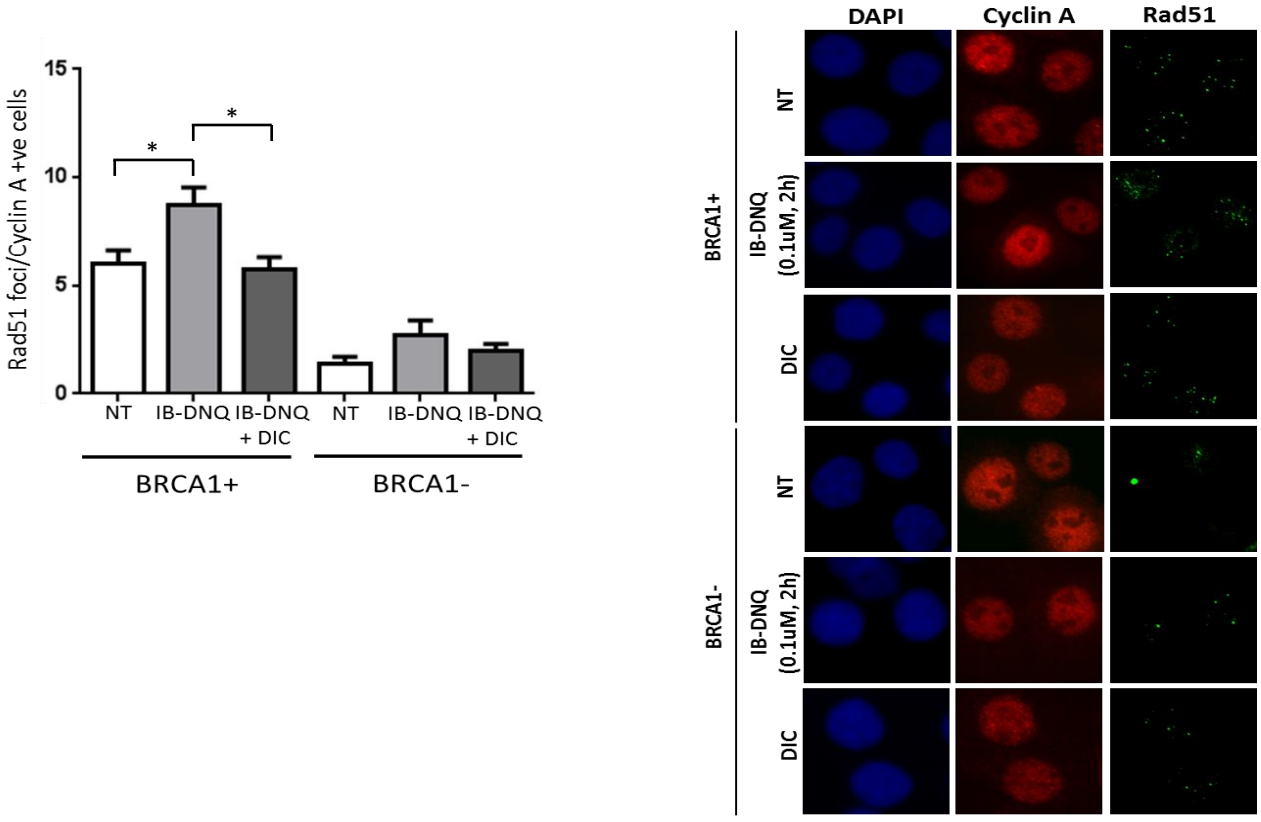

Figure 3.6. **BRCA1-deficient breast cancer cells cannot respond to IB-DNQ-induced DNA damage partly due to their HR deficiency.** HCC1937 (BRCA1+/-) cells were treated with 0.1 µM IB-DNQ for 2 h and co-stained for Rad51 and Cyclin A to delineate cells in S/G2 phase where HR is the preferred repair pathway.

HCC1937 BRCA1-deficient cancer cells are more sensitive to IB-DNQ due to their high NQO1 activity. To assess the sensitivity of MCF7 cells (shScr and shBRCA8) to IB-DNQ we did ATP assays and a long-term relative survival assays **(Fig 3.7).**

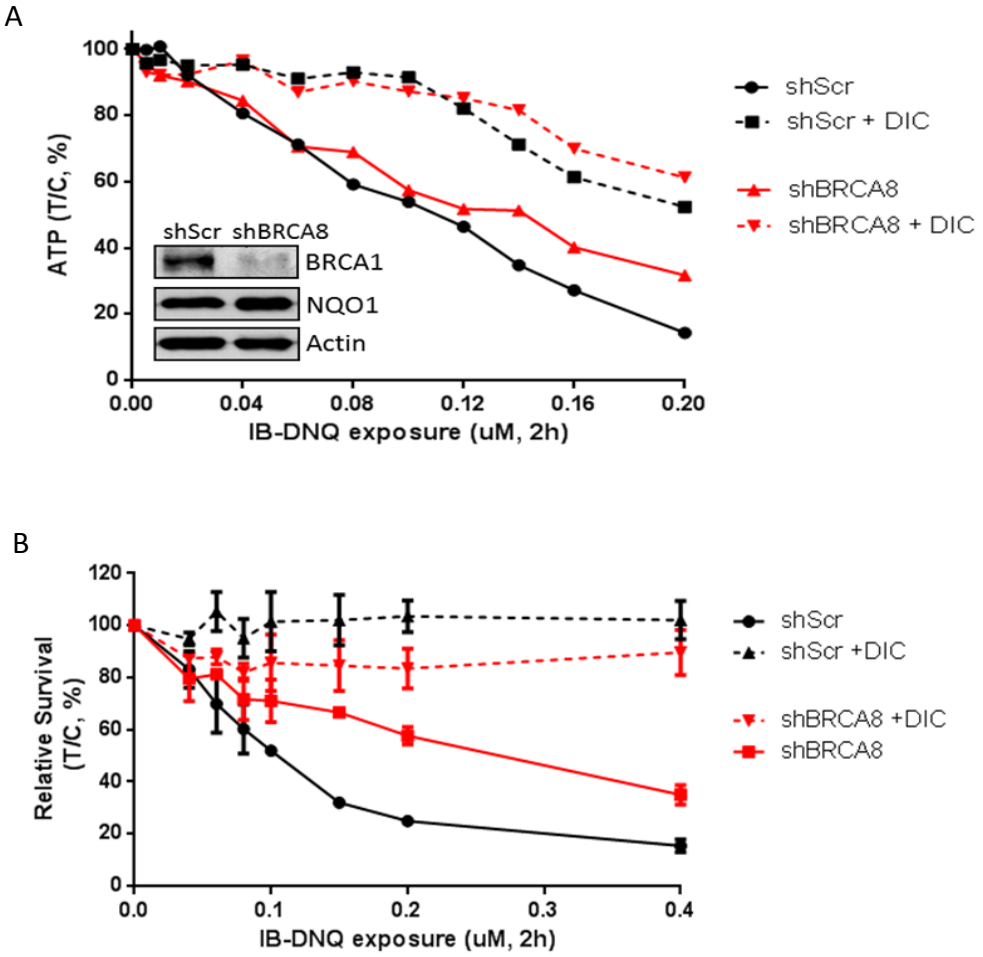

Figure 3.7. MCF7 shScr and shBRCA8 show equivalent sensitivity to IB-DNQ. A. As IB-DNQ doses increased, MCF7 shScr and shBRCA8 decreased their ATP levels to the same extent. Western blot showed the protein levels of BRCA1 and NQO1 in MCF7 shScr and shBRCA8. B. Long-term survival of MCF7 shScr vs. shBRCA8 treated with increasing doses of IB-DNQ for 2 h, with or without 50 µM DIC.

The data showed that both cell lines, with or without BRCA1, were sensitive to IB-DNQ due to their NQO1 enzyme activity (discussed in Chapter II). This led us to question the role of BRCA1 in modulating the sensitivity of these cells to IB-DNQ. Thus, we wanted to determine if the amount of ROS (mainly H_2O_2) produced after IB-DNQ exposure is the same in HCC1937 BRCA1+ vs. BRCA1- breast cancer cells **(Fig 3.8).**

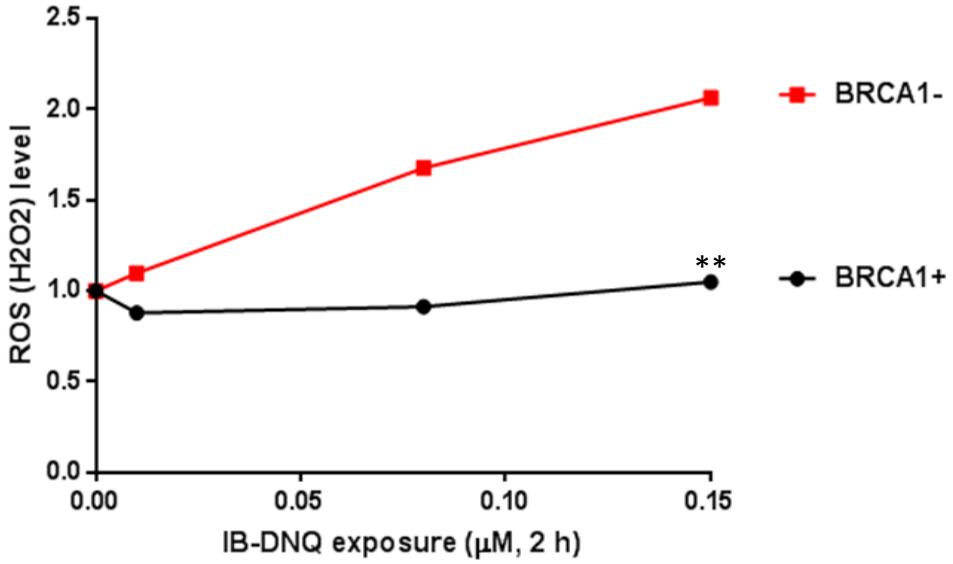

Figure 3.8. BRCA1-deficient breast cancer cells have higher amount of ROS. HCC1937 cells (BRCA1+ and BRCA1-) were exposed to increasing doses of IB-DNQ for 2 h, and the amount of H_2O_2 was measured using ROS-Glo H_2O_2 Assay (Promega).

Even though both HCC1937 BRCA1+ and BRCA1- had the same amount of NQO1 **(Fig 3.2A, Western blot),** BRCA1- cells had two and a half fold higher ROS levels. The NQO1-driven IB-DNQ futile cycle produces high amount of ROS; therefore, we determined the NQO1 enzyme activity in HCC1937 cells (BRCA1+ and BRCA1-). We found that the two cell lines, BRCA1+ and BRCA1-, did not have the same activity of NQO1, in fact, BRCA1- had almost 3-fold higher NQO1 activity **(Fig 3.9A).** This result is a possible explanation for the increased ROS levels in BRCA1- cells. However, MCF7 shScr and shBRCA8 had similar NQO1 enzyme activity **(Fig 3.9B).**

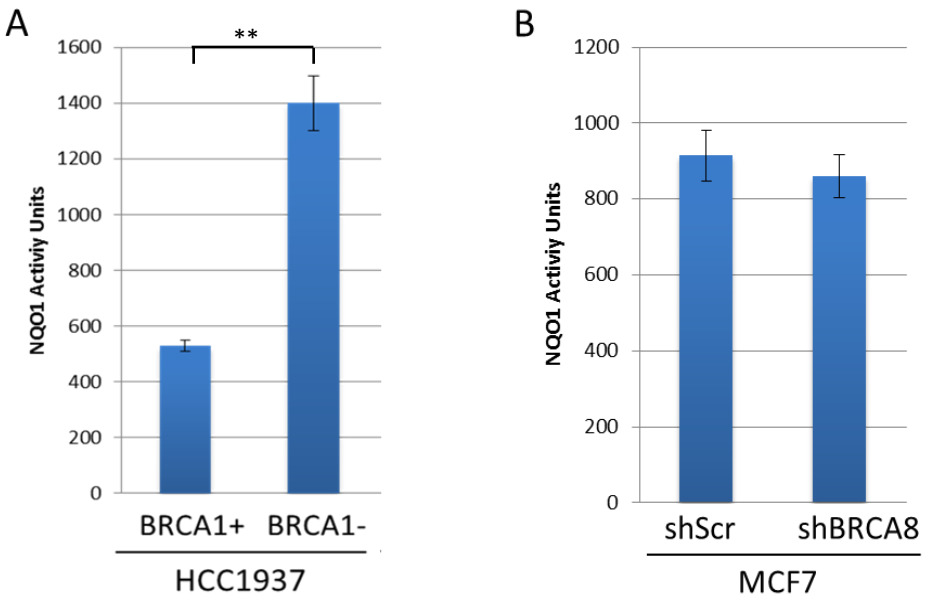

Figure 3.9. BRCA1-deficient HCC1937 cells have higher NQO1 enzyme activity while NQO1 activity is equal between MCF7 shScr and shBRCA8. Fresh cell pellets from HCC1937, BRCA1+ and BRCA1- , and MCF7 shScr and shBRCA8 were analyzed by NQO1 enzyme assay as described in (Materials and Methods).

Therefore, we could conclude that the sensitivity of these breast cancer cells to IB-DNQ is mainly driven by NQO1 activity, not by BRCA1 status. Future studies with additional BRCA1-deficient cancers are needed to confirm this conclusion.

DISCUSSION

About 5-10% of breast cancers are BRCA1/2-deficient, which makes them particularly vulnerable to replication-associated drugs like camptothecin (CPT) (L. F. Liu et al., 2000). We hypothesized that BRCA1/2-deficient cancers would be particularly sensitive to the cytotoxic effects of IB-DNQ, demonstrating an example of synthetic lethality. We already determined that IB-DNQ causes significant amount of DSBs (Chapter II), which activates ATR (pChk1) and ATM (pChk2) **(Fig 2.7)**. In order to determine whether IB-DNQ induced DNA damage in all cell cycle phases, we delineated cells in G1 versus cells in S/G2 phase by staining with Cyclin A, a protein with high levels in S/G2 phases. Both, cells in G1 (Cyclin A negative) and cells in S/G2 phase (Cyclin A positive) had three fold higher DSB number than background **(Fig 2.7E).** However, cells in S/G2 phase showed increased overall damage possibly due to intrinsic replication stress. DNA lesions that occur due to replication stress and damage that was induced when cells are in S/G2 phase are mainly repaired by the error-free HR pathway. Indeed, IB-DNQ-induced DNA damage activated HR, as seen by Rad51 foci in Cyclin A

positive cells **(Fig 3.6).** Due to the HR activation, we hypothesized that breast cancers with impaired HR would be excellent targets for IB-DNQ. We investigated the IB-DNQ-induced lethality in HCC1937 breast cancer cell line deficient in BRCA1. These BRCA1-deficient cells were complemented with wild-type BRCA1 to establish a genetically matched pair with the sole difference being BRCA1 protein status. Cancer cells lacking BRCA1 were extremely sensitive to low dose IB-DNQ compared to BRCA1-proficient cells. The addition of DIC significantly reduced the cytotoxic effects of the agent, however, it did not completely reverse the effect possibly due to other one-electron reductases present in the cell, such as P450R and B5R that can bioreduce quinones (Bey et al., 2013). BRCA1-deficient breast cancers have shown a response to PARP1 inhibitors, and currently there are over 13 PARP1 inhibitors in clinical trials, used both as a mono therapy or in combination with other chemotherapy (Lord, Tutt, & Ashworth, 2014). However, there is a rising amount of evidence for intrinsic resistance or acquired tolerance following drug exposure. Studies have identified possible mechanisms for resistance to PARP1 inhibitors in preclinical models and patients: (1) secondary mutations that partially restore BRCA1/2 function, (2) increased activity of Rad51, (3) decreased levels or activity of PARP1, (4) and decreased intracellular availability of PARP1 inhibitors due to p-glycoproteins (P-gp) involved in the efflux of PARP1 inhibitors (Montoni et al. 2013, Lord et al. 2013, Fojo et al. 2014). When we treated HCC1937 cells with the PARP1

inhibitor ABT-888 we saw the expected sensitivity of BRCA1-deficient cells to the inhibitor, albeit to a lesser degree than when we treated the same cells with IB-DNQ **(Fig 3.2C).** Comparing the two agents, IB-DNQ and the PARP1 inhibitor, we established the superiority of IB-DNQ by showing extreme sensitivity in BRCA1-deficient cells after short exposure time and at very low doses. Both BRCA1-proficient and deficient cells responded to IB-DNQ due to the presence of NQO1, however, BRCA1-deficient cells were more sensitive to IB-DNQ at these particular low doses possibly because of the overwhelming IB-DNQ-induced damage and their inability to repair it partly due to their HR deficiency. IB-DNQ-induced lethality is possibly the result of "crossing a threshold" of DNA damage that the cells cannot cope with, as with the case of BRCA1-deficient cells. That is why it is important to determine the status of HR and NHEJ, the two main pathways that repair DSBs, in every patient and determine a "personalized dose" for IB-DNQ in order to deliver the most efficacious cancer treatment.

To confirm that BRCA1 loss can further sensitize breast cancers to IB-DNQ, we generated a MCF7 cell line with a stable knockdown of BRCA1 **(Fig 3.4).** When we assessed the ATP levels in MCF7 shScr and shBRCA8 after treatment with increasing doses of IB-DNQ, we did not find a difference in ATP levels between the two cell lines. Furthermore, after a long-term relative survival assay, both shScr and shBRCA8 cells showed similar sensitivity to IB-DNQ. This

unexpected result prompted us to assess the NQO1 enzyme activity in HCC1937 cells (BRCA1+ and BRCA1) and MCF7 (shScr and shBRCA1). HCC1937 cells deficient in BRCA1 had an almost 3-fold greater NQO1 activity than BRCA1 complemented cells **(Fig 3.9A).** This was not the case with MCF7 cells with stable knockdown of BRCA1; both cell lines had equal NQO1 activity **(Fig 3.9B).** We speculate that due to greater genomic instability and increased metabolism, over the course of its tumor evolution, BRCA1-deficient cancer cells could have upregulated the activity of detoxifying enzymes such as NQO1. After measuring ROS levels in HCC1937 cells, we found that BRCA1-deficient cells had 2-fold higher ROS level **(Fig 3.8),** possibly due to the higher NQO1 activity. Thus, these observations bolstered the major role NQO1 plays in IB-DNQ-induced toxicity. Once again, these results proved that NQO1 is absolutely essential for IB-DNQ-induced lethality, and the particular cell death (NAD-Keresis, described in Chapter II) that IB-DNQ causes is a combination of DNA damage and metabolic changes, and it is BRCA1-independent.

Nevertheless, BRCA1/2-deficient breast cancers are good candidates for treatment with IB-DNQ. A recent study by Da Li et al. showed that intracellular NAD levels were dramatically increased in BRCA1-mutated breast cancer compared with adjacent normal tissue (D. Li et al., 2014). However, NADH levels were not affected by BRCA1 patterns. Therefore, the elevated NAD/ NADH ratio that they observed was mainly dependent on the increased NAD

levels in BRCA1-mutated breast cancer tissue. Although intracellular PARP1 levels and activity were increased in non-BRCA1-mutated breast cancer compared with adjacent normal tissue, BRCA1-mutated breast cancer showed dramatically increased intracellular PARP1 levels and activity compared with the other groups. Therefore, the results from this study suggest that BRCA1 inactivation may be involved in the induction of NAD synthesis, PARP1 expression, and elevated PARP1 activity. We have already established in Chapter II that IB-DNQ-induced lethality is dependent on PARP1 hyperactivation, thus these BRCA1-deficient breast cancers with elevated PARP1 level and activity could benefit from IB-DNQ treatment at low doses and with reduced potential side effects. In this particular population of breast cancers, where PARP1 activity is upregulated, a lower amount of DNA damage could tip over the "threshold" of lesions necessary to cause PARP1 hyperactivation and elicit NAD-Keresis. These results indicate that screening BRCA1-deficient breast cancers for NQO1 and PARP1 expression and activity may lead to better treatment outcome.

CHAPTER IV

Factors modulating the response of BRCA1/2-deficient breast cancers to PARP1 inhibitors

INTRODUCTION:

The highly conserved Mre11–Rad50–Nbs1 (MRN) complex is thought to have a key role in the sensing, processing and repair of DSBs (Williams, Williams, & Tainer, 2007). In addition to binding the DNA and bridging its broken ends **(Fig 4.1)**, a lot of in vitro studies have shown enzymatic roles for this complex.

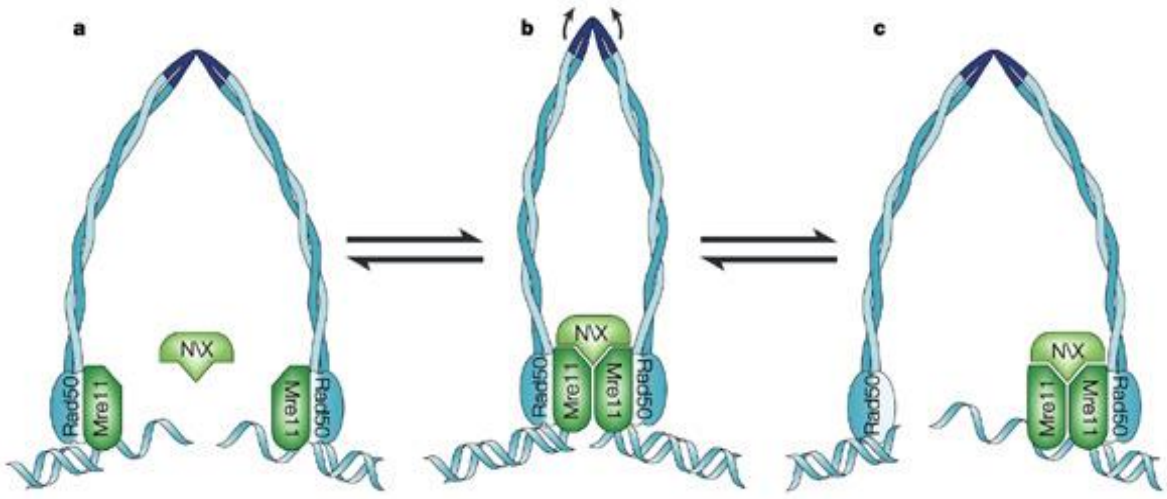

Figure 4.1. Structure of the MRN complex. The MRN complex is composed of dimers of Rad50 and Mre11 associated with a single Nbs1. In **a** and **c** Rad50 is in partly open conformations, whereas **b** shows the dimer in a completely folded 'closed' structure. Mre11 is the core of the complex and associates with Rad50 at the interface of its globular ATP-binding motifs and coiled–coil arms. Nbs1 binds to Mre11 independently of Rad50. *Figure adapted from (D'Amours & Jackson, 2002).*

Biochemical experiments have shown that Mre11 functions as both a single and double-strand DNA endonuclease, as well as a 3′–5′ dsDNA exonuclease (Zhuang, Jiang, Willers, & Xia, 2009). After DNA damage, the MRN complex is recruited to the sites of damage via zinc hooks at the ends of the long, flexible arms of Rad50 (Hopfner et al., 2002). The MRN complex also interacts with BRCA1 and CtIP, which may be essential for DSB end resection to generate 3' overhanging single-stranded DNA during initiation of HR (Chen, Nievera, Lee, & Wu, 2008). The malfunction of these mechanisms can result in the fusion of DNA ends that were originally distant from one another in the genome, which generates chromosomal rearrangements such as inversions, translocations and deletions. The disruption of gene expression can perturb normal cell profile, or lead to cancer (Yun & Hiom, 2009b).

A study done by J. Bartkova et al. reported that among a large series of approximately 1000 breast cancers, around 7 % of the tumors showed aberrantly reduced protein expression for Mre11 (Bartkova et al., 2008). The availability of clinical specimens from both sporadic and familial breast tumor cases, led them to consider potential differences between sporadic and familial cases. Indeed, there was an overall trend for the MRN complex defects to occur more frequently among familial breast cancers. The most striking result was the statistically highly significantly enhanced incidence of the MRN-aberrant tumors among the familial breast cancers linked to carriers of BRCA1 and BRCA2 mutations, as compared

to all non-BRCA1/2 tumors (Bartkova et al., 2008). The analysis identified two putatively disease-associated sequence variants in Mre11: Arg202Gly missense mutation in exon 7 and Arg633STOP nonsense mutation in exon 17. Importantly, both of these identified Mre11 mutations are associated with aberrant reduction or loss of not only Mre11 protein itself, but also the other proteins of the MRN complex. The fact that all three MRN proteins are still detectable in the normal stromal cells within the tumors, while selectively absent in the cancer cells is consistent with the heterozygous germline mutation of Mre11 in the patients, and the subsequent silencing or loss of the second allele only in the tumor. Furthermore, Mre11 defects were observed in 30 % of BRCA1 tumors (14/47), and 14 % of BRCA2 tumors (6/42), which may present Mre11 as a new candidate to the list of breast cancer-predisposing genes (Bartkova et al., 2008).

Another interesting role of Mre11 is its involvement in replication fork restart after release from replication block. PARP1 binds to and is activated by stalled replication forks that contain small gaps. PARP1 collaborates with Mre11 to promote replication fork restart most likely by recruiting Mre11 to the replication fork to promote resection of DNA (Bryant et al., 2009). As it has been reported, a significant number of breast cancers have defects in Mre11 and BRCA1, which leads to defective HR repair, leaving the cells with no other choice but to attempt to repair the DNA breaks through “back-up” error-prone pathways. However, there are still unanswered questions as to why PARP1 inhibitors are not effective

for all patients with BRCA1/2 mutations (Balmana, Domchek, Tutt, & Garber, 2011). PARP1 inhibitors are currently undergoing extensive testing as potential anticancer agents (Telli & Ford, 2010). These drugs were initially developed as agents that could enhance the cytotoxicity of DNA damaging treatments such as IR and temozolomide (TMZ) (Curtin & Szabo, 2013). Interest in these agents was heightened by the demonstration that BRCA1/2 mutant cancer cells are selectively killed by single-agent PARP1 inhibitor treatment (Farmer et al., 2005). Consistent with these preclinical observations, the PARP1 inhibitor olaparib has exhibited substantial single-agent activity in BRCA1/2-mutant breast and ovarian cancer (Fong et al., 2009). Nonetheless, fewer than 50 % of patients with BRCA1/2-mutant cancers respond to these drugs, raising important questions about identifying patients most likely to derive benefit from PARP1 inhibition (Balmana et al., 2011). With that in mind, we focused on identifying factors that modulate the response of BRCA1/2-deficient breast cancers to PARP1 inhibitors.

We found that there is an overall trend for the HR protein Mre11 defects to occur more frequently among familial breast cancers as compared to all non-BRCA1/2 tumors (Bartkova et al., 2008). Also, this can open a therapeutic window for patients with BRCA1 and Mre11 loss to be treated with PARP1 inhibitors alone, and potentially substitute the current radiation and chemotherapy treatments. The goal of this study was to determine whether PARP1 inhibitors increase tumor cell killing in patients with BRCA1 and Mre11 loss, and to

investigate the role of Mre11 in increasing genomic instability in the presence of PARP1 inhibitors in familial BRCA1-deficient breast cancers.

MATERIAL AND METHODS

Cell culture, PARP1 and CDK inhibition. U2OS, HCC1937, UWB1 (obtained from the American Type Culture Collection) were maintained in α-MEM, RPMI, RPMI+MEBM (1:1 ratio) medium, respectively, supplemented with 10 % fetal bovine serum and penicillin/streptomycin in a humidified atmosphere with 5 % CO_2. A U2OS line with stable shRNA-mediated knockdown of BRCA1 was generated by transfection with a pGIPZ vector (5′-TATGTGGTCACACTTTGTG-3′; No.: V2LHS_254648, Thermo Scientific) using Lipofectamine2000 (Invitrogen) followed by selection and continued maintenance in puromycin (1 μg ml^{-1}, Invitrogen). Control cells were generated by transfection with a pGIPZ vector expressing scrambled shRNA (No.: RHS4346, Thermo Scientific). For PARP1 inhibition, cells were incubated for 24 h in 10 μM veliparib (ABT-888) or 10 μM olaparib (AZD-2281). For CDK inhibition, cells were incubated with 2 μM AZD5438 (Selleck) or 10 μM Roscovitine (Sigma) for 5 h before cells were harvested or irradiated.

Transfection of cells. Depletion of Mre11 was carried out by transfection with siRNA (5′-AGU UGA UCU CUU CUC CUG U(d T)(d T); Invitrogen) using electroporation (Amaxa) followed by Lipofectamine2000 (Invitrogen) 24 h after

the electroporation. Cells were harvested 48 h later to verify knockdown by western blotting.

Western blotting and antibodies. Nuclear extracts for western blotting were prepared by re-suspending cell pellets in hypotonic lysis buffer (10 mM Tris–HCl pH 7.5, 1.5 mM MgCl2, 5 mM KCl, protease and phosphatase inhibitors), followed by nuclear extraction buffer (50 mM Tris–HCl pH 7.5, 0.5 M NaCl, 2 mM EDTA, 10 % sucrose, 10 % glycerol, protease and phosphatase inhibitors). The following primary antibodies were used: Rad51 (H-92), 53BP1 (H-300; Santa Cruz), actin (Sigma), RPA (Calbiochem), BrdU (Becton, Dickinson and Company), cyclin A (6E6), BRCA1, Mre11, γH2AX and Ku80 (a kind gift from Dr BP Chen). The following secondary antibodies were used: horseradish peroxidase-conjugated secondary antibodies (Bio-Rad) and Alexa488/568/647-conjugated secondary antibodies (Invitrogen). Antibody dilutions were 1:1000.

Irradiation of cells. Cells in culture media were irradiated with gamma rays from a cesium source ^{137}Cs (JL Shepherd and Associates) at 23^{o} C temperature, 400cGy/min dose/rate.

Immunofluorescence staining. Cells were seeded onto glass chamber slides (Lab-Tek) and immunostained with anti-RPA antibody or co-immunostained with anti-Rad51 and anti-cyclin A antibodies 3 h after irradiation with 6 Gy. Cells were fixed with 4 % paraformaldehyde/PBS and permeabilized with 0.5 % Triton X-

100 before incubation with antibodies. To obtain clear RPA foci, cells were subject to in situ fractionation (Tomimatsu et al., 2009). The average number of RPA foci per nucleus or mean Rad51 foci for cyclin A-positive (S/G2) nuclei was determined after scoring at least 50 nuclei and subtracting background (average numbers of foci in mock-irradiated cells). For quantifying DSB repair kinetics, cells were co-immuno stained with anti-53BP1 and anti-cyclin A antibodies at different time points post irradiation (1 Gy). The average numbers of 53BP1 foci for cyclin A-positive (S/G2) and cyclin A-negative (G1) nuclei were determined after scoring at least 50 nuclei and subtracting background. Images were captured using a Leica DH5500B fluorescence microscope (40 X objective lens) coupled to a Leica DFC340 FX camera using Leica Application Suite v3 acquisition software.

BrdU/ssDNA assay. Cells grown in the presence of 10 μM BrdU (Sigma) for 16 h were irradiated with 10 Gy of gamma rays and fixed 1 h after irradiation. Cells were immunofluorescence stained with anti-BrdU antibody under non-denaturing conditions (to detect BrdU incorporated into ssDNA). For clarifying BrdU/ssDNA foci, cells were subject to in situ fractionation (Cuadrado et al., 2006). The percentage of BrdU-positive cells (cells with 10 or more foci) was determined after scoring at least 50 nuclei and subtracting background.

Metaphase chromosome preparations. Cells were irradiated with 6 Gy of gamma rays. Colcemid (Sigma), along with 1 mM caffeine (Sigma) to bypass

G2/M arrest, was added at 8 h post IR. Metaphase chromosome spreads were prepared after 16 h and scored for radial chromosomes (McEllin et al., 2010).

Colony formation assays. Cells were treated for 24 h with ABT-888 as indicated. After that, cells were plated in triplicate onto 60 mm dishes (1,000 cells per dish). Surviving colonies were fixed and stained with methanol/crystal violet ~10–14 days later.

RESULTS

Loss of Mre11 leads to increased radial chromosomes in BRCA1-deficient breast and ovarian cancer cells. Due to Mre11's role in sensing and signaling of DSBs, and its endo- and exonuclease activities, we hypothesized that reduced levels, or absence of Mre11, in BRCA1 mutant breast cancer cells may lead to increased deficiency in HR and increased chromosomal aberrations. We used HCC1937 breast cancer cells that lack BRCA1 due to mutation in the BRCT domain (Scully et al., 1999). HCC1937 cell line was initiated from a primary ductal carcinoma and it was classified as TNM Stage IIB, grade 3 tumor. BRCA1 analysis revealed that the cell line is homozygous for the BRCA1 5382C mutation, whereas the lymphoblastoid cell line derived from the same patient is heterozygous for the same mutation (Greenberg et al., 2006). To study the effect of Mre11 on HR in these cells, we knocked down Mre11 with siRNA, and used scrambled siRNA as a control. We performed chromosomal aberrations analysis

in HCC1937 BRCA1-complemented (complemented with vector containing wt BRCA1) and HCC1937 BRCA1-null (contains empty vector pcDNA3.1 as a control) **(Fig 4.2).**

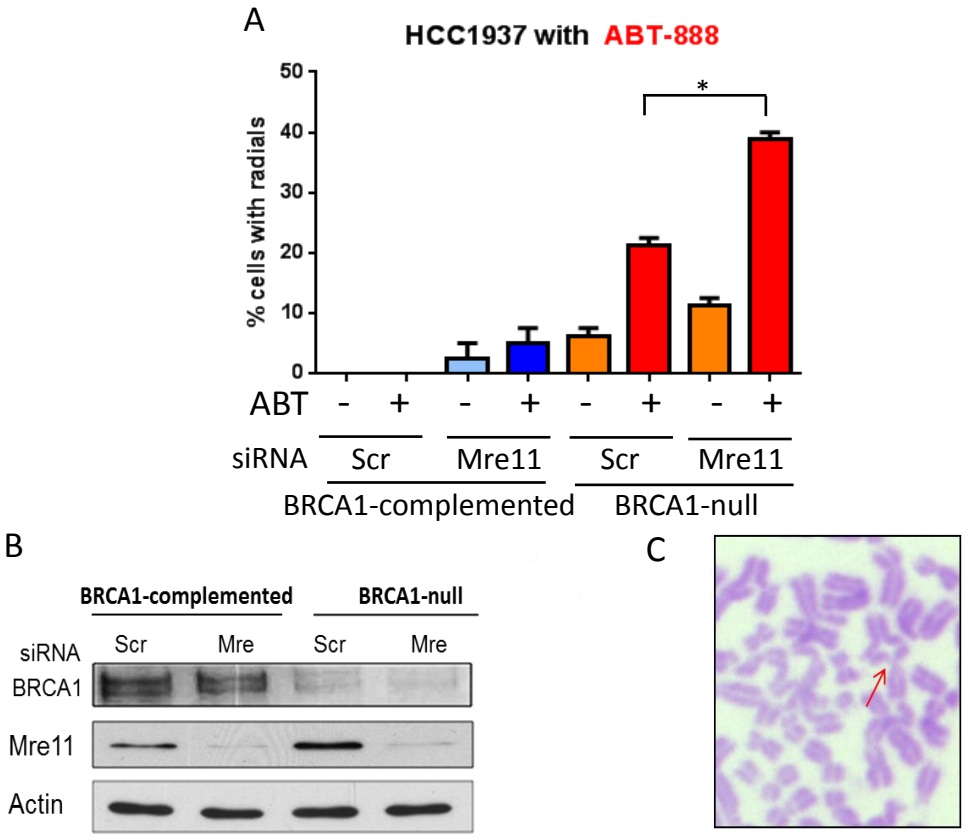

Figure 4.2. Loss of Mre11 leads to increased radial chromosomes in BRCA1-deficient breast cancer cells. A. siRNA-mediated knockdown of Mre11 in HCC1937 BRCA-complemented and HCC1937 BRCA1-null breast cancer cells was accomplished through electroporation followed by lipofection the next day to increase the efficiency of Mre11 knockdown. Cells were treated with 10 μM ABT-888 for 24 h, and colcemid and caffeine were added to the media (Tomimatsu et al., 2014). Metaphase chromosome spreads were prepared after 16 h and scored for radial chromosomes (McEllin et al., 2010). B. Western blot with antibodies against Mre11 verified the knockdown. C. A representative picture of BRCA1-null cells after treatment with ABT-888. Quadradial chromosome structure in BRCA1-null with Mre11 knockdown after ABT-888 treatment is indicated by the red arrow.

We found the same phenotype in UWB1 ovarian cancer cell line, with germline BRCA1 mutation within exon 11 and a deletion of the wild-type allele. UWB1 cell line is estrogen and progesterone receptor negative and has an acquired somatic mutation in p53, similar to the commonly used BRCA1-null breast cancer cell line HCC1937. UWB1 was complimented with wt BRCA1 to establish a genetically matched pair (DelloRusso et al., 2007) **(Fig 4.3).**

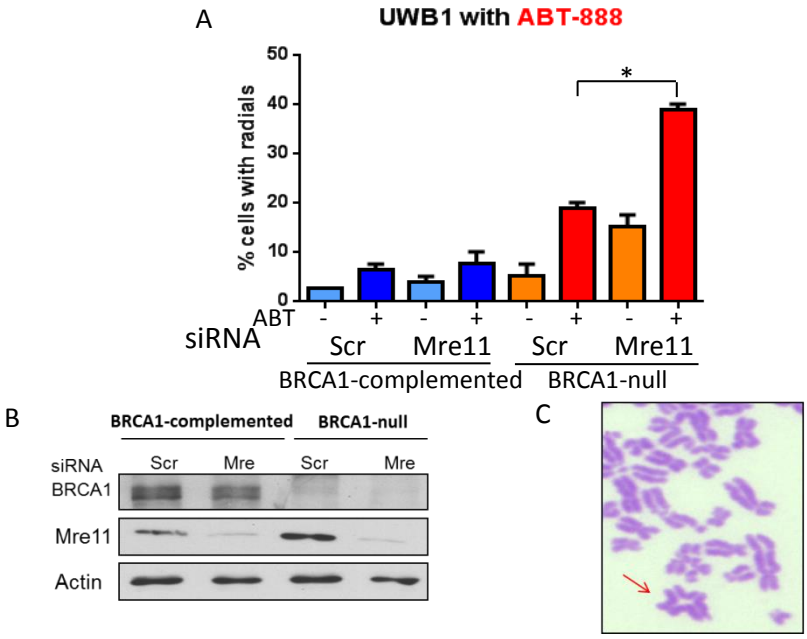

Figure 4.3. Loss of Mre11 leads to increased radial chromosomes in BRCA1-deficient ovarian cancer cells. A. siRNA-mediated knockdown of Mre11 in UWB1 BRCA-complemented and UWB1 BRCA1-null ovarian cancer cell line was accomplished through electroporation followed by lipofection the next day to increase the efficiency of Mre11 knockdown. Cells were treated with 10 μM ABT-888 for 24 h, and colcemid and caffeine were added to the media (Tomimatsu et al., 2014). Metaphase chromosome spreads were prepared after 16 h and scored for radial chromosomes (McEllin et al., 2010). B. Western blot with antibodies against Mre11 verified the knockdown. C. A representative picture of BRCA1-null with Mre11 loss after treatment with ABT-888. Quadradial chromosome structure is indicated by the red arrow.

There was a significant increase in the frequency of radial chromosomes when BRCA1-null cancer cells were treated with ABT-888. The highest sensitivity was seen in BRCA1/Mre11-deficient cells (~ 40 %). When we compared both IR and ABT-888 treatments and their effect on chromosomal stability in BRCA1-null verses BRCA1/Mre11-deficient cells, we observed greater sensitivity to these agents in BRCA1/Mre11-deficient cells probably due to their grossly aberrant HR. Due to the induced damage, we predicted probable cell cycle arrest which may prevent the cells from entering metaphase and leading to insufficient count of chromosomal spreads. To prevent that we added caffeine to inhibit ATM, which senses the DNA damage first and signals to cell cycle arrest proteins such as Chk1 and Chk2. The inhibition of ATM allowed the cells to continue the division and reach metaphase.

Lack of Mre11 further decreases HR in BRCA1-deficient breast and ovarian cancer cells. Due to loss of BRCA1 and Mre11, HR's crucial step of resection to produce single-strand 3' tail is abrogated and faithful repair cannot be executed. To investigate whether HR was greatly reduced when Mre11 was lost, we assessed the formation of Rad51 foci after treatment with ABT-888. Rad51 is involved in the search for homology and strand pairing stages of HR. Rad51 foci are good surrogate marker for single-stand DNA formed after resection because they bind to it and form nucleofilaments. If HR is compromised at the resection

step, no single-stand DNA will be formed leading to no Rad51 foci. We studied Rad51 foci formation by performing immunofluorescence in HCC1937 breast cancer cells and UWB1 ovarian cancer cells. In these cells we knocked down Mre11 with siRNA, and used scrambled siRNA as a control. These cells were treated with 6 Gy IR and after 3 h cells were fixed and fluorescent antibodies against Rad51 were added. Since we were interested in HR, which predominates in S/G2 phase, we stained the cells with antibodies against cyclin A. Cyclin A positive cells enabled us to analyze formation of Rad51 foci only in S/G2 phase cells **(Fig 4.4).**

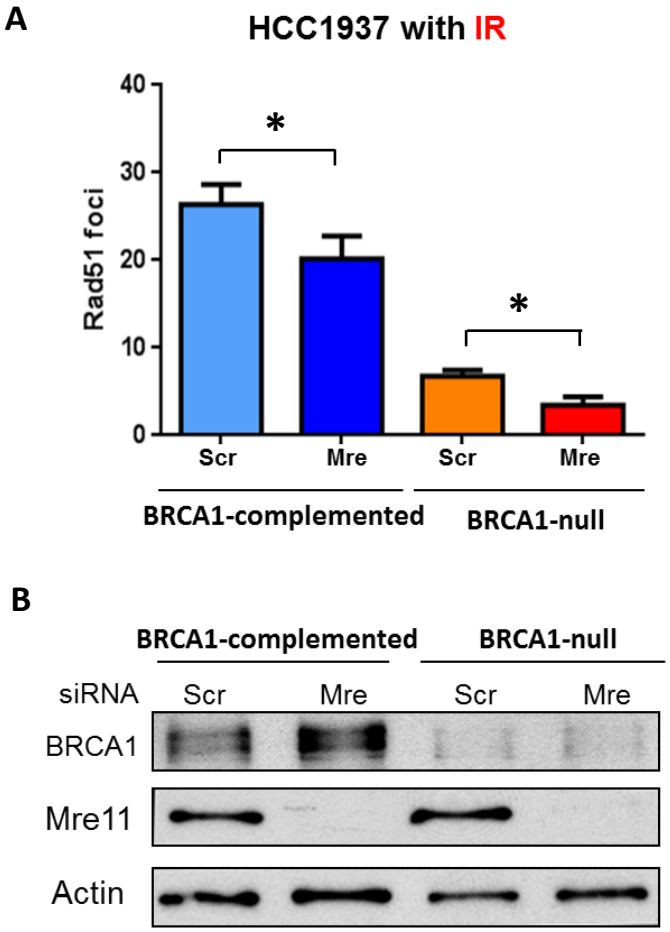

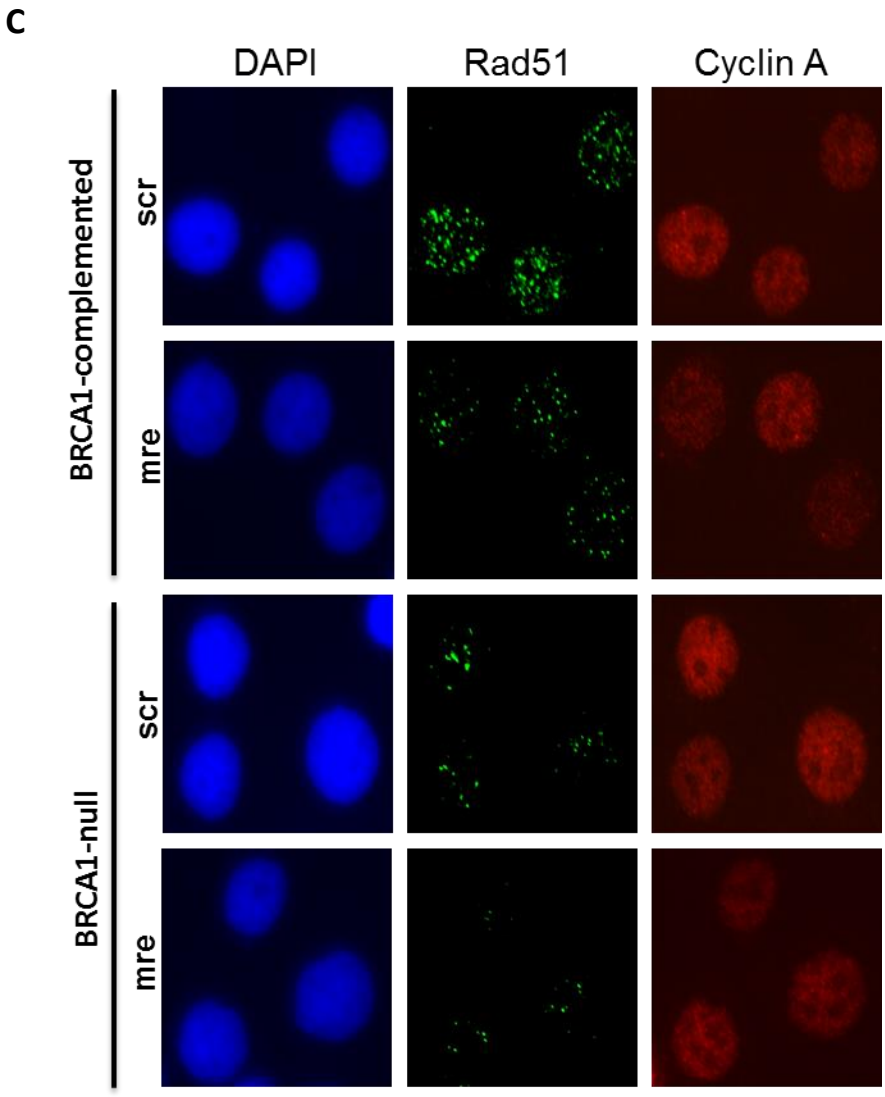

Figure 4.4. Lack of Mre11 further decreases HR in BRCA1-deficient breast cancer cells. A. In HCC1937 cells (BRCA1-complemented and BRCA1-null) Mre11 was knocked down by electroporation followed by lipofection (24 h later). B. Western blot confirmed the knock down. HCC1937 BRCA1-complemented and BRCA1-null cells were irradiated with 6 Gy and after 3 h cells were fixed. Fluorescent antibodies against Rad51 and cyclin A were used. C. Rad51 foci were scored from 50 cells in S/G2 phase (cyclin A +), and after subtracting background (number of foci in untreated nuclei), average foci per nucleus were plotted.

Mre11 loss in BRCA1-complemented breast cancer cells led to ~ 25 % decrease in Rad51, however, absence of Mre11 in BRCA1-null cells further augmented HR deficiency and decreased Rad51 foci with ~ 50 %. This result, along with the increased radial chromosomes **(Figs 4.2 and 4.3)** showed that BRCA1/Mre11-deficent breast cancers had grossly compromised HR. Same conclusion was made in UWB1 ovarian cancer cells **(Fig 4.5).**

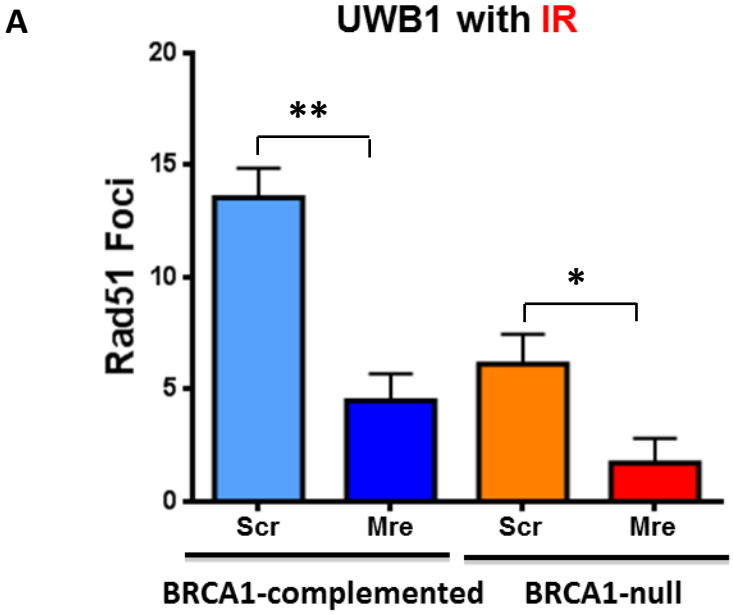

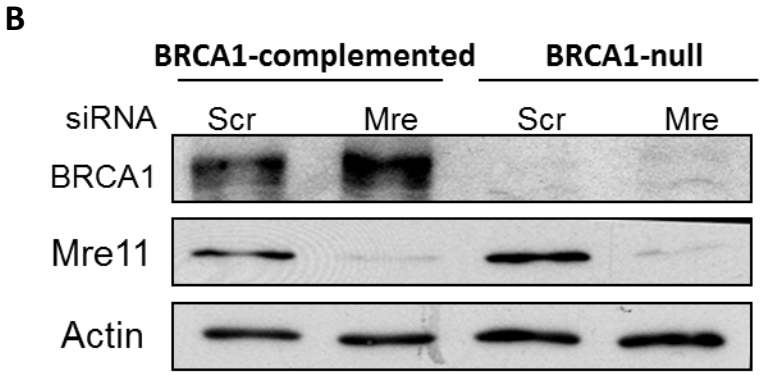

C

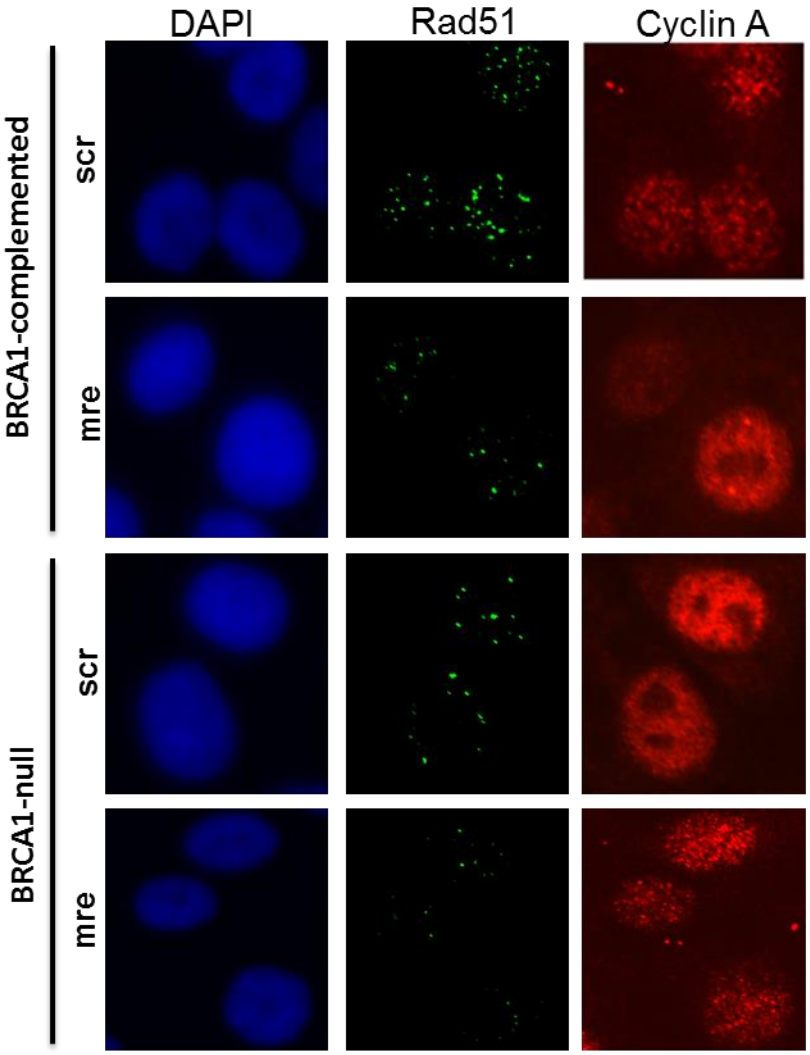

Figure 4.5. Lack of Mre11 further decreases HR in BRCA1-deficient breast cancer cells. A. In UWB1 cells (BRCA1-complemented and BRCA1-null) Mre11 was knocked down by electroporation followed by lipofection (24 h later). B. Western blot confirmed the knock down. UWB1 BRCA1-complemented and BRCA1-null cells were irradiated with 6 Gy and after 3 h cells were fixed. Fluorescent antibodies against Rad51 and cyclin A were used. C. Rad51 foci were scored from 50 cells in S/G2 phase (cyclin A +), and after subtracting background (number of foci in untreated nuclei), average foci per nucleus were plotted.

Depletion of Mre11 rendered BRCA1-deficient cancer hyper-sensitive to PARP1 inhibitors. We hypothesized that the loss of Mre11 in BRCA1-deficient tumors would further exacerbate the sensitivity of these cancers to PARP1 inhibitors due to the loss of functional HR. In order to test if there is an increased sensitivity to PARP1 inhibitor ABT-888, due to loss of Mre11, we performed colony formation assay with UWB1 ovarian cancer cells with siRNA mediated knockdown of Mre11. This allowed us to examine the sensitivity to the inhibitor when both BRCA1 and Mre11were absent **(Fig 4.6).**

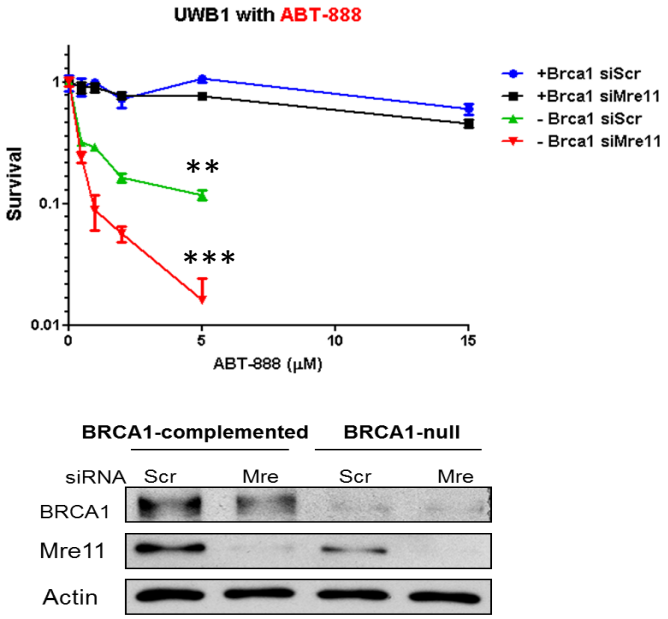

Figure 4.6. Mre11 loss leads to increased sensitivity to PARP1 inhibitor ABT-888 in BRCA1-null ovarian cells. UWB1 ovarian cancer cells (+BRCA1 siScr, +BRCA1 siMre11, -BRCA1 siScr, -BRCA1 siMre11) were plated in triplicate onto 60-mm dishes (1000 cells per dish) and treated with increasing concentrations of ABT-888. Surviving colonies were fixed and stained with methanol/crystal violet about 14 days later and colonies containing 50 cells and above were counted.

Stable knockdown of BRCA1 in U2OS cancer cells recapitulated defects in HR and sensitivity to PARP1 inhibitors. In addition, we generated another cell line, U2OS osteosarcoma cancer cell line, with stable knock down of BRCA1 **(Fig 4.7).** Clone #43 was used for the rest of the experiments.

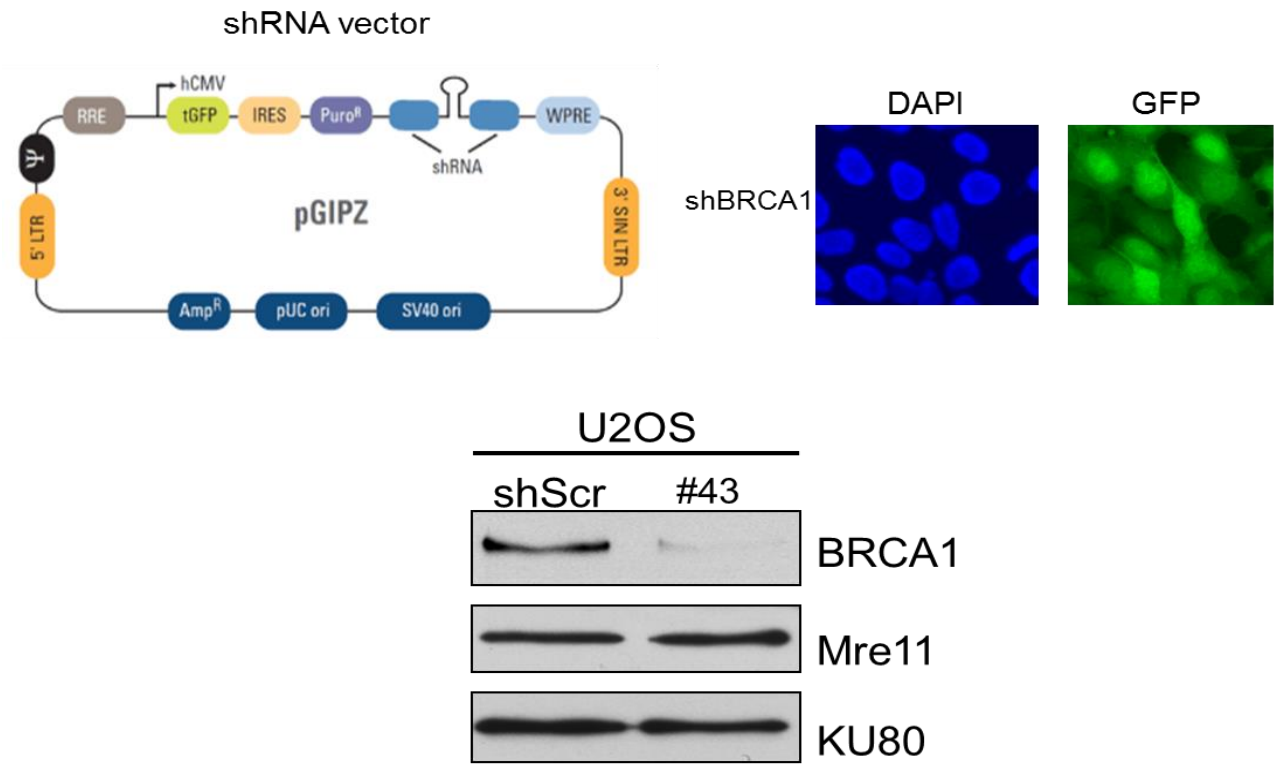

Figure 4.7. Generation of U2OS cell line with stable knockdown of BRCA1. U2OS cell line with stable shRNA-mediated knockdown of BRCA1 was generated by transfection with a pGIPZ vector (5′-TATGTGGTCACACTTTGTG-3′; No.: V2LHS_254648, Thermo Scientific) using Lipofectamine2000 (Invitrogen) followed by selection and continued maintenance in puromycin (1 μg/ml, Invitrogen). Control cells were generated by transfection with a pGIPZ vector expressing scrambled shRNA (No.: RHS4346, Thermo Scientific). pGIPZ vector contained GFP, and its expression helped estimate the transfection efficiency. The rest of the experiments would be done with clone #43 (shBRCA1).

U2OS cancer cells deficient in BRCA1 and Mre11 showed increased radial chromosomes after IR and ABT-888 treatment. Mre11 loss in BRCA1-null cells increased the toxic radial chromosomal structures several fold **(Fig 4.8).** Interestingly, sole depletion of Mre11 in both BRCA1-complemented or BRCA1-null cells did not lead to radial chromosomes, only BRCA1/Mre11-deficient cells in the presence of DNA damaging agent showed several fold increase.

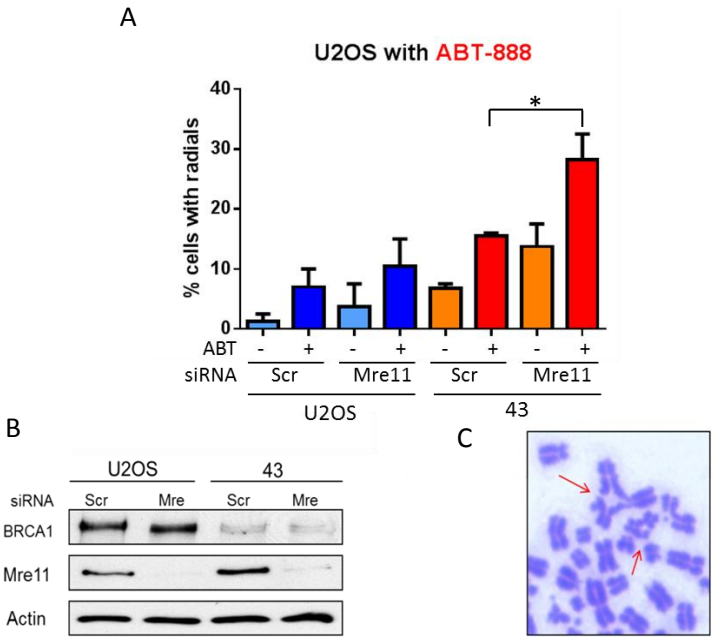

Figure 4.8. Loss of Mre11 leads to increased radial chromosomes in BRCA1-deficient U2OS cancer cells. A. siRNA-mediated knockdown of Mre11 in U2OS BRCA-proficient and #43 BRCA1-deficient cancer cells was accomplished through electroporation followed by lipofection the next day to increase the efficiency of Mre11 knockdown. Cells were treated with 10 µM ABT-888 for 24 h, and colcemid and caffeine were added to the media (Tomimatsu et al., 2014). Metaphase chromosome spreads were prepared after 16 h and scored for radial chromosomes (McEllin et al., 2010). B. Western blot with antibodies against Mre11 verified the knockdown. C. A representative picture of BRCA1-null with knockdown of Mre11 after treatment with ABT-888. Quadradial chromosome structure is indicated by the red arrow.

Mre11 loss in BRCA1-null cancer cells after treatment with ABT-888 caused further abrogation of HR, as seen with greatly reduced Rad51 foci.

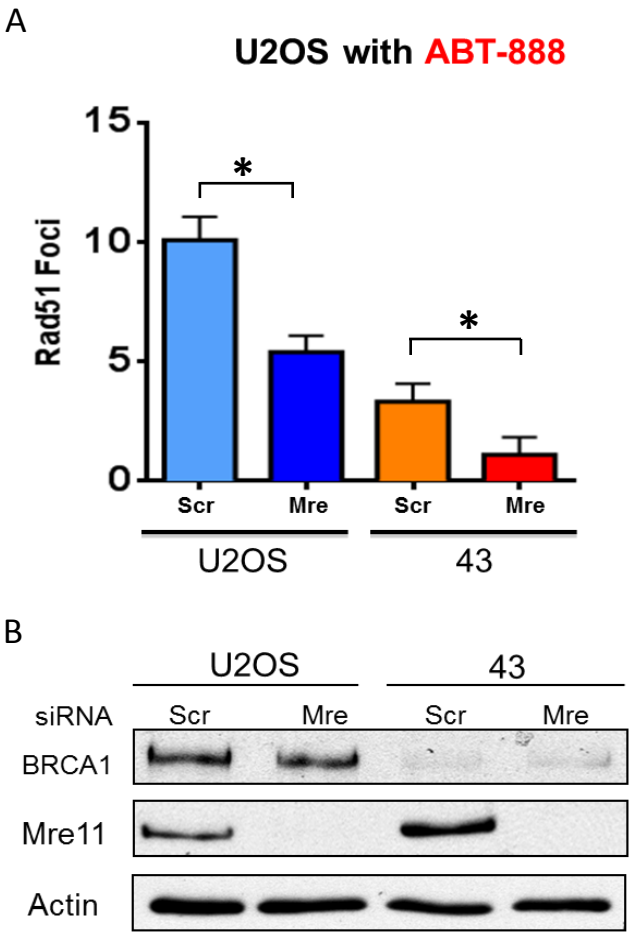

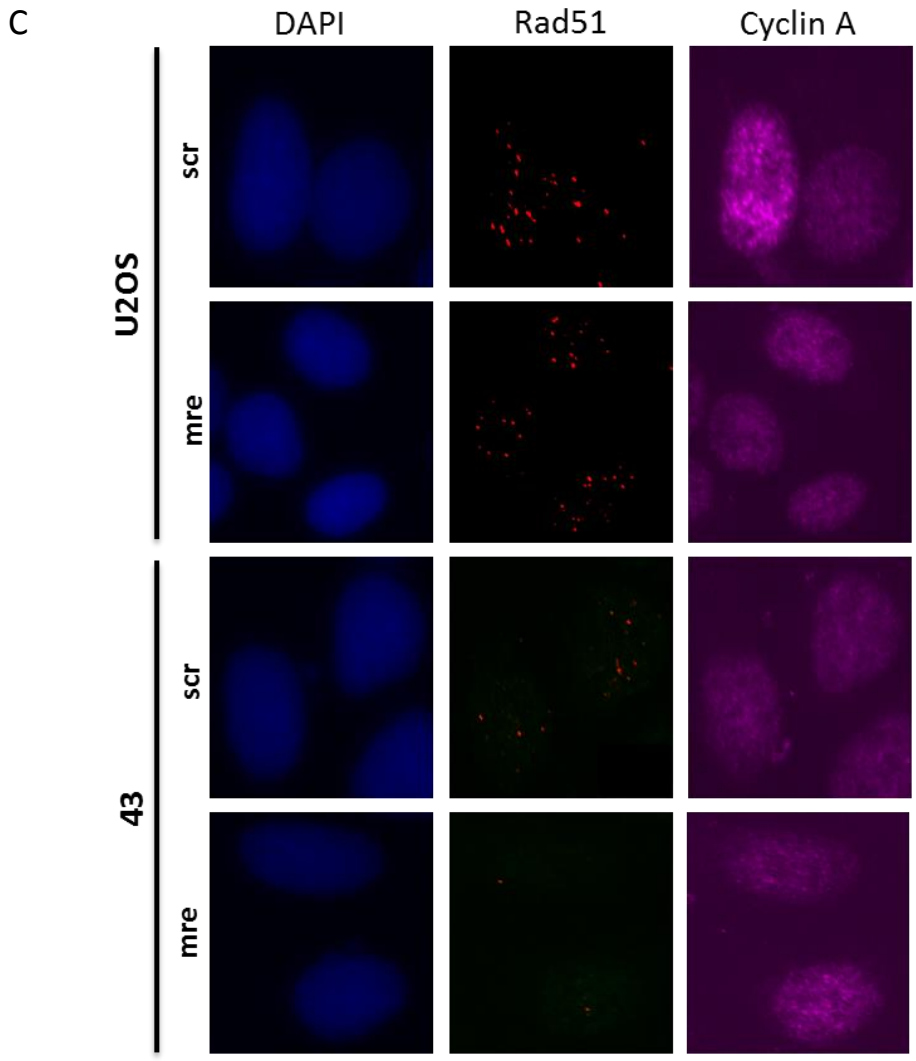

Figure 4.9. Lack of Mre11 further decreases HR in BRCA1-deficient cancer cells. A. In U2OS cells (BRCA1-proficient and BRCA1-null) Mre11 was knocked down by electroporation followed by lipofection (24 h later). B. Western blot confirmed the knock down. U2OS BRCA1-proficient and BRCA1-null cells were treated with 10 μM ABT-888 and after 24 h cells were fixed. Fluorescent antibodies against Rad51 and cyclin A were used. C. Rad51 foci were scored from 50 cells in S/G2 phase (cyclin A +), and after subtracting background (number of foci in untreated nuclei), average foci per nucleus were plotted.

When we measured the sensitivity of U2OS cancer cells to PARP1 inhibitor ABT-888 we observed the expected sensitivity of BRCA1-null cells due to the compromised HR. However, the depletion of Mre11 in BRCA1-null cancer cells led to even greater sensitivity to ABT-888. Again, loss of Mre11 on its own did not significantly increase the sensitivity to the inhibitor in BRCA1-proficient cells, but had a greater impact in BRCA1-null cancer cells.

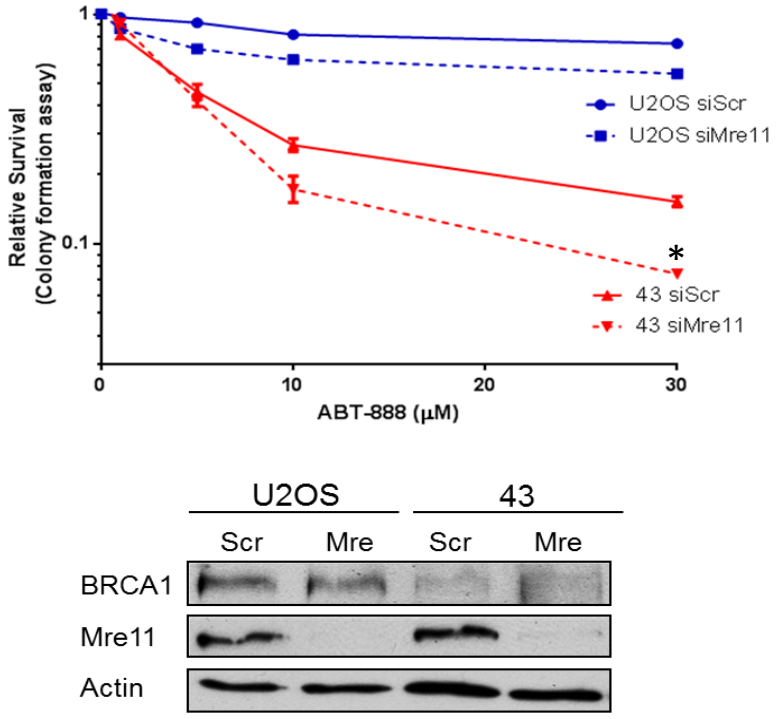

Figure 4.10. Mre11 loss leads to increased sensitivity to the PARP1 inhibitor ABT-888 in U2OS BRCA1-null cancer cells. U2OS cells (BRCA1-proficient and BRCA1-null) with siRNA-mediated knock down of Mre11 were plated in triplicate onto 60-mm dishes (1000 cells per dish) and treated with increasing concentrations of ABT-888. Surviving colonies were stained with crystal violet about 14 days later and colonies containing 50 cells and above were counted.

Mre11 loss led to modest reduction of the hyper-resection in BRCA1-deficient cells. The first step in HR repair is the resection of 5' strands from the DSB ends to develop 3′ tails of single-strand DNA that are bound initially by RPA, which is subsequently exchanged for the Rad51 recombinase (Symington, 2014). Due to loss of BRCA1 and Mre11 in 30 % of BRCA1-deficient breast cancers (Bartkova et al., 2008), we predicted that HR's crucial step of resection is abrogated, and faithful repair cannot be executed. To investigate if resection is greatly reduced when Mre11 is lost, we assessed the formation of RPA foci after treatment with ABT-888, as a surrogate marker for resection **(Fig 4.11).**

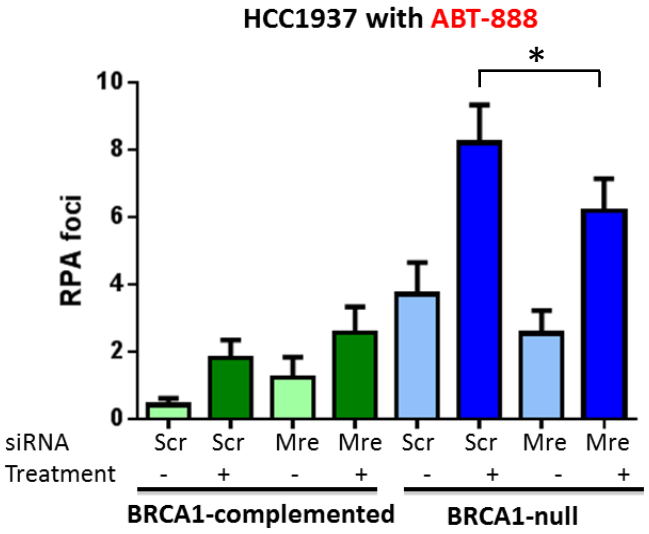

Figure 4.11. Resection is increased in BRCA1-null breast cancers, and Mre11 loss leads to modest decrease. HCC1937 cells (BRCA1-complemented and BRCA1-null) were depleted of endogenous Mre11 using siRNA, and were treated with 10 μM ABT-888 for 24 h. Cells were assayed for RPA foci as an indicator for resection.

Overall DNA end resection, assessed by the number of RPA foci, was increased after treatment with ABT-888 as expected. However, it was a surprise to us that resection in BRCA1-null cells was higher than BRCA1-complemented cells given the role of BRCA1 in HR and resection. On the other hand, Mre11 depletion in BRCA1-null cells reduced resection. The same findings were observed with BrdU/ssDNA assay **(Fig 4.12).**

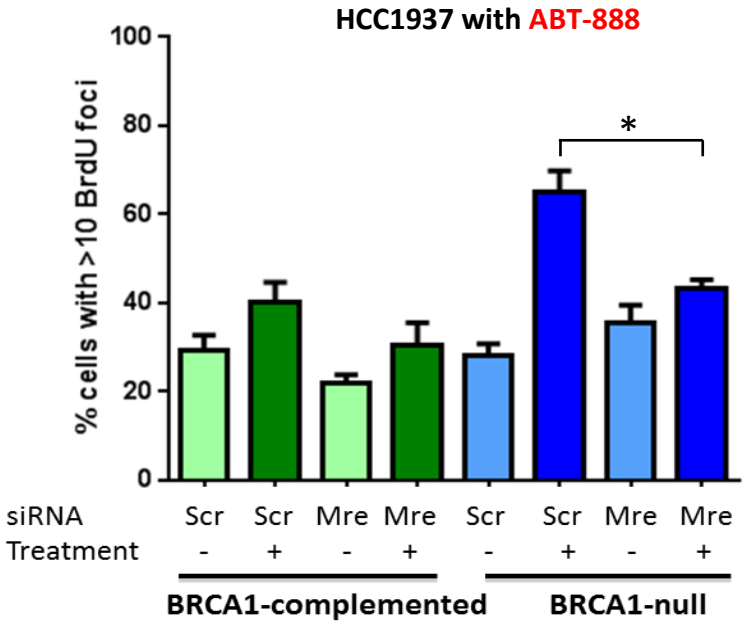

Figure 4.12. Resection is increased in BRCA1-null breast cancers, and Mre11 loss leads to its decrease. HCC1937 cells (BRCA1-complemented and BRCA1-null) with siRNA-mediated knock down of Mre11were treated with 10 μM ABT-888 for 24 h. Nuclei with > 10 BrdU foci were scored as an indicator for resection.

BrdU/ssDNA assay detects DNA incorporated BrdU only if the DNA strand that contains it is exposed to the BrdU antibody, and that serves as a proxy for end resection. Again, BRCA1-null cells had ~ 40% higher resection level than BRCA1-complemented cells after ABT-888 treatment, and Mre11 depletion brought it down with ~ 30%.

Other studies have also reported the same hyper-resection in BRCA1-deficient breast cancers (Durant & Nickoloff, 2005). A study by Tanya Paull, showed that via its ability to bind dsDNA, BRCA1 directly inhibits the endonuclease activity of the MRN complex, and the exonuclease activity of Mre11 alone (Paull, Cortez, Bowers, Elledge, & Gellert, 2001). In our observations, loss of Mre11 reduced the hyper-resection of BRCA1-null cells, albeit not to a great extent, possibly due to the activity of other independent exonucleases such as Exo1, Dna2.

Elucidating the role of Mre11 as a therapeutic target would be beneficial not only to the BRCA1/Mre11-deficient breast cancer population, but Mre11 inhibitors could be assigned in combination with PARP1 inhibitors to target all BRCA1/BRCA2-deficient cancers. The combination of the two inhibitors would reduce the dose required to achieve the therapeutic benefit, hence reducing potential side effects. Currently, there is only one inhibitor of Mre11, Mirin (Dupre et al., 2008). Unfortunately, Mirin is also toxic to normal cells and it is not

clinically available. There is a need for second generation Mre11 inhibitors with better selectivity towards cancer cells.

CDK1/2 inhibition altered HR capacity. We wanted to find another way to further inhibit resection and HR in BRCA1-deficient breast cancer and hyper-sensitize them to PARP inhibitors. Our strategy was to focus on other regulators of end resection, such as CDK1/2 (Trovesi, Manfrini, Falcettoni, & Longhese, 2013). Both short-and long-range resection factors are potentially regulated by CDK1/2 phosphorylation. CDK1/2 phosphorylates MRN complex, CtIP, Ku, PIN1, RPA, Exo1, and DNA2 (Ferretti, Lafranchi, & Sartori, 2013). Due to the crucial role of CDK1/2 in resection and HR overall, we predicted that CDK inhibition would exacerbate the resection defect of BRCA1-deficient cancer cells and hyper-sensitize them to PARP1 inhibitors.

PARP1 inhibitors require one round of replication to induce DSBs. Increased amount of SSBs results in increased replication fork collapse and conversion to DSBs. These one-ended DSBs become substrates for HR repair.

HR is the predominant pathway for repairing one-ended DSB arising in S phase when the replication fork encounters SSB or base damage (Jeggo, Geuting, & Lobrich, 2011). Thus, we wanted to follow the induction kinetics of DSBs in U2OS cells after treatment with ABT-888 in order to find the time of maximum damage **(Fig 4.13).**

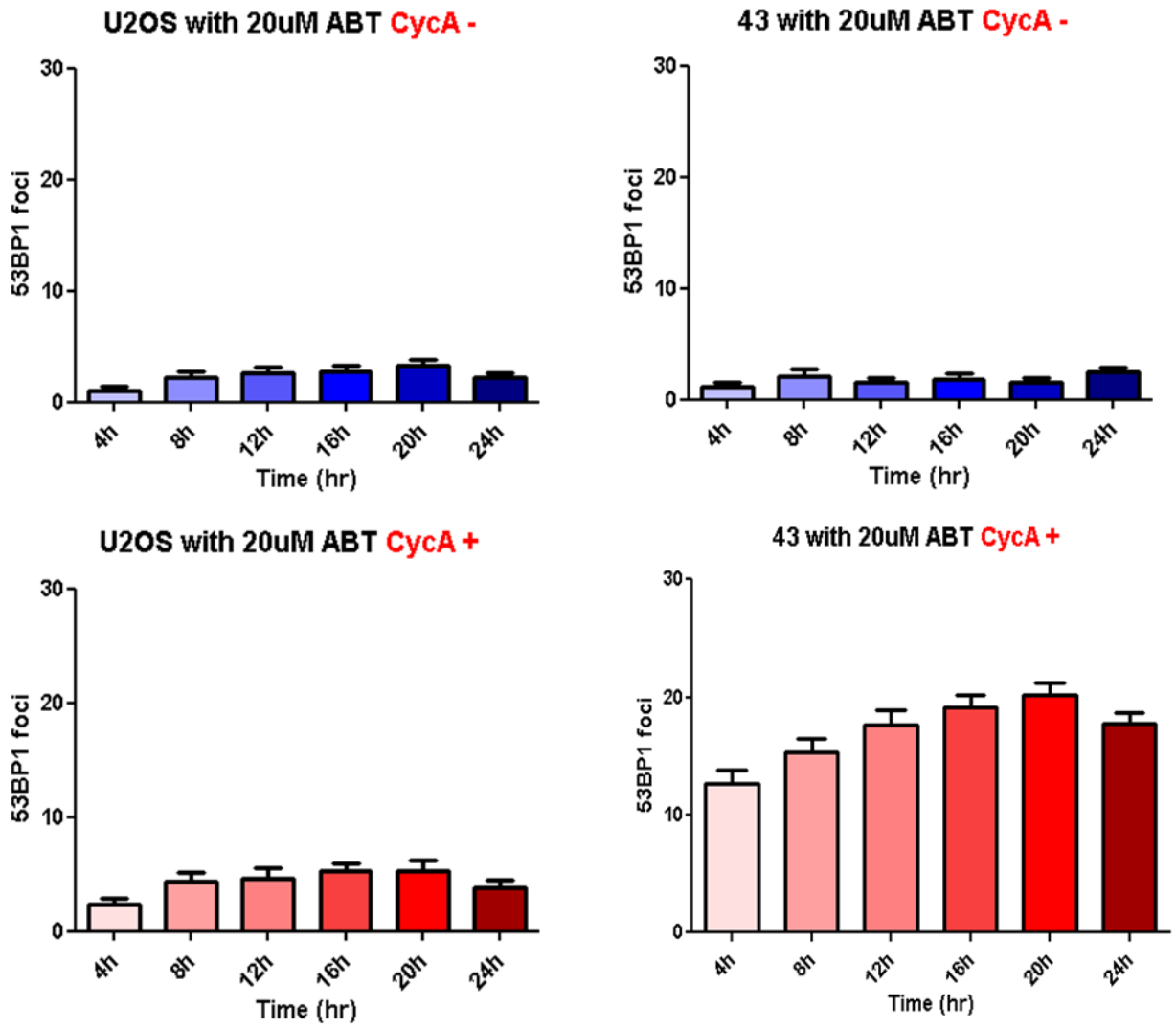

Figure 4.13. Induction kinetics of DSBs in U2OS after ABT-888 treatment. U2OS (BRCA1-proficient) and 43 (BRCA1-deficient) cells were treated with 20 μM ABT-888 over a time-course of 24 h. Every 4 h the cells were fixed and stained for 53BP1 and cyclin A, as markers for DSBs and cell cycle stage, respectively.

As expected BRCA1-proficient cells were not very sensitive to the PARP1 inhibitor, and there was not a significant difference in 53BP1 foci numbers between cyclin A- (G1 phase) and cyclin A+ cells (S/G2 phase). On the other hand, BRCA1-deficient cancer cells showed extensive difference between cyclin A- and cyclin A+ cells. Cyclin A- cells had only a few breaks above background level, while cyclin A+ cells had a ten-fold increase in DSBs. The same result was observed after treatment with another PARP1 inhibitor, olaparib (AZD-2281) **(Fig 4.14)**

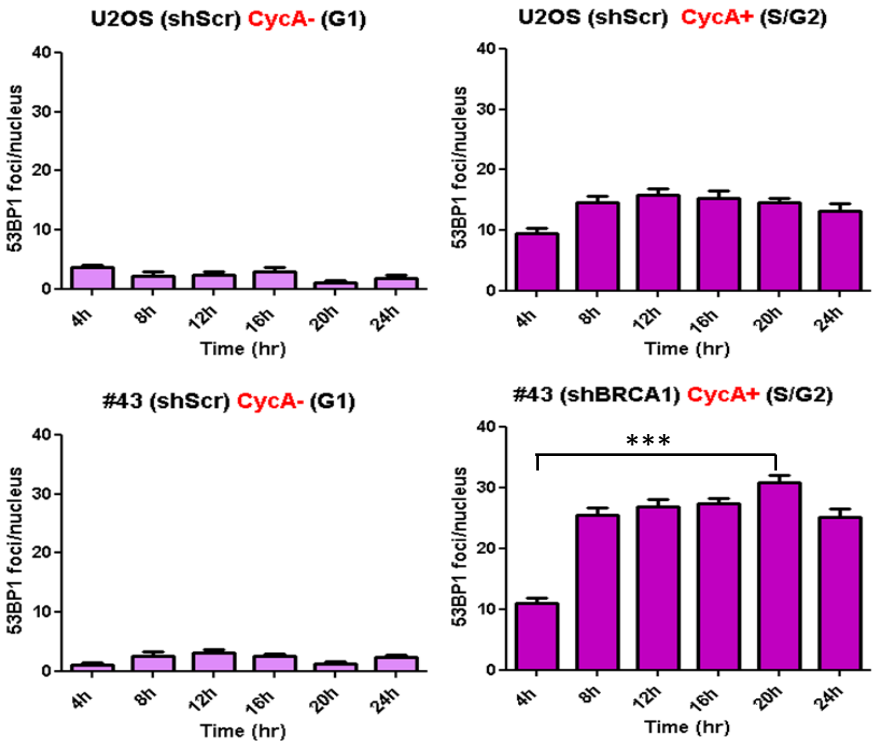

Figure 4.14. PARP1 inhibitor olaparib induced DSBs in S/G2 phase. U2OS (shScr) and #43 (shBRCA1) cells were treated with 10 μM AZD-2281 over a time-course of 24 h. Every 4 h the cells were fixed and stained for 53BP1 and cyclin A, as markers for DSBs and cell cycle stage, respectively.

Maximum induction of DSBs in BRCA1-deficient cells was seen after 20 h of PARP1 inhibitor treatment (both ABT-888 and AZD-2281 showed the same trend). The 20 h treatment confirmed that one round of replication is needed to convert the SSBs, produced after PARP1 inhibition, into DSBs which would be repaired by HR.

To further confirm the induction of DSBs in S/G2 phase after treatment with PARP1 inhibitor, we performed flow cytometry in U2OS cells **(Fig 4.15).** The result verified the above mentioned observations **(Fig 4.13 and 4.14).**

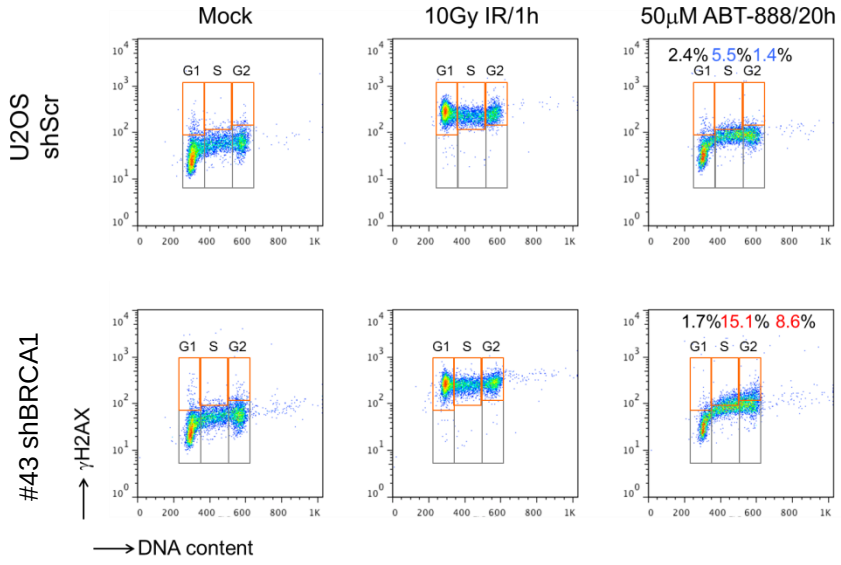

Figure 4.15. PARP1 inhibitor ABT-888 induced DSBs in S/G2 phase. BRCA1-proficient (U2OS shScr) and BRCA1-deficient (#43 shBRCA1) cells were treated with PARPi ABT-888 or irradiated with 10 Gy and harvested at the indicated times. The cells were stained for γH2AX, a marker for DSBs, and propidium iodide which delineates the phases of the cell cycle. #43(shBRCA1) cells showed greater sensitivity to ABT-888 as seen with the increased γH2AX staining. Cells in S/G2 phase of the cell cycle were more sensitive to the PARPi compared to cells in G1 phase.

DSB repair kinetics showed compromised resolution of damage in BRCA1-deficient cells. Furthermore, we wanted to assess the repair of DSBs caused by PARP1 inhibition. Following the repair kinetics in U2OS cells over 24 h showed that BRCA1-deficient cancer cells had ~ 40 % DSBs remaining while BRCA1-proficient cells completely repaired the induced damage **(Fig 4.16).**

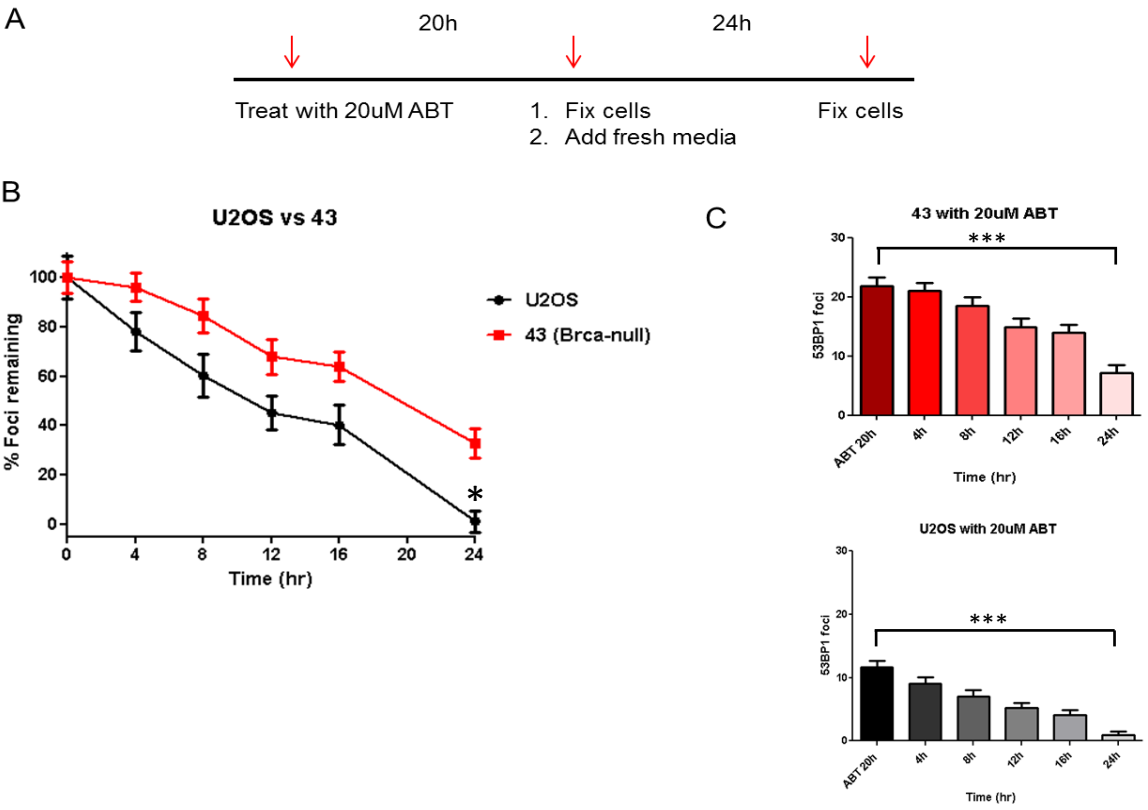

Figure 4.16. DSB repair kinetics in U2OS cells after ABT-888 treatment.
A. U2OS cells (BRCA1-proficient and BRCA1-deficient) were treated with 20 µM ABT-888 for 20 h in order to induce damage. One set of cells were fixed, and in another set of cells, drug-containing media was replaced with fresh media to allow cells to carry out repair for 24 h. Cells were fixed and stained with 53BP1 antibody. B. Percent of 53BP1 foci remaining unrepaired was plotted over 24 h course. C. Figure shows the actual number of 53BP1 foci in U2OS and #43 over the 24 h time-course.

Treatment with CDK1/2 inhibitors further abrogated repair in BRCA1-deficient cancer cells. In order to further abrogate repair in BRCA1-deficient cancer cells we added CDK1/2 inhibitor (AZD-5438) after treatment with PARP1 inhibitor **(Fig 4.17).**

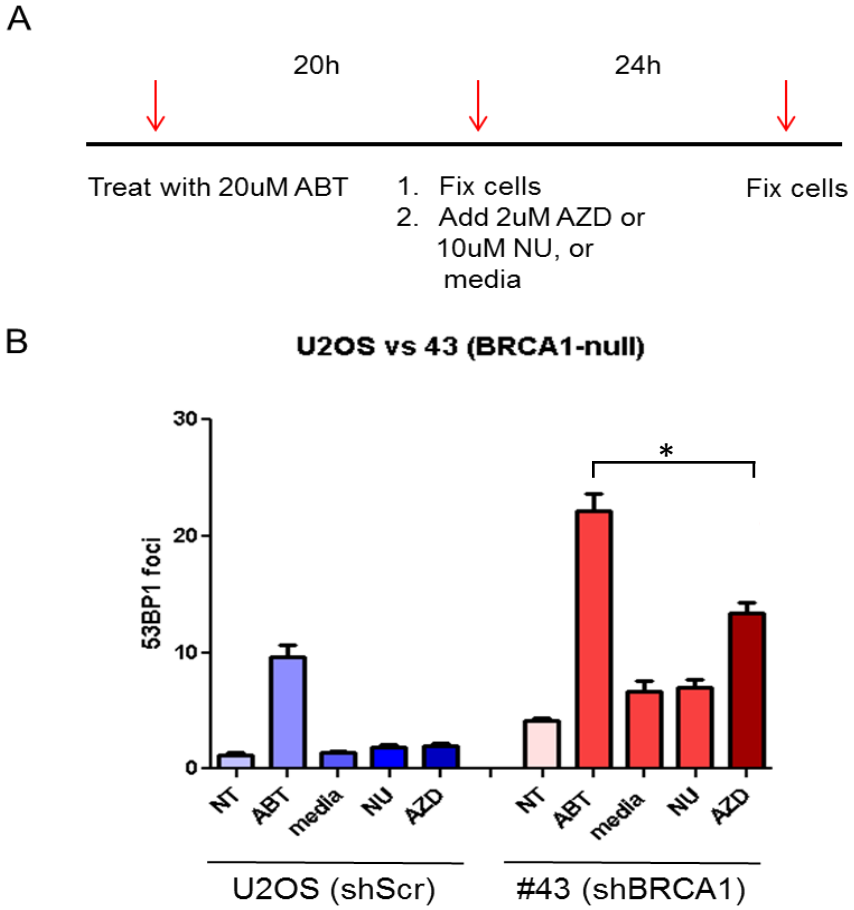

Figure 4.17. Treatment with CDK inhibitor AZD-5438 further abrogates repair in BRCA1-deficient cancer cells. A. U2OS (shScr) and #43 (shBRCA1) cells were treated with 20 μM ABT-888 for 20 h to induce damage. After that cells were either fixed, or treated with10 μM NU-7026 (DNA-PKcs inhibitor), or 2 μM AZD-5438 (CDK1/2 inhibitor), or left in drug-free media for 24 h. B. Cells were stained with 53BP1 antibody and the number of foci was plotted for both cell lines.

The repair of DSBs in BRCA1-deficient cancer cells was abrogated after addition of CDK1/2 inhibitor, while cells left in fresh media repaired the damage more efficiently. In order to rule out repair by NHEJ we treated the cells with potent DNA-PKcs inhibitor (NU-7026). There was no difference between cells left in media or treated with NU-7026; therefore, NHEJ had no contribution to the repair of PARP1 inhibitor induced breaks. Please note that AZD-5438 did not affect the repair of breaks in BRCA1-proficient cells. Thus, combination treatment with CDK1/2 inhibitors would increase the therapeutic window of PARP1 inhibitors in BRCA1-deficient cancer patients. Please note that treatment with CDK1/2 inhibitor AZD-5438 alone did not induce DSBs and was not toxic to the cells **(Fig 4.18).**

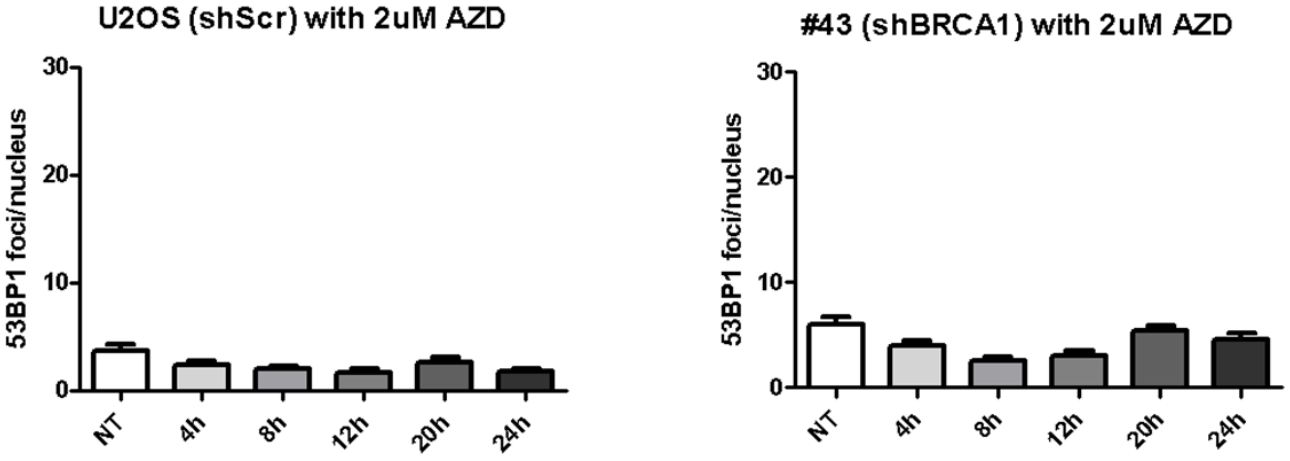

Figure 4.18. CDK1/2 inhibitor AZD-5438 does not induce DSBs. U2OS (shScr) and #43(shBRCA1) cells were treated with 2 μM AZD-5438 over a time-course of 24 h, and cells were fixed every 4 h and stained with 53BP1 antibody. The average number of 53BP1 foci from 50 cells was graphed.

CDK1/2 inhibition rendered BRCA1-deficient cancer cells hyper-sensitive to PARP1 inhibitors. To determine whether CDK1/2 inhibition hyper-sensitized BRCA1-deficient cancer cells to PARP1 inhibitor, we performed colony formation assay **(Fig 4.19).**

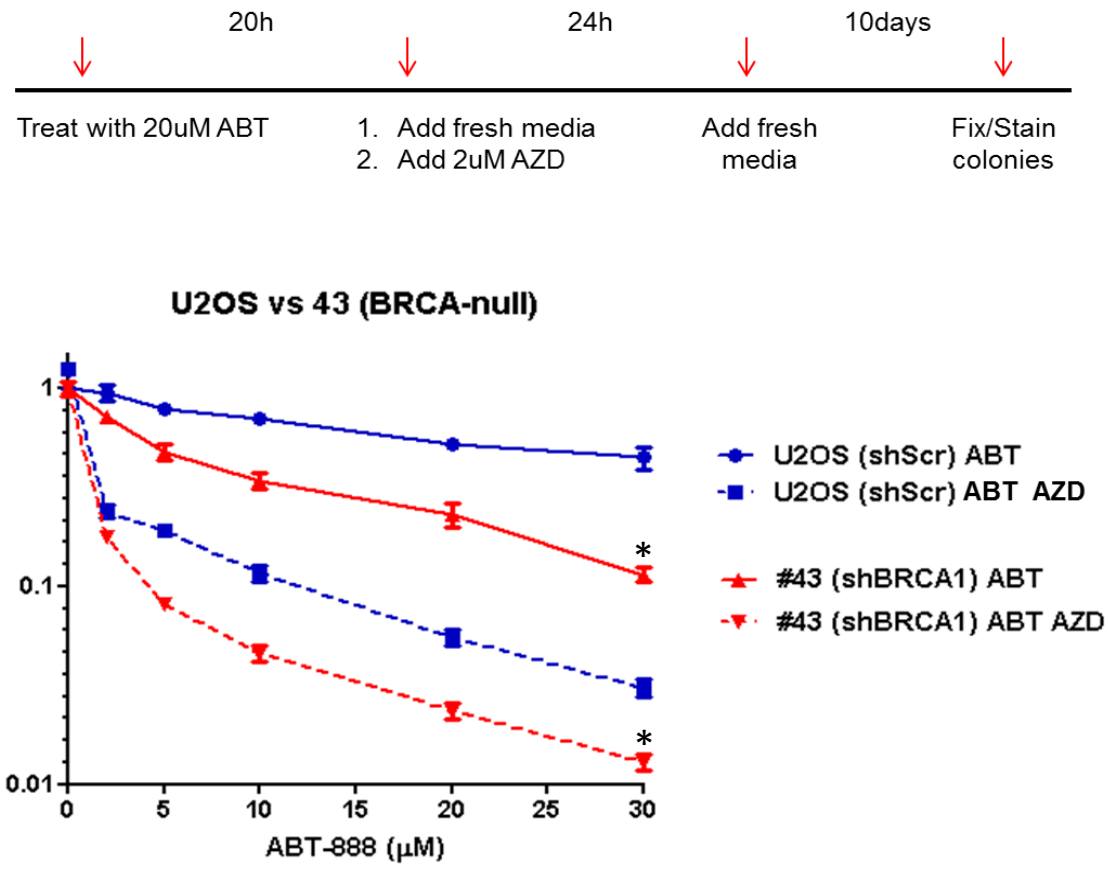

Figure 4.19. CDK inhibition increased the sensitivity of BRCA1-deficient cancer cells to PARP1 inhibitor ABT-888. U2OS cells (shScr and shBRCA1) were treated with 20 μM ABT-888 for 20 h, and after that they were treated with 2 μM AZD-5438 alone for 24 h, or left in fresh media. After 24 h AZD-5438 was removed and fresh media was added. Cells were allowed to grow for ~ 10 days until they reached 50 cells/colony and were stained with crystal violet.

CDK1/2 inhibition led to increased sensitivity to PARP1 inhibitor in both BRCA1-proficient and BRCA1-deficient cancer cells, excluding any role of BRCA1. A possible explanation for the observed result is the fact that CDK1/2 inhibition abrogates not only BRCA1 function, but also Nbs1, CtIP, Exo1, Dna2 which are normally phosphorylated by CDK1. CDK1 inhibition compromises HR due to its important role in both short and long-range resection (Johnson et al., 2011).

This result was not a complete surprise considering the recent study by Johnson N. et al., which showed that depletion or inhibition of CDK1 compromised the ability of cells to repair DNA by HR. Combined inhibition of CDK1 and PARP1 in BRCA1-wild-type cancer cells resulted in reduced colony formation, delayed growth of human tumor xenografts and tumor regression with prolonged survival in a mouse model of lung adenocarcinoma. Reduced CDK1 activity impairs BRCA1 function and consequently repair by HR, thus inhibition of CDK1 represents a favorable strategy for expanding the utility of PARP1 inhibitors to BRCA1-proficient cancers (Johnson et al., 2011).

DISCUSSION

BRCA1 plays an important role in the HR repair pathway, specifically in the initial step of DNA end resection, producing ssDNA substrates for homologous repair. Even though BRCA1-deficient cancers show significant reduction of Rad51 focus formation, indicating compromised HR, this repair pathway is not completely absent in breast cancers (Nakamura et al., 2010). Rad51 foci were reduced by ~ 60 % in BRCA1-deficient cells, however there were 40 % remaining Rad51 foci, thus, HR was still present (Mukhopadhyay et al., 2010). Several independent studies (Nakamura et al., 2010; Schlegel, Jodelka, & Nunez, 2006) showed the same trend, there were ~ 40 % Rad51 foci remaining in BRCA1-deficient cancer cells after cisplatin, HU, AG014699, or radiation treatment. Even though the HR pathway is impaired in BRCA1 mutant cells, it is still present, albeit at lower level.

The role of BRCA1 in DNA-end resection still remains unclear. In 2014, Cruz-Garcia and colleagues have developed a high-resolution method to measure the extent of DNA resection following DNA breaks (Cruz-Garcia, Lopez-Saavedra, & Huertas, 2014). They found that resection occurred in the absence of a BRCA1-CtIP interaction, but the rate of resection was slow, suggesting that BRCA1 modulates its speed. Resection is slower, but still takes place, thus it was imperative for us to find another way to compromise resection and HR. It was very important to find factors that modulate the response of BRCA1-deficient

breast cancers to agents that induce DSBs, mainly occurring in S/G2 phase. We focused our efforts on the Mre11 protein due to its role in resection initiation, and also the fact that 30 % of BRCA1-deficient breast cancers lack Mre11 (Bartkova et al., 2008).

Failure of the BiPar/Sanofi phase III clinical trial of iniparib (BSI-201) had prompted investigations into how the effect of PARP1 inhibitors may be modulated by additional genetic changes, and also how the effectiveness of these inhibitors could be increased. An example of a genetic factor that modulates the sensitivity of BRCA1-deficient cancers to PARP1 inhibitors was shown in 2010 by S.F. Bunting et al., describing the opposing roles of 53BP1 and BRCA1 in DNA end resection. While BRCA1 plays an important role in HR by recruiting nucleases necessary for DNA end resection, 53BP1 protein, a factor for the NHEJ pathway, inhibits HR by blocking resection of DNA breaks. The study showed that loss of 53BP1 alleviates the hypersensitivity of BRCA1 mutant cells to PARP1 inhibition and restores error-free repair by HR (Bunting et al., 2010). Additional studies by Bouwman et al. clearly showed 53BP1 as a factor modulating the response of BRCA1-deficient tumors to PARP1 inhibitors. But is it only 53BP1, or are there additional genetic changes that may modulate the response of these cancers to PARP1 inhibitors? The main goal of this study was to identify and characterize the effects of additional genetic factors that regulate the sensitivity of BRCA1-deficient cancers to PARP1 inhibitors. An excellent

candidate for that role was the Mre11 protein because it is reduced in 30 % of BRCA1-deficient cancers (Bartkova et al., 2008), and also it is involved in HR repair.

In wild-type cells, HR is the predominant repair pathway of DSBs in S/G2 phase, and inter-chromosomal radial fusions are rarely produced. In contrast, BRCA1 deficiency prevents normal HR, so that chromatid breaks, instead of being faithfully repaired, are resolved into aberrant chromatid fusions between heterologous chromosomes (Huen et al., 2010). Characteristic HR aberrations are radial chromosomes, which are abnormal chromosome structures that result from pairing of homologous or non-homologous metaphase chromosomes (Venkitaraman, 2004). These radial chromosomal fusions are dependent on LIG4 (Bunting, 2010), an essential component of the NHEJ pathway. We observed a significant increase in radial chromosomal structures in BRCA1-deficient cancer cells (HCC1937, UWB1 and U2OS) after the loss of Mre11 and treatment with PARP1 inhibitor **(Fig 4.2 and 4.3)**. When we further evaluated the status of HR after Mre11 depletion in BRCA1-proficient and deficient cancer cells after treatment with a PARP1 inhibitor, we found a greater decrease of Rad51 foci in cells lacking both BRCA1 and Mre11 **(Fig 4.4 and 4.5).** Furthermore, the absence of Mre11 in these cancers led to a heightened sensitivity to PARP1 inhibitors **(Fig 4.6).** We speculate that breast cancer cells can handle individual loss of BRCA1, or Mre11, but the loss of both proteins at the same time is detrimental for HR.

We hypothesized that the elevated sensitivity to PARP1 inhibitor after loss of Mre11 was due to the essential role of Mre11 in resection initiation. We expected further reduction of resection in BRCA1-deficient cells, which we quantified by RPA and BrdU foci. To our surprise, we saw the opposite effect; there was an increased number of RPA and BrdU foci in BRCA1-deficient cells, indicating increased resection **(Fig 4.7).** In fact, the same observation was seen by Choudhary S.K. et al. in HCC1937 cells. They reported that after IR treatment BRCA1 and RPA form punctate nuclear staining patterns that co-localize with each other and, in BRCA1-deficient cells, the number of RPA foci increased significantly. Therefore, BRCA1 may remove RPA at the site of a DSB and facilitate the loading of proteins such as Rad51 (Choudhary & Li, 2002). Also, the mechanism of hyper-resection in BRCA1-deficient cancer cells has been addressed by the studies of Hu et al., and Dever et al. They found that ablation of the BRCA1-Abraxas interaction promotes extensive resection, as visualized by an increase in ssDNA abundance and chromatin retention of RPA. Elevated binding of RPA is indicative of more abundant or longer stretches of resected ssDNA.

Furthermore, Paull et al. showed that BRCA1 protein binds strongly to DNA, an activity conferred by a domain in the center of the BRCA1 polypeptide, and as a result of this binding BRCA1 inhibits the nucleolytic activities of the MRN complex (Paull et al., 2001).

Loss of Mre11 did not further increase resection in BRCA1-deficient cancer cells, on the contrary; it reduced its level, albeit not to the wild-type level. This is probably due to the endo- and exonuclease activity of Mre11, and its role in short-range resection. However, Mre11 loss did not restore resection to wild type levels in BRCA1-deficient cells possible due to the activity of other nucleases such as CtIP, Exo1, and Dna2. Also the hyper-resection could be the result of the long-range resection where Mre11 does not play a role.

Since there is no Mre11 inhibitor available in the clinic (due to high toxicity), we devised another strategy to further alter resection and HR in BRCA1-deficient cancers. We pharmacologically targeted the important regulator of resection, CDK1/2. A study done by Neil Johnson et al., showed that non-transformed cells, which arrested in G2-M after inhibition of CDK1, probably did not accumulate SSBs followed by DSBs because they did not accumulate γ-H2AX, and were therefore not sensitive to the combined inhibition of CDK1 and PARP1,thus presenting a therapeutic window. Based on the principle of synthetic lethality, PARP1 and CDK1/2 inhibition has the potential to improve the effectiveness of breast cancer therapy.

CHAPTER V

Conclusions and Future Directions

CONCLUSIONS AND FUTURE DIRECTIONS

Failure to properly repair damaged DNA contributes to the development of many diseases including cancer. This work focused on DNA damage responses and ways to utilize them to improve the efficacy of breast cancer therapy.

Among all types of cancer, breast cancer is the second leading cause of cancer death for women in the United States (American Cancer Society, 2015). Specifically, the tumor suppressor BRCA1 has taken central stage being involved in diverse cellular processes that ensure genome stability and promote cell survival. BRCA1 plays an important role in the HR repair pathway, taking part in the initial step of resecting the DNA ends and producing ssDNA substrates for HR. Germline mutations of the BRCA1 gene account for most hereditary cases of breast and ovarian cancer.

In 2005, two independent groups, H. Bryant et al. and H. Farmer et al., discovered the highly selective anticancer activity of PARP1 inhibition in BRCA1 and BRCA2-deficient breast cancers. Since then, PARP1 inhibitors have proven to be a very effective treatment, either alone or in combination with chemotherapy, in the fight against specific subtypes of breast cancer. Despite the initial success of PARP1 inhibitors, not all BRCA1-deficient breast cancers respond to it, or there is an acquired resistance to the inhibitors. Thus, it was very important to find other effective treatments, and/or factors that could improve the sensitivity of BRCA1-deficient breast cancers to PARP1 inhibitors.

The work presented here is the first attempt to describe the mechanism of action of a novel anti-cancer agent, IB-DNQ, for improving the efficacy of breast cancer therapy. Also, we evaluated the role of BRCA1 in modulating the sensitivity of breast cancers to IB-DNQ. Another major goal of this work was to assess the role of Mre11 as a factor modulating the response of BRCA1-deficient breast cancers to PARP-1 inhibitors. We speculated that additional loss of Mre11 in BRCA1-deficient breast cancers may exacerbate the DNA resection defect of these cancers and hyper-sensitize them to PARP1 inhibitors. The first part of this work focused on PARP1 hyperactivation, while the second part focused on hypersensitivity to PARP1 inhibitors.

We discovered that IB-DNQ is an excellent drug for the treatment of solid cancers, such as breast cancers, with higher potency than β-lapachone. IB-DNQ undergoes a futile cycle, where it is bioreduced by NQO1 enzyme to produce overwhelmingly high levels of ROS (H_2O_2). Normally, cells eliminate toxic H_2O_2 using endogenous catalase. The selectivity of IB-DNQ is based on the fact that ~ 60 % of cancers have high amount of NQO1 and low level of catalase, while normal cells have high catalase and low or no NQO1 **(Fig 2.1).** The different NQO1: Catalase ratios between tumor and normal tissue allow discrimination of the two populations, presenting excellent therapeutic window. The amount of ROS, produced by IB-DNQ in NQO1- expressing cancer cells, exceeds a "tolerable threshold" and hyperactivates PARP1. The core mechanism of IB-

DNQ-induced cytotoxicity lies on PARP1 hyperactivation. We want to emphasize that hyperactivated PARP1 does not mean that PARP1 is more active in DNA repair, on contrary, PARP1 hyperactivation inhibits PARP1 repair activity. PARP1 and PARG are responsible for a tight balance between PAR production and degradation. Any dysregulation of this balance towards an over production of PAR is detrimental for the cell due to NAD+ over consumption. The PARP1 hyperactivation, upon massive IB-DNQ-induced DNA damage, was responsible for 80-90% loss of cellular NAD+/ATP **(Fig 2.5).**

A cell can die through apoptosis, necrosis, or even necroptosis (programmed necrosis) (Han et al., 2011). The type of cell death that IB-DNQ induced we named NAD-Keresis, described in (Moore et al., 2015). NAD-Keresis death is due to the extensive loss of NAD+/ATP, not to the increased amount of PAR formed in the cell (as with parthanatos death).

Preliminary data from Boothman lab showed that IB-DNQ-induced damage activated BER, NHEJ and HR repair pathways. When we tried to synergize IB-DNQ with inhibitors of these pathways, only BER inhibitor (MeOX) increased the sensitivity of breast cancer cells to IB-DNQ. After removal of the damaged bases by glycosylases, MeOX binds to AP sites and prevents further repair of the base damage. Methoxyamine potentiates IB-DNQ cytotoxicity and allows the use of very low doses of IB-DNQ, significantly reducing potential side effects. Future in vivo studies will address the predicted equivalent antitumor efficacy of IB-

DNQ to β-lapachone and DNQ, but with much greater potency at lower doses. These findings offer preclinical proof-of-concept for IB-DNQ as a potent chemotherapeutic agent for the treatment of breast cancers, especially in combination with MeOX.

In addition, we wanted to determine if breast cancers with vulnerability, such as BRCA1-deficient cancers with impaired HR, would have increased sensitivity to IB-DNQ, thus lower doses of the agent could be used to achieve the same efficacy. We used HCC1937 breast cancer cells, deficient in BRCA1, which showed ten-fold greater sensitivity to IB-DNQ than their BRCA1-complemented counterparts. However, when we tried to recapitulate the same phenotype in another breast cancer cell line with stable knock down of BRCA1 (MCF7 shScr and shBRCA8), we could not find substantial difference between BRCA1-proficient and BRCA1-deficient cancer cells. After assessing the amount of ROS produced in HCC1937 cells after treatment with IB-DNQ, we found that BRCA1-deficient cells had two-fold higher ROS levels. The elevated ROS production was a result of the increased NQO1 enzyme activity in BRCA1-deficient cells compared to BRCA1-proficient cells (1000 U vs. 400 U, respectively). This observation was surprising considering the recent study by Li et al. showing that β-lapachone-mediated cell death requires > 90 enzymatic units of NQO1. Cells having NQO1 activity above 90 U, as with the case of BRCA1-deficient and BRCA1-proficinet HCC1937 cells, should be equally sensitive to IB-DNQ. The

HCC1937 cell line might be an exception, and additional BRCA1-deficient breast cancers need to be analyzed.

Future studies will be focused on potentiating the cytotoxicity of IB-DNQ by combination treatment with agents that can increase the H_2O_2 levels in the cell. Excellent candidates for that are SOD (superoxide dismutase) inhibitors such as diethyldithiocarbamate (Khazaei, Moien-Afshari, Elmi, Mirdamadi, & Laher, 2009). Also, we need to optimize the solubility of IB-DNQ in vivo and ensure that it reaches its target and kills the cancer cells.

In addition, we need to explore the relationship between BRCA1 and PARP1, and find ways to exploit it. There are a few studies starting to uncover the crosstalk between BRCA1 and PARP1 (D. Li et al., 2014) showing that BRCA1 inactivation events were accompanied by increased PARP1 and NAD levels, and a subsequent increase in PARP1 activity. We suggest screening breast cancer patients to determine the status of BRCA1, PARP1 and NQO1, and based on their activities to design the optimal personalized treatment.

The main objective of this work was to improve the efficacy of breast cancer treatment utilizing PARP1's role in DNA damage repair. The first strategy to achieve that was based on PARP1 hyperactivation and programmed necrosis (NAD-Keresis), while the second one was based on factors increasing the sensitivity to PARP1 inhibition and apoptosis. We focused on Mre11 protein as a factor modulating the response of BRCA1-deficient breast cancers to PARP1

inhibitors due to its role in resection initiation, and the fact that 30 % of BRCA1-deficient breast cancers have very low or no Mre11 protein (Bartkova et al., 2008). After treatment with PARP1 inhibitor BRCA1/Mre11-deficient breast cancers showed increased genomic instability, as seen with increased radial chromosomes, and impaired resolution of DSBs. Knockdown of Mre11 rendered BRCA1-deficient cancers hypersensitive to PARP1 inhibitors. Hypersensitivity to PARP1 inhibitors in BRCA1/Mre11-deficient cells may be due to defect in HR (due to low Rad51 foci), but this defect was not on the level of resection as we discovered (Chapter IV). The increased chromosomal aberrations seen after treatment with PARP1 inhibitor in BRCA1/Mre11-deficient cancer cells might be due to Mre11's role in proper metaphase chromosome alignment. It has been reported that loss of MRN function triggers a metaphase delay and disrupts the RCC1-dependent RanGTP gradient (Rozier et al., 2013).

CDK1/2 inhibition was another good strategy to hypersensitize BRCA1-deficient cancers to PARP1 inhibitors. The combination treatment of PARP1 and CDK1/2 inhibitors prevented complete repair of DSBs, and increased the sensitivity to PARP1 inhibitors.

Also, Polθ (also known as PolQ) was recently identified as a crucial alternative NHEJ factor in mammalian cells (Mateos-Gomez et al., 2015). Although POLQ expression in normal human tissues is generally repressed, it is upregulated in a wide range of human cancers and associates with poor clinical

outcome in breast tumors (Higgins et al., 2010). The findings that cells with compromised HR activity depend on this mutagenic polymerase for survival establish the foundation for the development of Polθ-targeted approaches for cancer treatment.

Future studies will utilize CRISPR Cas9 system to completely eliminate Mre11 and evaluate the function of HR in its absence. Furthermore, we will expand our studies in a panel of breast cancer cell lines with different levels of Mre11, and evaluate their sensitivity to PARP1 inhibitors. Certainly, we need to examine other factors that could modulate the sensitivity to PARP1 inhibitors. Studies done by Simon Powell and colleagues report of a HR "back-up" pathway, in the absence of BRCA1, that is mediated by Rad52 (Lok & Powell, 2012). We need to focus not only on factors involved in resection initiation, but also on long-range resection and find targetable proteins. Another consideration is the role of Rad51 in HR; overexpression of Rad51 in cells with normal HR can be deleterious, while overexpression in cells with HR defect can be beneficial (Martin et al., 2007). Thus, it is important to evaluate patients for their Rad51 status.

Another emerging question is 'what is the role of the 16 additional PARPs', most of which modify proteins with mono-ADP-ribose (MAR); their biology is less well understood. Recent data identified potentially cancer-relevant functions

for these PARPs, which indicates that we need to understand more about these PARPs to effectively target them (Vyas & Chang, 2014).

We need to consider the role of NHEJ in the absence of HR pathway. There are several studies that show PARP1's function in suppressing various components of NHEJ pathway, such as Ku and LIG4 (Hochegger et al., 2006). Moreover, Ku and DNA-PKcs are capable of binding to PAR (Gagne et al., 2008). PARP1 inhibition induces phosphorylation of DNA-PK targets and enhances NHEJ (Patel et al., 2011). It would be important to determine the effect of combined treatment with PARP1 and DNA-PK inhibitors.

An important future study would be to find out how the extent of resection is regulated, and how hyper-resection or hypo-resection is prevented. BRCA1 has been shown to inhibit the nuclease activity of Mre11, and this inhibition is required for precise DSB repair. But how is resection regulated in BRCA1-deficient cancers? We observed hyper-resection in BRCA1-deficient cancers, which could result in the acquisition of new mutations leading to more aggressive tumors. Therefore, it would be important to understand how BRCA1/Mre11-deficient breast cancers repair replication associated DSBs, and how they escape from mitotic catastrophe.

BIBLIOGRAPHY

BIBLIOGRAPHY

Alexander, N. M. (1957). Catalase inhibition by normal and neoplastic tissue extracts. *J Biol Chem, 227*(2), 975-985.

Aly, A., & Ganesan, S. (2011). BRCA1, PARP, and 53BP1: conditional synthetic lethality and synthetic viability. *J Mol Cell Biol, 3*(1), 66-74. doi: 10.1093/jmcb/mjq055

Andrabi, S. A., Kim, N. S., Yu, S. W., Wang, H., Koh, D. W., Sasaki, M., . . . Dawson, T. M. (2006). Poly(ADP-ribose) (PAR) polymer is a death signal. *Proc Natl Acad Sci U S A, 103*(48), 18308-18313. doi: 10.1073/pnas.0606526103

Aparicio, T., Baer, R., & Gautier, J. (2014). DNA double-strand break repair pathway choice and cancer. *DNA Repair (Amst), 19*, 169-175. doi: 10.1016/j.dnarep.2014.03.014

Ashworth, A. (2008). Drug resistance caused by reversion mutation. *Cancer Res, 68*(24), 10021-10023. doi: 10.1158/0008-5472.can-08-2287

Balmana, J., Domchek, S. M., Tutt, A., & Garber, J. E. (2011). Stumbling blocks on the path to personalized medicine in breast cancer: the case of PARP inhibitors for BRCA1/2-associated cancers. *Cancer Discov, 1*(1), 29-34. doi: 10.1158/2159-8274.cd-11-0048

Bartkova, J., Tommiska, J., Oplustilova, L., Aaltonen, K., Tamminen, A., Heikkinen, T., . . . Bartek, J. (2008). Aberrations of the MRE11-RAD50-NBS1 DNA damage sensor complex in human breast cancer: MRE11 as a candidate familial cancer-predisposing gene. *Mol Oncol, 2*(4), 296-316. doi: 10.1016/j.molonc.2008.09.007

Bassing, C. H., & Alt, F. W. (2004). The cellular response to general and programmed DNA double strand breaks. *DNA Repair (Amst), 3*(8-9), 781-796. doi: 10.1016/j.dnarep.2004.06.001

Bentle, M. S., Bey, E. A., Dong, Y., Reinicke, K. E., & Boothman, D. A. (2006). New tricks for old drugs: the anticarcinogenic potential of DNA repair inhibitors. *J Mol Histol, 37*(5-7), 203-218. doi: 10.1007/s10735-006-9043-8

Bentle, M. S., Reinicke, K. E., Bey, E. A., Spitz, D. R., & Boothman, D. A. (2006). Calcium-dependent modulation of poly(ADP-ribose) polymerase-1 alters cellular metabolism and DNA repair. *J Biol Chem, 281*(44), 33684-33696. doi: 10.1074/jbc.M603678200

Bentle, M. S., Reinicke, K. E., Dong, Y., Bey, E. A., & Boothman, D. A. (2007). Nonhomologous end joining is essential for cellular resistance to the novel antitumor agent, beta-lapachone. *Cancer Res, 67*(14), 6936-6945. doi: 10.1158/0008-5472.can-07-0935

Berger, N. A. (1985). Poly(ADP-ribose) in the cellular response to DNA damage. *Radiat Res, 101*(1), 4-15.

Bey, E. A., Reinicke, K. E., Srougi, M. C., Varnes, M., Anderson, V. E., Pink, J. J., . . . Boothman, D. A. (2013). Catalase abrogates beta-lapachone-induced PARP1

hyperactivation-directed programmed necrosis in NQO1-positive breast cancers. *Mol Cancer Ther, 12*(10), 2110-2120. doi: 10.1158/1535-7163.mct-12-0962

Blanco, E., Bey, E. A., Khemtong, C., Yang, S. G., Setti-Guthi, J., Chen, H., . . . Gao, J. (2010). Beta-lapachone micellar nanotherapeutics for non-small cell lung cancer therapy. *Cancer Res, 70*(10), 3896-3904. doi: 10.1158/0008-5472.can-09-3995

Bryant, H. E., Petermann, E., Schultz, N., Jemth, A. S., Loseva, O., Issaeva, N., . . . Helleday, T. (2009). PARP is activated at stalled forks to mediate Mre11-dependent replication restart and recombination. *EMBO J, 28*(17), 2601-2615. doi: 10.1038/emboj.2009.206

Bryant, H. E., Schultz, N., Thomas, H. D., Parker, K. M., Flower, D., Lopez, E., . . . Helleday, T. (2005). Specific killing of BRCA2-deficient tumours with inhibitors of poly(ADP-ribose) polymerase. *Nature, 434*(7035), 913-917. doi: 10.1038/nature03443

Buis, J., Stoneham, T., Spehalski, E., & Ferguson, D. O. (2012). Mre11 regulates CtIP-dependent double-strand break repair by interaction with CDK2. *Nat Struct Mol Biol, 19*(2), 246-252. doi: 10.1038/nsmb.2212

Bunting, S. F., Callen, E., Wong, N., Chen, H. T., Polato, F., Gunn, A., . . . Nussenzweig, A. (2010). 53BP1 inhibits homologous recombination in Brca1-deficient cells by blocking resection of DNA breaks. *Cell, 141*(2), 243-254. doi: 10.1016/j.cell.2010.03.012

Cao, L., Xu, X., Bunting, S. F., Liu, J., Wang, R. H., Cao, L. L., . . . Finkel, T. (2009). A selective requirement for 53BP1 in the biological response to genomic instability induced by Brca1 deficiency. *Mol Cell, 35*(4), 534-541. doi: 10.1016/j.molcel.2009.06.037

Chen, L., Nievera, C. J., Lee, A. Y., & Wu, X. (2008). Cell cycle-dependent complex formation of BRCA1.CtIP.MRN is important for DNA double-strand break repair. *J Biol Chem, 283*(12), 7713-7720. doi: 10.1074/jbc.M710245200

Choudhary, S. K., & Li, R. (2002). BRCA1 modulates ionizing radiation-induced nuclear focus formation by the replication protein A p34 subunit. *J Cell Biochem, 84*(4), 666-674.

Chuang, H. C., Kapuriya, N., Kulp, S. K., Chen, C. S., & Shapiro, C. L. (2012). Differential anti-proliferative activities of poly(ADP-ribose) polymerase (PARP) inhibitors in triple-negative breast cancer cells. *Breast Cancer Res Treat, 134*(2), 649-659. doi: 10.1007/s10549-012-2106-5

Cortazzo, J. A., & Lichtman, A. D. (2014). Methemoglobinemia: a review and recommendations for management. *J Cardiothorac Vasc Anesth, 28*(4), 1055-1059. doi: 10.1053/j.jvca.2013.02.005

Cruz-Garcia, A., Lopez-Saavedra, A., & Huertas, P. (2014). BRCA1 accelerates CtIP-mediated DNA-end resection. *Cell Rep, 9*(2), 451-459. doi: 10.1016/j.celrep.2014.08.076

Cuadrado, M., Martinez-Pastor, B., Murga, M., Toledo, L. I., Gutierrez-Martinez, P., Lopez, E., & Fernandez-Capetillo, O. (2006). ATM regulates ATR chromatin

loading in response to DNA double-strand breaks. *J Exp Med, 203*(2), 297-303. doi: 10.1084/jem.20051923

Curtin, N. J., & Szabo, C. (2013). Therapeutic applications of PARP inhibitors: anticancer therapy and beyond. *Mol Aspects Med, 34*(6), 1217-1256. doi: 10.1016/j.mam.2013.01.006

D'Amours, D., & Jackson, S. P. (2002). The Mre11 complex: at the crossroads of dna repair and checkpoint signalling. *Nat Rev Mol Cell Biol, 3*(5), 317-327. doi: 10.1038/nrm805

David, K. K., Andrabi, S. A., Dawson, T. M., & Dawson, V. L. (2009). Parthanatos, a messenger of death. *Front Biosci (Landmark Ed), 14*, 1116-1128.

De Lorenzo, S. B., Patel, A. G., Hurley, R. M., & Kaufmann, S. H. (2013). The Elephant and the Blind Men: Making Sense of PARP Inhibitors in Homologous Recombination Deficient Tumor Cells. *Front Oncol, 3*, 228. doi: 10.3389/fonc.2013.00228

de Murcia, J. M., Niedergang, C., Trucco, C., Ricoul, M., Dutrillaux, B., Mark, M., . . . de Murcia, G. (1997). Requirement of poly(ADP-ribose) polymerase in recovery from DNA damage in mice and in cells. *Proc Natl Acad Sci U S A, 94*(14), 7303-7307.

Dedes, K. J., Wetterskog, D., Mendes-Pereira, A. M., Natrajan, R., Lambros, M. B., Geyer, F. C., . . . Reis-Filho, J. S. (2010). PTEN deficiency in endometrioid endometrial adenocarcinomas predicts sensitivity to PARP inhibitors. *Sci Transl Med, 2*(53), 53ra75. doi: 10.1126/scitranslmed.3001538

Dedes, K. J., Wilkerson, P. M., Wetterskog, D., Weigelt, B., Ashworth, A., & Reis-Filho, J. S. (2011). Synthetic lethality of PARP inhibition in cancers lacking BRCA1 and BRCA2 mutations. *Cell Cycle, 10*(8), 1192-1199.

DelloRusso, C., Welcsh, P. L., Wang, W., Garcia, R. L., King, M. C., & Swisher, E. M. (2007). Functional characterization of a novel BRCA1-null ovarian cancer cell line in response to ionizing radiation. *Mol Cancer Res, 5*(1), 35-45. doi: 10.1158/1541-7786.mcr-06-0234

Dong, Y., Bey, E. A., Li, L. S., Kabbani, W., Yan, J., Xie, X. J., . . . Boothman, D. A. (2010). Prostate cancer radiosensitization through poly(ADP-Ribose) polymerase-1 hyperactivation. *Cancer Res, 70*(20), 8088-8096. doi: 10.1158/0008-5472.can-10-1418

Drost, R., Bouwman, P., Rottenberg, S., Boon, U., Schut, E., Klarenbeek, S., . . . Jonkers, J. (2011). BRCA1 RING function is essential for tumor suppression but dispensable for therapy resistance. *Cancer Cell, 20*(6), 797-809. doi: 10.1016/j.ccr.2011.11.014

Dumitriu, I. E., Voll, R. E., Kolowos, W., Gaipl, U. S., Heyder, P., Kalden, J. R., & Herrmann, M. (2004). UV irradiation inhibits ABC transporters via generation of ADP-ribose by concerted action of poly(ADP-ribose) polymerase-1 and glycohydrolase. *Cell Death Differ, 11*(3), 314-320. doi: 10.1038/sj.cdd.4401348

Dupre, A., Boyer-Chatenet, L., Sattler, R. M., Modi, A. P., Lee, J. H., Nicolette, M. L., . . . Gautier, J. (2008). A forward chemical genetic screen reveals an inhibitor of the

Mre11-Rad50-Nbs1 complex. *Nat Chem Biol, 4*(2), 119-125. doi: 10.1038/nchembio.63

Durant, S. T., & Nickoloff, J. A. (2005). Good timing in the cell cycle for precise DNA repair by BRCA1. *Cell Cycle, 4*(9), 1216-1222.

Eliasson, M. J., Sampei, K., Mandir, A. S., Hurn, P. D., Traystman, R. J., Bao, J., . . . Dawson, V. L. (1997). Poly(ADP-ribose) polymerase gene disruption renders mice resistant to cerebral ischemia. *Nat Med, 3*(10), 1089-1095.

Farmer, H., McCabe, N., Lord, C. J., Tutt, A. N., Johnson, D. A., Richardson, T. B., . . . Ashworth, A. (2005). Targeting the DNA repair defect in BRCA mutant cells as a therapeutic strategy. *Nature, 434*(7035), 917-921. doi: 10.1038/nature03445

Ferretti, L. P., Lafranchi, L., & Sartori, A. A. (2013). Controlling DNA-end resection: a new task for CDKs. *Front Genet, 4*, 99. doi: 10.3389/fgene.2013.00099

Fojo, T., & Bates, S. (2013). Mechanisms of resistance to PARP inhibitors--three and counting. *Cancer Discov, 3*(1), 20-23. doi: 10.1158/2159-8290.cd-12-0514

Fong, P. C., Boss, D. S., Yap, T. A., Tutt, A., Wu, P., Mergui-Roelvink, M., . . . de Bono, J. S. (2009). Inhibition of poly(ADP-ribose) polymerase in tumors from BRCA mutation carriers. *N Engl J Med, 361*(2), 123-134. doi: 10.1056/NEJMoa0900212

Gagne, J. P., Isabelle, M., Lo, K. S., Bourassa, S., Hendzel, M. J., Dawson, V. L., . . . Poirier, G. G. (2008). Proteome-wide identification of poly(ADP-ribose) binding proteins and poly(ADP-ribose)-associated protein complexes. *Nucleic Acids Res, 36*(22), 6959-6976. doi: 10.1093/nar/gkn771

Gottipati, P., Vischioni, B., Schultz, N., Solomons, J., Bryant, H. E., Djureinovic, T., . . . Helleday, T. (2010). Poly(ADP-ribose) polymerase is hyperactivated in homologous recombination-defective cells. *Cancer Res, 70*(13), 5389-5398. doi: 10.1158/0008-5472.can-09-4716

Greenberg, R. A., Sobhian, B., Pathania, S., Cantor, S. B., Nakatani, Y., & Livingston, D. M. (2006). Multifactorial contributions to an acute DNA damage response by BRCA1/BARD1-containing complexes. *Genes Dev, 20*(1), 34-46. doi: 10.1101/gad.1381306

Han, J., Zhong, C. Q., & Zhang, D. W. (2011). Programmed necrosis: backup to and competitor with apoptosis in the immune system. *Nat Immunol, 12*(12), 1143-1149. doi: 10.1038/ni.2159

Harper, J. W., & Elledge, S. J. (2007). The DNA damage response: ten years after. *Mol Cell, 28*(5), 739-745. doi: 10.1016/j.molcel.2007.11.015

Hartwell, L. H., Szankasi, P., Roberts, C. J., Murray, A. W., & Friend, S. H. (1997). Integrating genetic approaches into the discovery of anticancer drugs. *Science, 278*(5340), 1064-1068.

Hemminki, K., Scelo, G., Boffetta, P., Mellemkjaer, L., Tracey, E., Andersen, A., . . . Brennan, P. (2005). Second primary malignancies in patients with male breast cancer. *Br J Cancer, 92*(7), 1288-1292. doi: 10.1038/sj.bjc.6602505

Higgins, G. S., Harris, A. L., Prevo, R., Helleday, T., McKenna, W. G., & Buffa, F. M. (2010). Overexpression of POLQ confers a poor prognosis in early breast cancer patients. *Oncotarget, 1*(3), 175-184.

Hochegger, H., Dejsuphong, D., Fukushima, T., Morrison, C., Sonoda, E., Schreiber, V., . . . Takeda, S. (2006). Parp-1 protects homologous recombination from interference by Ku and Ligase IV in vertebrate cells. *EMBO J, 25*(6), 1305-1314. doi: 10.1038/sj.emboj.7601015

Hoeijmakers, J. H. J. (2001). Genome maintenance mechanisms for preventing cancer. *Nature, 411*(6835), 366-374.

Hopfner, K. P., Craig, L., Moncalian, G., Zinkel, R. A., Usui, T., Owen, B. A., . . . Tainer, J. A. (2002). The Rad50 zinc-hook is a structure joining Mre11 complexes in DNA recombination and repair. *Nature, 418*(6897), 562-566. doi: 10.1038/nature00922

Huang, X., Dong, Y., Bey, E. A., Kilgore, J. A., Bair, J. S., Li, L. S., . . . Boothman, D. A. (2012). An NQO1 substrate with potent antitumor activity that selectively kills by PARP1-induced programmed necrosis. *Cancer Res, 72*(12), 3038-3047. doi: 10.1158/0008-5472.can-11-3135

Huen, M. S., Sy, S. M., & Chen, J. (2010). BRCA1 and its toolbox for the maintenance of genome integrity. *Nat Rev Mol Cell Biol, 11*(2), 138-148. doi: 10.1038/nrm2831

Irizarry, R. A., Hobbs, B., Collin, F., Beazer-Barclay, Y. D., Antonellis, K. J., Scherf, U., & Speed, T. P. (2003). Exploration, normalization, and summaries of high density oligonucleotide array probe level data. *Biostatistics, 4*(2), 249-264. doi: 10.1093/biostatistics/4.2.249

Iyama, T., & Wilson, D. M., 3rd. (2013). DNA repair mechanisms in dividing and non-dividing cells. *DNA Repair (Amst), 12*(8), 620-636. doi: 10.1016/j.dnarep.2013.04.015

Jaspers, J. E., Kersbergen, A., Boon, U., Sol, W., van Deemter, L., Zander, S. A., . . . Rottenberg, S. (2013). Loss of 53BP1 causes PARP inhibitor resistance in Brca1-mutated mouse mammary tumors. *Cancer Discov, 3*(1), 68-81. doi: 10.1158/2159-8290.cd-12-0049

Jeggo, P. A., Geuting, V., & Lobrich, M. (2011). The role of homologous recombination in radiation-induced double-strand break repair. *Radiother Oncol, 101*(1), 7-12. doi: 10.1016/j.radonc.2011.06.019

Jemal, A., Siegel, R., Xu, J., & Ward, E. (2010). Cancer statistics, 2010. *CA Cancer J Clin, 60*(5), 277-300. doi: 10.3322/caac.20073

Johnson, N., Johnson, S. F., Yao, W., Li, Y. C., Choi, Y. E., Bernhardy, A. J., . . . Shapiro, G. I. (2013). Stabilization of mutant BRCA1 protein confers PARP inhibitor and platinum resistance. *Proc Natl Acad Sci U S A, 110*(42), 17041-17046. doi: 10.1073/pnas.1305170110

Johnson, N., Li, Y. C., Walton, Z. E., Cheng, K. A., Li, D., Rodig, S. J., . . . Shapiro, G. I. (2011). Compromised CDK1 activity sensitizes BRCA-proficient cancers to PARP inhibition. *Nat Med, 17*(7), 875-882. doi: 10.1038/nm.2377

Kennedy, R. D., & D'Andrea, A. D. (2005). The Fanconi Anemia/BRCA pathway: new faces in the crowd. *Genes Dev, 19*(24), 2925-2940. doi: 10.1101/gad.1370505

Khanna, K. K., & Jackson, S. P. (2001). DNA double-strand breaks: signaling, repair and the cancer connection. *Nat Genet, 27*(3), 247-254. doi: 10.1038/85798

Khazaei, M., Moien-Afshari, F., Elmi, S., Mirdamadi, A., & Laher, I. (2009). The effects of diethyldithiocarbamate, a SOD inhibitor, on endothelial function in sedentary and exercised db/db mice. *Pathophysiology, 16*(1), 15-18. doi: 10.1016/j.pathophys.2008.11.002

Kumar, R., & Cheok, C. F. (2014). RIF1: a novel regulatory factor for DNA replication and DNA damage response signaling. *DNA Repair (Amst), 15*, 54-59. doi: 10.1016/j.dnarep.2013.12.004

Langerak, P., Mejia-Ramirez, E., Limbo, O., & Russell, P. (2011). Release of Ku and MRN from DNA ends by Mre11 nuclease activity and Ctp1 is required for homologous recombination repair of double-strand breaks. *PLoS Genet, 7*(9), e1002271. doi: 10.1371/journal.pgen.1002271

Li, D., Bi, F. F., Chen, N. N., Cao, J. M., Sun, W. P., Zhou, Y. M., . . . Yang, Q. (2014). A novel crosstalk between BRCA1 and poly (ADP-ribose) polymerase 1 in breast cancer. *Cell Cycle, 13*(21), 3442-3449. doi: 10.4161/15384101.2014.956507

Li, L. S., Bey, E. A., Dong, Y., Meng, J., Patra, B., Yan, J., . . . Boothman, D. A. (2011). Modulating endogenous NQO1 levels identifies key regulatory mechanisms of action of beta-lapachone for pancreatic cancer therapy. *Clin Cancer Res, 17*(2), 275-285. doi: 10.1158/1078-0432.ccr-10-1983

Li, M. L., & Greenberg, R. A. (2012). Links between genome integrity and BRCA1 tumor suppression. *Trends Biochem Sci, 37*(10), 418-424. doi: 10.1016/j.tibs.2012.06.007

Lindahl, T., & Barnes, D. E. (2000). Repair of endogenous DNA damage. *Cold Spring Harb Symp Quant Biol, 65*, 127-133.

Lindahl, T., & Wood, R. D. (1999). Quality control by DNA repair. *Science, 286*(5446), 1897-1905.

Liu, L., Taverna, P., Whitacre, C. M., Chatterjee, S., & Gerson, S. L. (1999). Pharmacologic disruption of base excision repair sensitizes mismatch repair-deficient and -proficient colon cancer cells to methylating agents. *Clin Cancer Res, 5*(10), 2908-2917.

Liu, L. F., Desai, S. D., Li, T. K., Mao, Y., Sun, M., & Sim, S. P. (2000). Mechanism of action of camptothecin. *Ann N Y Acad Sci, 922*, 1-10.

Liu, X., Han, E. K., Anderson, M., Shi, Y., Semizarov, D., Wang, G., . . . Shoemaker, A. R. (2009). Acquired resistance to combination treatment with temozolomide and ABT-888 is mediated by both base excision repair and homologous recombination DNA repair pathways. *Mol Cancer Res, 7*(10), 1686-1692. doi: 10.1158/1541-7786.mcr-09-0299

Lok, B. H., & Powell, S. N. (2012). Molecular pathways: understanding the role of Rad52 in homologous recombination for therapeutic advancement. *Clin Cancer Res, 18*(23), 6400-6406. doi: 10.1158/1078-0432.ccr-11-3150

Lord, C. J., Tutt, A. N., & Ashworth, A. (2014). Synthetic Lethality and Cancer Therapy: Lessons Learned from the Development of PARP Inhibitors. *Annu Rev Med*. doi: 10.1146/annurev-med-050913-022545

Lovato, A., Panasci, L., & Witcher, M. (2012). Is there an epigenetic component underlying the resistance of triple-negative breast cancers to parp inhibitors? *Front Pharmacol, 3*, 202. doi: 10.3389/fphar.2012.00202

Luo, X., & Kraus, W. L. (2012). On PAR with PARP: cellular stress signaling through poly(ADP-ribose) and PARP-1. *Genes Dev, 26*(5), 417-432. doi: 10.1101/gad.183509.111

Martin, R. W., Orelli, B. J., Yamazoe, M., Minn, A. J., Takeda, S., & Bishop, D. K. (2007). RAD51 up-regulation bypasses BRCA1 function and is a common feature of BRCA1-deficient breast tumors. *Cancer Res, 67*(20), 9658-9665. doi: 10.1158/0008-5472.can-07-0290

Mateos-Gomez, P. A., Gong, F., Nair, N., Miller, K. M., Lazzerini-Denchi, E., & Sfeir, A. (2015). Mammalian polymerase theta promotes alternative NHEJ and suppresses recombination. *Nature, 518*(7538), 254-257. doi: 10.1038/nature14157

McEllin, B., Camacho, C. V., Mukherjee, B., Hahm, B., Tomimatsu, N., Bachoo, R. M., & Burma, S. (2010). PTEN loss compromises homologous recombination repair in astrocytes: implications for glioblastoma therapy with temozolomide or poly(ADP-ribose) polymerase inhibitors. *Cancer Res, 70*(13), 5457-5464. doi: 10.1158/0008-5472.can-09-4295

McVey, M., & Lee, S. E. (2008). MMEJ repair of double-strand breaks (director's cut): deleted sequences and alternative endings. *Trends Genet, 24*(11), 529-538. doi: 10.1016/j.tig.2008.08.007

Miki, Y., Swensen, J., Shattuck-Eidens, D., Futreal, P. A., Harshman, K., Tavtigian, S., . . . et al. (1994). A strong candidate for the breast and ovarian cancer susceptibility gene BRCA1. *Science, 266*(5182), 66-71.

Moore, Z., Chakrabarti, G., Luo, X., Ali, A., Hu, Z., Fattah, F. J., . . . Boothman, D. A. (2015). NAMPT inhibition sensitizes pancreatic adenocarcinoma cells to tumor-selective, PAR-independent metabolic catastrophe and cell death induced by beta-lapachone. *Cell Death Dis, 6*, e1599. doi: 10.1038/cddis.2014.564

Moroni, F. (2008). Poly(ADP-ribose)polymerase 1 (PARP-1) and postischemic brain damage. *Curr Opin Pharmacol, 8*(1), 96-103. doi: 10.1016/j.coph.2007.10.005

Moskwa, P., Buffa, F. M., Pan, Y., Panchakshari, R., Gottipati, P., Muschel, R. J., . . . Chowdhury, D. (2011). miR-182-mediated downregulation of BRCA1 impacts DNA repair and sensitivity to PARP inhibitors. *Mol Cell, 41*(2), 210-220. doi: 10.1016/j.molcel.2010.12.005

Mukhopadhyay, A., Elattar, A., Cerbinskaite, A., Wilkinson, S. J., Drew, Y., Kyle, S., . . . Curtin, N. J. (2010). Development of a functional assay for homologous recombination status in primary cultures of epithelial ovarian tumor and correlation with sensitivity to poly(ADP-ribose) polymerase inhibitors. *Clin Cancer Res, 16*(8), 2344-2351. doi: 10.1158/1078-0432.ccr-09-2758

Nakamura, K., Kogame, T., Oshiumi, H., Shinohara, A., Sumitomo, Y., Agama, K., . . . Taniguchi, Y. (2010). Collaborative action of Brca1 and CtIP in elimination of covalent modifications from double-strand breaks to facilitate subsequent break repair. *PLoS Genet, 6*(1), e1000828. doi: 10.1371/journal.pgen.1000828

Oplustilova, L., Wolanin, K., Mistrik, M., Korinkova, G., Simkova, D., Bouchal, J., . . . Bartek, J. (2012). Evaluation of candidate biomarkers to predict cancer cell sensitivity or resistance to PARP-1 inhibitor treatment. *Cell Cycle, 11*(20), 3837-3850. doi: 10.4161/cc.22026

Parkinson, E. I., Bair, J. S., Cismesia, M., & Hergenrother, P. J. (2013). Efficient NQO1 substrates are potent and selective anticancer agents. *ACS Chem Biol, 8*(10), 2173-2183. doi: 10.1021/cb4005832

Patel, A. G., Sarkaria, J. N., & Kaufmann, S. H. (2011). Nonhomologous end joining drives poly(ADP-ribose) polymerase (PARP) inhibitor lethality in homologous recombination-deficient cells. *Proc Natl Acad Sci U S A, 108*(8), 3406-3411. doi: 10.1073/pnas.1013715108

Pathania, S., Bade, S., Le Guillou, M., Burke, K., Reed, R., Bowman-Colin, C., . . . Livingston, D. M. (2014). BRCA1 haploinsufficiency for replication stress suppression in primary cells. *Nat Commun, 5*, 5496. doi: 10.1038/ncomms6496

Paull, T. T., Cortez, D., Bowers, B., Elledge, S. J., & Gellert, M. (2001). Direct DNA binding by Brca1. *Proc Natl Acad Sci U S A, 98*(11), 6086-6091. doi: 10.1073/pnas.111125998

Pieper, A. A., Walles, T., Wei, G., Clements, E. E., Verma, A., Snyder, S. H., & Zweier, J. L. (2000). Myocardial postischemic injury is reduced by polyADPripose polymerase-1 gene disruption. *Mol Med, 6*(4), 271-282.

Pink, J. J., Planchon, S. M., Tagliarino, C., Varnes, M. E., Siegel, D., & Boothman, D. A. (2000). NAD(P)H:Quinone oxidoreductase activity is the principal determinant of beta-lapachone cytotoxicity. *J Biol Chem, 275*(8), 5416-5424.

Prasad, R., Horton, J. K., Chastain, P. D., 2nd, Gassman, N. R., Freudenthal, B. D., Hou, E. W., & Wilson, S. H. (2014). Suicidal cross-linking of PARP-1 to AP site intermediates in cells undergoing base excision repair. *Nucleic Acids Res, 42*(10), 6337-6351. doi: 10.1093/nar/gku288

Rehman, F. L., Lord, C. J., & Ashworth, A. (2010). Synthetic lethal approaches to breast cancer therapy. *Nat Rev Clin Oncol, 7*(12), 718-724.

Robinson, M. D., & Speed, T. P. (2007). A comparison of Affymetrix gene expression arrays. *BMC Bioinformatics, 8*, 449. doi: 10.1186/1471-2105-8-449

Ross, D., Kepa, J. K., Winski, S. L., Beall, H. D., Anwar, A., & Siegel, D. (2000). NAD(P)H:quinone oxidoreductase 1 (NQO1): chemoprotection, bioactivation,

gene regulation and genetic polymorphisms. *Chem Biol Interact, 129*(1-2), 77-97.

Rouse, J., & Jackson, S. P. (2002). Interfaces between the detection, signaling, and repair of DNA damage. *Science, 297*(5581), 547-551. doi: 10.1126/science.1074740

Rozier, L., Guo, Y., Peterson, S., Sato, M., Baer, R., Gautier, J., & Mao, Y. (2013). The MRN-CtIP pathway is required for metaphase chromosome alignment. *Mol Cell, 49*(6), 1097-1107. doi: 10.1016/j.molcel.2013.01.023

Russell, P. A., Pharoah, P. D., De Foy, K., Ramus, S. J., Symmonds, I., Wilson, A., . . . Gayther, S. A. (2000). Frequent loss of BRCA1 mRNA and protein expression in sporadic ovarian cancers. *Int J Cancer, 87*(3), 317-321.

San Filippo, J., Sung, P., & Klein, H. (2008). Mechanism of eukaryotic homologous recombination. *Annu Rev Biochem, 77*, 229-257. doi: 10.1146/annurev.biochem.77.061306.125255

Schlegel, B. P., Jodelka, F. M., & Nunez, R. (2006). BRCA1 promotes induction of ssDNA by ionizing radiation. *Cancer Res, 66*(10), 5181-5189. doi: 10.1158/0008-5472.can-05-3209

Scott, T. L., Rangaswamy, S., Wicker, C. A., & Izumi, T. (2014). Repair of oxidative DNA damage and cancer: recent progress in DNA base excision repair. *Antioxid Redox Signal, 20*(4), 708-726. doi: 10.1089/ars.2013.5529

Scully, R., Ganesan, S., Vlasakova, K., Chen, J., Socolovsky, M., & Livingston, D. M. (1999). Genetic analysis of BRCA1 function in a defined tumor cell line. *Mol Cell, 4*(6), 1093-1099.

Sharma, A., Singh, K., & Almasan, A. (2012). Histone H2AX phosphorylation: a marker for DNA damage. *Methods Mol Biol, 920*, 613-626. doi: 10.1007/978-1-61779-998-3_40

Sourisseau, T., Maniotis, D., McCarthy, A., Tang, C., Lord, C. J., Ashworth, A., & Linardopoulos, S. (2010). Aurora-A expressing tumour cells are deficient for homology-directed DNA double strand-break repair and sensitive to PARP inhibition. *EMBO Mol Med, 2*(4), 130-142. doi: 10.1002/emmm.201000068

Speit, G., Hochsattel, R., & Vogel, W. (1984). The contribution of DNA single-strand breaks to the formation of chromosome aberrations and SCEs. *Basic Life Sci, 29 Pt A*, 229-244.

Symington, L. S. (2014). End resection at double-strand breaks: mechanism and regulation. *Cold Spring Harb Perspect Biol, 6*(8). doi: 10.1101/cshperspect.a016436

Tagliarino, C., Pink, J. J., Reinicke, K. E., Simmers, S. M., Wuerzberger-Davis, S. M., & Boothman, D. A. (2003). Mu-calpain activation in beta-lapachone-mediated apoptosis. *Cancer Biol Ther, 2*(2), 141-152.

Telli, M. L., & Ford, J. M. (2010). PARP inhibitors in breast cancer. *Clin Adv Hematol Oncol, 8*(9), 629-635.

Thomas, C., & Tulin, A. V. (2013). Poly-ADP-ribose polymerase: machinery for nuclear processes. *Mol Aspects Med, 34*(6), 1124-1137. doi: 10.1016/j.mam.2013.04.001

Tomimatsu, N., Mukherjee, B., & Burma, S. (2009). Distinct roles of ATR and DNA-PKcs in triggering DNA damage responses in ATM-deficient cells. *EMBO Rep, 10*(6), 629-635. doi: 10.1038/embor.2009.60

Tomimatsu, N., Mukherjee, B., Catherine Hardebeck, M., Ilcheva, M., Vanessa Camacho, C., Louise Harris, J., . . . Burma, S. (2014). Phosphorylation of EXO1 by CDKs 1 and 2 regulates DNA end resection and repair pathway choice. *Nat Commun, 5*, 3561. doi: 10.1038/ncomms4561

Trovesi, C., Manfrini, N., Falcettoni, M., & Longhese, M. P. (2013). Regulation of the DNA damage response by cyclin-dependent kinases. *J Mol Biol, 425*(23), 4756-4766. doi: 10.1016/j.jmb.2013.04.013

Valko, M., Rhodes, C. J., Moncol, J., Izakovic, M., & Mazur, M. (2006). Free radicals, metals and antioxidants in oxidative stress-induced cancer. *Chem Biol Interact, 160*(1), 1-40. doi: 10.1016/j.cbi.2005.12.009

Venkitaraman, A. R. (2004). Tracing the network connecting BRCA and Fanconi anaemia proteins. *Nat Rev Cancer, 4*(4), 266-276. doi: 10.1038/nrc1321

Vyas, S., & Chang, P. (2014). New PARP targets for cancer therapy. *Nat Rev Cancer, 14*(7), 502-509. doi: 10.1038/nrc3748

Walsh, C. S. (2015). Two decades beyond BRCA1/2: Homologous recombination, hereditary cancer risk and a target for ovarian cancer therapy. *Gynecol Oncol*. doi: 10.1016/j.ygyno.2015.02.017

Wang, J., Bian, C., Li, J., Couch, F. J., Wu, K., & Zhao, R. C. (2008). Poly(ADP-ribose) polymerase-1 down-regulates BRCA2 expression through the BRCA2 promoter. *J Biol Chem, 283*(52), 36249-36256. doi: 10.1074/jbc.M803693200

Wang, Y., Huang, J. W., Calses, P., Kemp, C. J., & Taniguchi, T. (2012). MiR-96 downregulates REV1 and RAD51 to promote cellular sensitivity to cisplatin and PARP inhibition. *Cancer Res, 72*(16), 4037-4046. doi: 10.1158/0008-5472.can-12-0103

Waters, C. A., Strande, N. T., Wyatt, D. W., Pryor, J. M., & Ramsden, D. A. (2014). Nonhomologous end joining: a good solution for bad ends. *DNA Repair (Amst), 17*, 39-51. doi: 10.1016/j.dnarep.2014.02.008

Williams, R. S., & Glover, J. N. (2003). Structural consequences of a cancer-causing BRCA1-BRCT missense mutation. *J Biol Chem, 278*(4), 2630-2635. doi: 10.1074/jbc.M210019200

Williams, R. S., Williams, J. S., & Tainer, J. A. (2007). Mre11-Rad50-Nbs1 is a keystone complex connecting DNA repair machinery, double-strand break signaling, and the chromatin template. *Biochem Cell Biol, 85*(4), 509-520. doi: 10.1139/o07-069

Wilson, D. M., 3rd, & Simeonov, A. (2010). Small molecule inhibitors of DNA repair nuclease activities of APE1. *Cell Mol Life Sci, 67*(21), 3621-3631. doi: 10.1007/s00018-010-0488-2

Wiltshire, T., Senft, J., Wang, Y., Konat, G. W., Wenger, S. L., Reed, E., & Wang, W. (2007). BRCA1 contributes to cell cycle arrest and chemoresistance in response to the anticancer agent irofulven. *Mol Pharmacol, 71*(4), 1051-1060. doi: 10.1124/mol.106.029504

Wuerzberger, S. M., Pink, J. J., Planchon, S. M., Byers, K. L., Bornmann, W. G., & Boothman, D. A. (1998). Induction of apoptosis in MCF-7:WS8 breast cancer cells by beta-lapachone. *Cancer Res, 58*(9), 1876-1885.

Yi, Y. W., Kang, H. J., & Bae, I. (2014). BRCA1 and Oxidative Stress. *Cancers (Basel), 6*(2), 771-795. doi: 10.3390/cancers6020771

Ying, W. (2013). Roles of NAD (+) , PARP-1, and Sirtuins in Cell Death, Ischemic Brain Injury, and Synchrotron Radiation X-Ray-Induced Tissue Injury. *Scientifica (Cairo), 2013*, 691251. doi: 10.1155/2013/691251

Yun, M. H., & Hiom, K. (2009a). CtIP-BRCA1 modulates the choice of DNA double-strand-break repair pathway throughout the cell cycle. *Nature, 459*(7245), 460-463. doi: 10.1038/nature07955

Yun, M. H., & Hiom, K. (2009b). Understanding the functions of BRCA1 in the DNA-damage response. *Biochem Soc Trans, 37*(Pt 3), 597-604. doi: 10.1042/bst0370597

Zhuang, J., Jiang, G., Willers, H., & Xia, F. (2009). Exonuclease function of human Mre11 promotes deletional nonhomologous end joining. *J Biol Chem, 284*(44), 30565-30573. doi: 10.1074/jbc.M109.059444